

Baryon asymmetry of the Universe in the standard model

Glennys R. Farrar

Department of Physics and Astronomy, Rutgers University, Piscataway, New Jersey 08855

M. E. Shaposhnikov*

CERN, TH Division, CH-1211, Geneva 23, Switzerland

(Received 19 May 1993)

We study the interactions of quarks and antiquarks with the changing Higgs field during the electroweak phase transition, including quantum mechanical and some thermal effects, with the only source of CP violation being the known CKM phase. We show that the GIM cancellation, which has been commonly thought to imply a prediction which is at least 10 orders of magnitude too small, can be evaded in certain kinematic regimes, for instance, when the strange quark is totally reflected but the down quark is not. We report on a quantitative calculation of the asymmetry in a one-dimensional approximation based on the present understanding of the physics of the high-temperature environment, but with some aspects of the problem oversimplified. The resulting prediction for the magnitude and sign of the present baryonic asymmetry of the Universe agrees with the observed value, with moderately optimistic assumptions about the dynamics of the phase transition. Both magnitude and sign of the asymmetry have an intricate dependence on quark masses and mixings, so that quantitative agreement between prediction and observation would be highly nontrivial. At present uncertainties related to the dynamics of the EW phase transition and the oversimplifications of our treatment are too great to decide whether or not this is the correct explanation for the presence of remnant matter in our Universe; however, the present work makes it clear that the minimal standard model cannot be discounted as a contender for explaining this phenomenon.

PACS number(s): 98.80.Cq, 12.15.Ji

I. INTRODUCTION

The nonzero ratio of baryon number to entropy, $n_B/s \sim (4 - 6) \times 10^{-11}$, is an important challenge to particle theory. Many possible mechanisms have been advanced to explain it [1–6] (for reviews and references to more recent work see, e.g., Refs. [7–13]). The standard electroweak theory contains in principle all the elements necessary [1] for generation of the baryonic asymmetry of the Universe (BAU). (1) C and CP violations, in the fundamental gauge and Higgs interactions of the quarks; (2) anomalous electroweak baryon number violation¹ [14, 15]; (3) a departure from thermal equilibrium, assuming the cosmological $SU(2) \times U(1)$ phase transition [19, 20] is first order.

However, conventional wisdom holds that the minimal standard model (MSM) cannot by itself cause the observed baryonic asymmetry of the Universe. The most important reason is that the CP violation present in

the MSM to account for the observed CP violation in kaon decays is commonly believed to be inadequate, by 10–12 orders of magnitude or more, to explain the observed $\sim 10^{-11}$ – 10^{-10} level of the asymmetry. The second reason is that such a large asymmetry can only be generated in a strongly first order phase transition, and the Higgs sector of the MSM may not produce a sufficiently strong phase transition. In particular, the rate of sphaleron transitions after the phase transition must be small enough not to wash out the asymmetry, so the mass of the W just after the phase transition must not be too small [21]. Using the one-loop high temperature effective potential together with the one-loop sphaleron rate results in the upper bound on the Higgs boson mass in the MSM: $M_H^{\text{crit}} = 45$ GeV [22, 23], which is in contradiction with the experimental lower bound reached at the CERN e^+e^- collider LEP:² $M_H \gtrsim 60$ GeV.

For these reasons, people have considered extensions of the standard model in a search for a mechanism for electroweak baryogenesis [16, 25–34]. Variants of the electroweak theory contain more free parameters than the MSM alone, allowing the introduction of an extra source of CP violation and allowing the upper bound on the Higgs boson mass to be relaxed [35–39]. The general con-

*On leave of absence from Institute for Nuclear Research of Russian Academy of Sciences, Moscow 117312, Russia.

¹It was shown in Ref. [16] (for earlier discussion see [17, 6, 18]) that although anomalous B violation is negligible at zero temperature, it is enormously enhanced at high temperature, so that it can be large enough that the baryonic asymmetry of the Universe may have been produced during the electroweak phase transition.

²For the current best limit from all four experiments, see [24].

clusion is quite optimistic: the baryon asymmetry of the Universe can plausibly be a natural consequence of several extended versions of the standard model, provided the electroweak phase transition is sufficiently strongly first order³ and the additional source of CP violation is strong enough. In these “scenarios,” however, the magnitude and sign of the asymmetry cannot be predicted; instead, the observed BAU must be used to constrain the parameters of the extended theory.

We shall demonstrate in this paper that, contrary to popular belief, known MSM physics alone may in fact be responsible for the production of the baryonic asymmetry, with no new source of CP violation required, as long as the usual requirement of a sufficiently strongly first order phase transition is met.⁴ We make a detailed calculation of the asymmetry which is produced when the quarks and antiquarks, treated as quasiparticle excitations of the plasma (whose dispersion relation we obtain using one-loop high temperature perturbation theory) are quantum-mechanically reflected from the barrier presented to them by the interface between the regions of small and large Higgs VEV. We simplify the problem in several important respects, neglecting incoherent scattering of the quasiparticles and considering only one-dimensional scattering. Since the results can be consistent with observation in sign and magnitude, our simplified treatment provides the necessary incentive to investigate MSM production of the BAU with a more realistic treatment. It also provides insight into the most important and problematic aspects of the physics, and thus can be of guidance in future work.

The bulk of this paper is devoted to elucidating the essential aspects of the physics involved in production of the BAU in the minimal standard model, developing necessary theoretical machinery for solving the problem, and presenting the quantitative results of a fairly realistic but nonetheless oversimplified calculation.

³All present models of electroweak baryogenesis depend on two essential aspects of the strength of the phase transition which are in principle independent, but which for simplicity we lump together when speaking of a requirement that the phase transition be strong enough: the vacuum expectation value (VEV) after the transition must be large enough that sphaleron transitions in the broken phase are turned off, and the bubbles of low temperature phase which expand to fill the Universe must not be too flimsy or slow moving. The first condition is the one which is better understood, so that it is normally the one whose constraint is given quantitatively.

⁴Whether or not the minimal standard model with a single Higgs boson produces a sufficiently strongly first order phase transition is a separate question from whether the MSM CP violation in the CKM matrix is sufficiently large. In fact, it is still an open question, since the uncertainties in the upper bound on the Higgs boson mass are rather large. Although the one loop calculation gives $M_H^{\text{crit}} = 45$ GeV, taking into account Debye screening effects reduces the critical mass to $M_H^{\text{crit}} = 35$ GeV [40, 41]. The two-loop corrections increase the latter number by about 5 GeV [42, 43], while nonperturbative effects may change it up to $M_H^{\text{crit}} \sim 100$ GeV [44].

The plan of the paper is as follows. We begin with a section describing CP violation in the MSM and the argument leading to the conventional wisdom on the smallness of MSM CP violation. We discuss CP violation in the K^0 system, which is known to be $\sim 10^{-3}$, in order to understand how the physics of the MSM may lead to C and CP violation at the level required for the production of the observed BAU. This allows us to identify aspects of the physics which must be treated adequately if we are to avoid missing the effect in cosmology.

In Sec. III we give an overview of the various dynamical mechanisms for electroweak baryogenesis which have been discussed in the literature, and describe the mechanism [32, 33, 45] which we quantitatively investigate in the latter portion of this paper. In this mechanism, the CP -violating scattering of thermal quarks from the bubble wall of the expanding Higgs VEV produces a baryonic current flowing from the unbroken to the broken phase. In Sec. IV we make a rough estimate of the size of the baryonic current which might be anticipated from this process, when the important region of phase space is not overlooked. The quantitative calculation of the current is deferred to the latter portion of the paper.

Given a nonzero current of baryon number produced by some process involving the bubble wall, we must estimate the ratio n_B/s which remains after the phase transition is complete, produced on account of sphaleron processes which diminish the antibaryon excess in the unbroken phase. We cannot give a firm estimate of this ratio as a function of the sphaleron rate in the unbroken phase, since it also depends on the nature of the bubble wall. However we can obtain a conservative estimate of the magnitude of n_B/s by considering the case that the bubble wall does not disequilibrate the medium as it passes, i.e., in quasistatic approximation. This analysis is presented in Sec. V. Presumably improvements on the quasistatic approximation will only increase the magnitude of n_B/s .

Interactions of the fermions with the gauge and Higgs fields of the high temperature plasma are crucial to the existence of nontrivial CP violation, as explained in Sec. II. Moreover they are quantitatively important in other regards. Thus we present in Sec. VI a discussion of the properties of quark excitations in the thermal plasma.

While the discussion in the first part of the paper is rather general, independent of the precise source of the baryonic current, in order to make a quantitative prediction of the asymmetry we must adopt a particular mechanism for its production. The formalism which we have developed in order to calculate the asymmetry in the reflection probabilities of quarks and antiquarks scattering from the domain wall, is given in Sec. VII and the Appendixes. Using this formalism, Sec. VIII is devoted to obtaining analytic results under various simplifying assumptions. The analytic expression presented here is helpful for understanding how the Glashow-Iliopoulos-Maiani (GIM) mechanism can be evaded, and explaining the final dependence on quark Yukawa couplings. However in order to do a calculation with sufficient accuracy to address the question of the sign of the result, we must do an exact numerical calculation. The results of this

are given in Sec. IX. We explore in some detail how the asymmetry depends on quark masses and mixings.

Having determined the asymmetry in the reflection probabilities, we then combine it with the estimates of the sphaleron conversion efficiency and the asymmetry in the fluxes, obtained in earlier sections, and give in Sec. X our final estimate for n_b/s . We review and elaborate on the uncertainties and inadequacies of the present calculation. The last section is the Conclusion, where we summarize the present situation, describe the problems which must be solved, and mention some consequences.

The main ideas of the paper can be understood by reading Secs. II–IV, IX, X, and the Conclusion, although Sec. V is important in that it shows how the final prediction is connected to the kinetics and dynamics near the bubble wall, and Sec. VI will aid in comprehending some of the unusual properties of the thermal excitations which are the actual eigenstates of the scattering problem. Many readers will also want to study the analytic formula derived in Sec. VIII in thin wall, small p/ω approximation, working to lowest nonvanishing order in the mixing angles, in order to understand the dependence on quark masses of the final asymmetry. Other sections and the Appendixes are intended for readers wanting to understand the details as well as the general ideas.

A brief description this work has been published in Ref. [46]. The present version of this paper corrects some typographical errors in the original version and has been somewhat reorganized (e.g., moving more to the Appendixes) and elaborated (especially the section on analytic results) in order to make it more readily understandable. In addition we include two effects which were previously neglected: $L - R$ mixing due to QCD sphalerons, and a diminution of the electroweak gauge and Higgs effects in the broken phase due to mass corrections in the one-loop approximation to the quasiparticle propagator. The results and conclusion are not significantly modified; the discussion of the various uncertainties is more complete and quantitative.

II. CP VIOLATION IN THE STANDARD MODEL

In the minimal standard model, CP violation occurs because of relative phases between the electroweak gauge

interactions and the Higgs interactions of the quarks. As shown by Kobayashi and Maskawa [47], if there are at least three generations of quarks, there can be a physically meaningful phase which leads to observable CP -violating effects. The part of the MSM Lagrangian which involves quarks is

$$\mathcal{L} = \mathcal{L}_G + \mathcal{L}_Y. \quad (2.1)$$

In the “gauge” basis

$$\mathcal{L}_G = \bar{Q}_L \not{D} Q_L + \bar{U}_R \not{D} U_R + \bar{D}_R \not{D} D_R \quad (2.2)$$

and

$$\mathcal{L}_Y = \frac{g_W}{\sqrt{2}M_W} \{ \bar{Q}_L^i K^{ij} M_d^{jj} D_R^j \phi + \bar{Q}_L^i M_u^{ii} U_R^i \tilde{\phi} + \text{H.c.} \}, \quad (2.3)$$

where \not{D} is the appropriate covariant derivative, Q_L^i are the left-handed quark doublets (i is the generation index), U_R^i and D_R^i are the right-handed quarks with electric charges $\frac{2}{3}$ and $-\frac{1}{3}$, respectively, K is the Cabibbo-Kobayashi-Maskawa (CKM) matrix, M_u and M_d are the diagonal mass matrices of the quarks, and $\tilde{\phi}_i = \epsilon_{ij} \phi_j^\dagger$. In this basis, the Lagrangian has been written in terms of the fields which are eigenstates of the $SU(2)_L$ gauge interactions, and the CP violation is contained in a phase in the matrix K , relating the gauge eigenstates to the mass eigenstates. When a specific parametrization of the CKM matrix is required, we adopt that of the Particle Data Group [48]. Note that by redefining the basis, any one of the three types of fermionic interactions, with charged or neutral Higgs bosons, or gauge bosons, can be made purely real. This means that in order for a process in the minimal standard model to violate CP , it must involve in an essential way two or more of these interactions.

If either mass matrix M_d or M_u has two or more degenerate elements, or if one or more of the mixing angles in the CKM matrix vanishes, then with a physically unobservable change of phases of the quark fields, the CKM matrix can be made purely real and there is no CP violation. Thus if the combination

$$d_{CP} = \sin(\theta_{12}) \sin(\theta_{23}) \sin(\theta_{13}) \sin \delta_{CP} (m_t^2 - m_c^2)(m_t^2 - m_u^2)(m_c^2 - m_u^2)(m_b^2 - m_s^2)(m_b^2 - m_d^2)(m_s^2 - m_d^2) \quad (2.4)$$

vanishes, CP violation vanishes. The basis-invariant formulation of this statement can be found in Ref. [49]. Furthermore, it is essential for baryogenesis that not only CP but also C be violated. Because of the chiral nature of the $SU(2)$ gauge interaction, left and right chiralities of quarks have different interactions, so that \mathcal{L}_{MSM} has both C -even and C -odd pieces.

The above remarks make it evident that in order for MSM processes to produce a baryon asymmetry, all 3 quark generations, as well as dynamics which distinguishes between chiralities and which involve quark in-

teractions with both neutral and charged bosons,⁵ must play a significant role. In the next section we will describe how both these elements are incorporated in the mechanism we investigate.

The “conventional wisdom,” that CP violation originating from the KM phase is too small to be relevant to

⁵I.e., not only the Higgs VEV but also W^\pm or charged components of the Higgs field.

the observed baryonic asymmetry, results from arguing⁶ that the only natural scale for the baryogenesis problem is the temperature of the electroweak phase transition, $T \sim 100$ GeV. One might think that at this temperature the Yukawa interaction can be treated as a perturbation, because quark masses are small compared with the temperature. Then, since the baryon asymmetry is a dimensionless number, the quantity (2.4) should be divided by something with the dimension of (mass)¹². The natural mass parameter at high temperatures seems to be the temperature itself, so that the asymmetry is argued to be at most

$$\frac{n_B}{s} \lesssim \frac{d_{CP}}{N_{\text{eff}} T^{12}} \sim 10^{-20}. \quad (2.5)$$

This reasoning has been widely accepted, but, as has been the case with many “no-go” theorems, proves not to be watertight when examined carefully.⁷

In order to reveal one important point of weakness in the above argument, it is instructive to consider CP violation in the K^0 system. Here the CP -violating parameter is known to be quite large, $\epsilon = 2 \times 10^{-3}$. By analogy with the above discussion one could say that since $K^0 \leftrightarrow \bar{K}^0$ oscillations are described by the box diagram, the typical scale associated with this process is the momentum in the loop, $p \sim M_W$, leading to the conclusion $\epsilon \sim d_{CP}/M_W^{12} \sim 10^{-17}$. This is, however, wrong by 14 orders of magnitude.

Of course, everybody knows why this “derivation” is incorrect. The mass of the W boson is not the only scale of the problem here. There are numerous other scales, such as the mass of the kaon itself. Moreover, since m_K is smaller than the masses of the c , b , and t quarks and $m_K \sim m_s$, a perturbative expansion in the quark masses does not work, so that detailed calculation is necessary. The box-diagram contribution was found [51], in the original KM basis, to be

$$\begin{aligned} \left| \frac{\text{Im } M_{12}}{\Delta m} \right| \sim & \frac{s_1^2 c_1 s_2 c_2 s_3 c_3 \sin \delta_{CP} (m_t^2 - m_c^2)}{s_1^2 c_1^2 c_3^2 \left[c_2^4 m_c^2 + s_2^4 m_t^2 + \frac{2s_2^2 c_2^2 m_t^2 m_c^2}{(m_t^2 - m_c^2)} \ln \left(\frac{m_t^2}{m_c^2} \right) \right]} \left\{ c_2^2 m_c^2 \left[\frac{m_t^2}{(m_t^2 - m_c^2)^2} \ln \left(\frac{m_t^2}{m_c^2} \right) - \frac{1}{m_t^2 - m_c^2} \right] \right. \\ & \left. + s_2^2 m_t^2 \left[\frac{m_c^2}{(m_t^2 - m_c^2)^2} \ln \left(\frac{m_c^2}{m_t^2} \right) + \frac{1}{m_t^2 - m_c^2} \right] \right\}. \end{aligned} \quad (2.7)$$

⁶Here we give a popular version of the more sophisticated treatment of Ref. [26].

⁷This paper is not the first one to look for and point out possible loopholes in this argument. In Refs. [26, 50] a mechanism of MSM baryogenesis was explored based on the possible existence of a Chern-Simons condensate in the high temperature phase and the decay of nontrivial fluctuations of gauge and Higgs fields during the first order electroweak phase transition. There, a measure of CP violation in the effective action for the gauge fields in the expanding Universe was found to be [50]

$$\frac{\alpha_W}{\pi^4} \left(\frac{\alpha_W}{m_W^2} \right)^4 \frac{s_2 s_3 \sin \delta m_t^4 m_b^4 m_s^2}{\alpha_s^2 (m_s^2 + s_2^2 m_b^2)} \sim 10^{-15} \quad (2.6)$$

which is not analytic in Yukawa coupling constants. More recently, in [45] it was observed that for some processes occurring in the hot plasma, Yukawa interactions cannot be treated as a perturbation neither in the unbroken nor in the broken phase due to mixing effects, so that the formal argument leading to the estimate (2.5) does not hold.

Evidently, the dependence on mixing angles and quark masses is much more complicated than in⁸ Eq. (2.4).

It is interesting to note that the expression for ϵ contains *no* dependence on the charge $-1/3$ quark masses. How then does CP violation disappear when $m_d = m_s$? If the d and s quarks were degenerate in mass, then kaons and pions would be degenerate, and the expression for mixing between particles and antiparticles would contain box diagrams connecting, e.g., $d\bar{d}$ with $d\bar{s}$ pairs, etc., in such a way that the sum would vanish (GIM cancella-

⁸Sometimes it is said that any CP -violating quantity, in particular the BAU, must be proportional to d_{CP} since it has a basis-invariant representation, the “Jarlskog determinant” [49]. This reasoning is incorrect, however, because d_{CP} is not the only CP -violating quantity with a basis-independent representation. Indeed ϵ itself, given in a particular basis in Eq. (2.7), provides an example of a quantity besides d_{CP} with a basis-independent representation, as is obvious since it is a physical observable.

tion). While it is surely true that CP violation must disappear if any pair of like-charge quarks is degenerate in mass, we see from this example that this does not mean that CP -violating quantities are manifestly proportional to all pairs of mass-squared differences. The first term in a Taylor expansion in mass-squared differences may be a very poor representation of the dependence on masses, for physically relevant values of masses.

We can draw two lessons for cosmology from the kaon example. First, one should look for a process involving some small energy scale so that perturbative expansion in the quark masses does not work. This scale should be of the order of the strange quark mass or less, since otherwise the contribution from the strange quark will tend to cancel the d -quark contribution. Second, the analysis must be concrete and based on some specific mechanism, otherwise one cannot know which scale is relevant.

There are many different energy scales at high temperatures. We shall argue that the most important of them (from the point of view of CP violation) may be the thermal momenta p of the quarks. While the typical momentum in the heat bath is of the order of the temperature, some fraction of the particles carry much smaller momenta and, for them, CP violation can be substantial. In order to make a real calculation of the effect, one must choose a mechanism for baryogenesis. In the next section we discuss some of them, and make a rough estimate of the asymmetry which can be generated in a particular one.

III. OVERVIEW OF MSM BARYOGENESIS

A number of schemes for baryogenesis at the electroweak scale have been suggested [16, 21, 22, 26, 25, 52, 53], [27–29, 31–34, 30, 54] (see also reviews [10, 55, 11, 9, 13, 12]). These mechanisms rely heavily on the dynamics of the first order phase transition [17, 57, 58] during the spontaneous breaking of the $SU(2)_C \times U(1)$ gauge symmetry, which is assumed to occur through the nucleation of bubbles of the new phase, at a temperature of about 100 GeV. Inside the bubbles, the vacuum expectation value (VEV) of the Higgs field is nonzero and assumed to be large enough that anomalous processes with B violation are switched off. However in the high temperature phase outside the bubbles, the electroweak symmetry is unbroken and the rate of B -violating sphaleron reactions is high, so that a net baryonic number density cannot be maintained. Hence baryogenesis must be related to the presence of the bubble wall.

Roughly speaking, the mechanisms for EW baryogenesis can be divided into two categories. In the first category [26, 52, 53, 27–29], nontrivial configurations of the gauge and/or Higgs fields (sphalerons or thermal fluctuations) are supposed to have CP -violating interactions with the moving domain wall, biasing the anomalous B -nonconserving processes in such a way that net fermionic number is produced when these field configurations decay. In the second class of mechanisms (“charge transport baryogenesis” [31, 32]), CP -noninvariant interactions between fermions and the bubble wall lead to a separa-

tion of some CP -odd charge by the bubble wall, which is then converted to an asymmetry in the baryonic number by sphaleron processes in the unbroken phase.

In Ref. [45], one of us [MS] observed that if the CP violation in the interaction of thermal quarks with the bubble wall in the Higgs field is strong enough, it could result in a direct separation of baryonic number in the second type of mechanism mentioned above, without the need for separation of a surrogate CP -odd charge. Baryons⁹ inside the bubble survive till the present time because the rate of B -violating reactions is (required to be) highly suppressed in the broken phase, while the anti-fermions outside the bubble (partially) disappear through equilibrium B -violating reactions.

In this paper we will elaborate this mechanism [33, 45] in more detail and compute the baryonic asymmetry in it in the framework of the MSM. This does not mean that we insist that this mechanism is the best one; others should be investigated as well. However this is a good first case, since the MSM CP -violation effects can be explored in a very simple and physically transparent way. If the wall is thin, as suggested by recent work [44], this is likely to be the dominant mechanism. The most important new element of the present work is the understanding of how the GIM cancellation, present when quarks are taken to have typical thermal momenta, can be circumvented in particular regions of momenta. One such relevant region of momentum is identified and its contribution is estimated. Presumably in the other mechanisms there may be a similar failure of the GIM cancellation when the relevant regions of momenta are treated sufficiently accurately.

Reference [45] both noted the importance of including thermal interactions with gauge and Higgs particles in the plasma, and proposed a specific mechanism for producing the asymmetry. While our work here is a natural extension of that work, it differs in several important ways. In Ref. [45] the asymmetry in reflection probabilities of quarks and antiquarks was estimated, taking a contribution near the top quark reflection threshold (the dominant region of phase space) and conjecturing that $O(\alpha_s)$ loop effects would produce phases which would cause the net asymmetry to be nonvanishing. In this paper we identify a mechanism which evades the GIM cancellation without invoking loop effects, and really calculate the asymmetry in reflection probabilities. We use a purely quantum mechanical treatment of the scattering, noting that the ordinary scattering phase shift provides the nontrivial CP -conserving phase needed to interfere with the CP -violating phase to give a difference in reflection probabilities between quarks and antiquarks. Our treatment of the fermionic excitations in the hot medium is more exact than that of [45] because we include some loop effects in the broken phase [45] which are necessary to get a quantitatively accurate result. In this paper

⁹As opposed to antibaryons, on account of the known sign of the present asymmetry.

we also relate the asymmetry in reflection probabilities to the final baryonic asymmetry by studying the baryon number diffusion in the vicinity of the bubble wall (Sec. V).

IV. ROUGH ESTIMATE OF THE BAU FROM MSM CP VIOLATION

We have $n_B/s \sim [J_{CP}][f_{sph}]/[\text{entropy}]$, where J_{CP} is the baryonic separation current produced by quark interactions with the wall and f_{sph} is the sphaleron efficiency in removing the antibaryon excess in the unbroken phase. Before going to the technical details of the full calculation in the latter portions of this paper we give a qualitative discussion of CP violation in quark scattering from the domain wall, ignoring higher order corrections in α_s . This will permit us to estimate the left baryonic current, J_{CP} .

Some difference in reflection probabilities between quarks and antiquarks is possible due to the interference between the CP -violating phase in the coupling of the thermal quarks¹⁰ to the bubble wall, which changes sign in going from quarks to antiquarks, and the ordinary (CP -conserving) scattering phase shift, which is the same for quarks and antiquarks and is nonvanishing even when $\delta_{CP} = 0$. However how can we expect to “evade” the GIM cancellation which lies at the heart of the conventional argument that CP violation from the CKM matrix is far too small to account for the observed baryonic asymmetry? Evidently, an important variable for the scattering problem is the momentum of the particle perpendicular to the bubble wall, p . The other essential scales are the mass, M , of the particle and the inverse thickness of the wall, a . The component of the momentum parallel to the wall is conserved in the scattering process and is unimportant in a qualitative discussion¹¹.

Let us discuss first the most typical situation, when $p \sim T$, $p \gg M$, and $p \gg a$. Then the interaction of fermions with the domain wall is suppressed semiclassically by the factor $\exp(-\pi p/a)$. According to several estimates [40, 41] $a \sim T/(40 - 10)$, so that for typical quark momenta in the plasma, $p \sim T$, the light fermions do not scatter off the wall at all. The only reflection coefficient which can be significantly different from zero is that for the t quark. It is clear, according to the discussion in Sec. II, that for this region of phase space one cannot expect any non-negligible CP -violating effect. If the domain wall is very thin ($p/a \ll 1$), the reflection amplitude is suppressed only by Yukawa coupling constants rather than by the exponential factor. Nevertheless, for $p \sim T$ the light quarks are effectively degenerate due

to the tiny difference between their masses as compared to their typical momenta, so that their contributions to the net separation of baryon number, when summed over all generations, cancel nearly perfectly due to the GIM mechanism. That is, even if the phase in the CKM matrix means, say, that a d is more likely to reflect than a \bar{d} , this contribution to the baryonic asymmetry will be nearly perfectly compensated by, say, the \bar{s} being more likely to reflect than the s , with the cancellation being perfect if $m_s = m_d$. In this region the “conventional wisdom” reasoning is correct.

Let us consider now the region of phase space in which the momentum perpendicular to the wall is low enough that the interactions of the s quark with the bubble wall are strong and its reflection coefficient does not contain any powers of Yukawa coupling constants. Roughly, we have

$$J_{CP} \sim [\text{fraction of phase space}] \times [\text{asymmetry of fluxes}] \times [CP \text{ violation}] \times [\text{dynamical details}].$$

The breaking of the GIM cancellation is most profound in the region of the thermal spectrum in which the s and \bar{s} are totally reflected, but the d and \bar{d} are partially reflected and partially transmitted. The fraction of phase space corresponding to this situation is of order $\frac{m_s - m_d}{T}$, so that CP violation vanishes when $m_s = m_d$, as required.

Another important factor arises because the contribution to the baryonic current coming from quarks incident from the two sides of the wall would exactly cancel if the Fermi distributions on the two sides of the wall were the same. How the distributions near the wall differ from the equilibrium distribution is not yet understood due to uncertainties in the physics of bubble propagation and interaction with the quarks. However just from the motion of the thermal medium with respect to the wall, the flux in the wall rest frame of particles of a given energy incident from the unbroken phase is generally greater than the flux incident from the broken phase, producing an asymmetry even for equilibrium distributions. The asymmetry in the fluxes is thus expected to be $\gtrsim 2v(p/T)n_F(1 - n_F)$ for small wall velocity v but less than $\sim n_F$, as it would be if the wall carried along all the quarks ahead of it, eliminating the flux from the broken phase.

The natural measure of CP violation is just $J \equiv \sin(\theta_{12}) \sin(\theta_{23}) \sin(\theta_{13}) \sin(\delta_{CP})$. Global fits to determine CKM parameters place J in the range [59] $(1.4 - 5.0) \times 10^{-5}$. Of course, there will be a further dependence on quark masses and dynamical details, but this can give us a very rough estimate to use as a guide for our expectations. The analogous estimate of ϵ is just J , so that for the kaon system the dynamics increases the ratio of CP -violating to CP -conserving rates by a factor of ~ 100 . An explicit analytic expression for the additional quark mass and other dynamical dependence under certain conditions is given in Sec. VIII.

Putting together the factors above and dividing by the entropy density, $s = 2\pi^2 N_{\text{eff}} T^3/45$, where $N_{\text{eff}} \sim 100$ is the total number of particle degrees of freedom, one anticipates a baryon asymmetry of order

¹⁰By working with the quasiparticles of the high temperature plasma, interactions with gauge and higgs particles are included and nontrivial CP violation is possible. See Sec. VI.

¹¹However parallel components play a nontrivial role in the dynamics, contrary to the $T = 0$ situation where no thermal medium breaks Lorentz invariance, and could be quantitatively significant, as discussed in Sec. X and Appendix E.

$$|n_b/s| \sim (3-9) \times 10^{-10} f_{\text{sph}} f_{\text{dyn}} f_{\text{flux}}, \quad (4.1)$$

where f_{dyn} accounts for additional dynamical effects which will be included in a real calculation. Studies of the behavior of the expanding bubble wall suggest that v is in the range 0.1–0.9, so the flux asymmetry factor f_{flux} can range from $10^{-1}p/T$ to 1. For the one dimensional problem, total reflection of the quasiparticles occurs for $p/T \sim 10^{-1}$. We shall see in Sec. V that f_{sph} is estimated to lie in the range $\sim 10^{-4}$ –1. We see, then, that the CP violation present in the CKM matrix may be sufficient to account for the observed baryonic asymmetry of the Universe. In any case, the conventional estimate $\lesssim 10^{-21}$ must be discarded.

Predicting the sign of the asymmetry requires a quantitative calculation. As shall be seen from the results given in Sec. IX, the crude estimate given in this section is roughly correct in magnitude. Moreover the sign predicted by the quantitative calculation does agree with the observed positive sign, corresponding to an excess in our Universe of baryons rather than antibaryons.

Another region of phase space which *a priori* might seem interesting is that in which the c quark and antiquark are totally reflected, but the u 's are not. However since $c-u$ is not the most degenerate like-charge pair, lifting their degeneracy dynamically is less significant than for the $d-s$ pair. As could be expected and is borne out in our quantitative results, the near degeneracy of the $d-s$ quarks asserts itself in a reduction of the degree of asymmetry in the scattering of charge $+2/3$ quarks. We also note that regions in which only the heaviest quark is totally reflected, or none are totally reflected, do not make important contributions to the separation of baryon number, since in these regions the dynamics of the d and s quarks are essentially indistinguishable.¹²

This qualitative discussion can only be considered as a guide for a real calculation. To be more quantitative, we must examine in greater detail the mechanism of baryonic number separation by the domain wall, which requires finding the correct excitations in the hot plasma, then computing the reflection coefficients for their scattering off the domain wall. One thus determines the baryonic current which is produced by a flux of equal numbers of quarks and antiquarks on the domain wall, from either side. In the next section we imagine that this current is known and we investigate the connection between this baryonic current and the present-day n_B/s . After devoting Secs. VI and VII and a number of appendixes to developing the necessary technology to do the quantitative calculation, we report the results of this calculation in Sec. IX, confirming the heuristic estimates presented in this section.

¹²This can cease to be true when higher order corrections, which mix momentum scales and can generate phases which do not rely on total reflection, are included. Then it may happen that in the tradeoff between minimizing the GIM cancellation and maximizing the volume of phase space, another region can be more important.

V. BARYONIC NUMBER SEPARATION AND BARYONIC ASYMMETRY

The interactions of thermal quarks and antiquarks with the domain wall are CP -noninvariant. Nevertheless, unitarity and CPT constraints relate different transition amplitudes in such a way that the net current of any C - or CP -odd number vanishes in thermal equilibrium (see Sec. VII and [33]). Of course, there is nothing surprising in this, since it would be too naive to expect BAU generation in thermal equilibrium in any mechanism.

A first order EW phase transition, however, provides a deviation from thermal equilibrium. In our case the important manifestation is in the movement of the domain wall. Because of the interaction with the medium, the domain wall is expected to move with a constant velocity, which is estimated [60, 40, 41, 61] to be $v \sim 0.1$ –0.9. Thus in the wall rest frame there is a net flux of particles and almost equal flux of antiparticles¹³ flowing from the side of unbroken phase toward the side of broken phase. A crucial quantity for the mechanism of baryogenesis which we study is the *difference* between the fluxes on the two sides of the wall, viewed from the wall rest frame. This difference of fluxes depends on the extent to which the passage of the wall disturbs the equilibrium distributions of the quarks. Treatments of the problem [60, 40, 41, 61] based on a perturbatively calculated Higgs potential have envisaged a wall which is sufficiently thick compared to a mean free path that the equilibrium is approximately maintained. That is, the velocity and temperature of the medium is essentially the same on either side of the wall. We present below a calculation of $n_B(J_{CP})$ in this case. However recent work (cf., [44]) suggests that non-perturbative effects may cause the transition in the Higgs VEV to occur much more abruptly than previously imagined, opening the possibility that the quasiequilibrium assumption is a poor approximation. We will return to the consequences of this possibility below.

Let us go to the rest frame of the wall and assume that the medium going through it with velocity v has the same temperature inside and outside the bubble. Since fluxes from the two sides are unequal, the unitarity constraints do not apply and the asymmetry in reflection coefficients can produce a nonzero baryonic current J_{CP} (as well as currents of other C - and CP -odd quantities such as left and right baryonic numbers, J_{CP}^L and J_{CP}^R). If B -violating processes are in equilibrium in the unbroken phase but not in the broken phase, such currents imply the separation of baryonic number and other numbers.

For small v , we will have an approximately static situation in the wall rest frame, in which each of these currents, say J_{CP}^L , is balanced by an opposite current through the wall due to an excess of the appropriate density, in this case L baryonic density. Particle densities will depend on the temperature and velocity in the usual

¹³In the absence of CP violation the fluxes would be precisely the same.

way, but will contain chemical potentials for the various CP - and C -odd numbers which are nonvanishing in the broken phase. To determine these chemical potentials, one must solve the kinetic equations in the vicinity of the domain wall. We shall write the kinetic equations in a diffusive approximation, which is valid when the characteristic length scale of the density variation is large compared with the mean free path of the quarks. As will be seen *a posteriori*, this condition is satisfied if the velocity of the domain wall is not too large ($v \lesssim 0.3$), although it would be very nice to find the relation between J_{CP} and n_B/s also for large velocities.

Quarks and leptons take part in many processes on both sides of the wall with many different time scales. In order to decide which processes must be included in the equation describing diffusion, one needs to define a relevant time scale and then include processes taking place on shorter scales than that. Let us follow the evolution of a particle after it has been reflected from the domain wall toward the unbroken phase. Its typical distance from the bubble wall is given by

$$\sqrt{Dt} - vt, \quad (5.1)$$

where the first term describes the random walk of the particle in the rest frame of the plasma (D is the diffusion coefficient for the particle of interest) and the second term describes the motion of the bubble wall. This particle will be trapped by the bubble after a time $t_D \sim D/v^2$, so one can neglect any process with a characteristic time $\tau \gg t_D$. (Of course, B violation must be included in any case, since if it is absent, no baryonic asymmetry can be produced.) The characteristic diffusion time t_D is much smaller than the time scale of the chirality breaking $L - R$ transitions coming from inelastic scatterings with Higgs particles, since those are suppressed by small Yukawa coupling constants.¹⁴ However the QCD sphaleron produces $L - R$ transitions at rate $\sim \frac{8}{3} \left(\frac{\alpha_s}{\alpha_w}\right)^4 \sim 300$ times larger than the EW sphaleron rate [62]. Thus even though the EW sphaleron only couples to L chiral particles and antiparticles, on account of the action of the QCD sphaleron, we can simply discuss the total baryonic number, with small modifications in the diffusion equations as compared to the case without the QCD sphaleron.

Let $n_B(x, t)$ and $n_L(x, t)$ be the densities of baryonic and leptonic numbers in the rest frame of the wall. We place the wall at $x = 0$ and take $x > 0$ to be the broken phase where sphaleron processes are switched off. Then the diffusion equations are, for $x > 0$,

$$\frac{\partial}{\partial t} \begin{pmatrix} n_B \\ n_L \end{pmatrix} = \begin{pmatrix} D_B \frac{\partial^2}{\partial x^2} - v \frac{\partial}{\partial x} & 0 \\ 0 & D_L \frac{\partial^2}{\partial x^2} - v \frac{\partial}{\partial x} \end{pmatrix} \begin{pmatrix} n_B \\ n_L \end{pmatrix}, \quad (5.2)$$

¹⁴Except for t quarks, however this can be neglected since the asymmetry resides in the charge $-1/3$ quark sector.

but for $x < 0$ we have

$$\frac{\partial}{\partial t} \begin{pmatrix} n_B \\ n_L \end{pmatrix} = \begin{pmatrix} D_B \frac{\partial^2}{\partial x^2} - v \frac{\partial}{\partial x} - \frac{3}{2}\Gamma & -\Gamma \\ -\frac{3}{2}\Gamma & D_L \frac{\partial^2}{\partial x^2} - v \frac{\partial}{\partial x} - \Gamma \end{pmatrix} \begin{pmatrix} n_B \\ n_L \end{pmatrix}, \quad (5.3)$$

where $\Gamma = 9\Gamma_{\text{sph}}/T^3$ and Γ_{sph} is the rate of sphaleron transitions per unit time and volume. (The relation between the rate of B violation and the sphaleron rate can be found in Refs. [23, 63].) D_B and D_L are diffusion constants for quarks and leptons, respectively.¹⁵

These equations must be supplemented by a number of boundary conditions. At $x \rightarrow -\infty$ (the unbroken phase far from the domain wall), n_B and $n_L \rightarrow 0$ because we are considering the case that the BAU does not exist prior to the EW phase transition. At $x \rightarrow +\infty$, n_B and n_L must be finite. The other boundary conditions are specified at $x = 0$; we will discuss them later.

We will assume that the velocity of the domain wall is low enough that some “steady state” solution to the kinetic equation can be established.¹⁶ In other words, in the rest frame of the domain wall the densities of particles are time independent. For $x > 0$ the only solutions consistent with the boundary conditions are constants:

$$n_B(x) \equiv B_+, \quad n_L(x) \equiv L_+. \quad (5.4)$$

For $x < 0$ they have the form

¹⁵According to the argument of Ref. [64], any kinetic equation written in terms of *bare particles* should also contain non-trivial corrections associated with Debye screening of the hypercharge. These corrections, however, are absent for Eqs. (5.2) and (5.3) describing quasiparticles. Precisely on account of the Debye screening phenomenon, quasiparticles do not carry hypercharge or any other gauged quantum number, while they can have nonzero global numbers like baryonic number and flavor. A physical excitation in the high temperature plasma with the global quantum numbers of a left quark would, for instance, be actually composed of a left chiral quark, gluons, electroweak gauge bosons, and Higgs bosons, such that it is actually an $SU(3) \times SU(2) \times U(1)$ singlet. This is discussed further in Sec. XD. Of course, the baryonic charges of quasiparticles differ from the baryonic charges of the bare particles. This fact is automatically taken into account in our approach, since we define the various currents in terms of quasiparticles (see Sec. VI). We thank S. Khlebnikov for a discussion of this point.

¹⁶Actually, this is only in order to enable us to solve the problem relatively simply. If the velocity is larger, the effects are presumably larger, but since we find an interesting level of asymmetry even in this very conservative approximation, we do not attempt to extend the treatment to large velocities. That is an interesting and important subject to develop, however.

$$\begin{pmatrix} n_B \\ n_L \end{pmatrix} = \sum C_i \xi_i \exp(k_i x), \quad (5.5)$$

where C_i are arbitrary constants, and ξ_i and k_i are eigenvectors and eigenvalues to be found from the condition

$$\begin{pmatrix} D_B k_i^2 - v k_i - \frac{3}{2}\Gamma & -\Gamma \\ -\frac{3}{2}\Gamma & D_L k_i^2 - v k_i - \Gamma \end{pmatrix} \xi_i = 0. \quad (5.6)$$

One of the eigenvalues, say k_4 , is zero independently of the parameters. It corresponds to a nonzero density of the conserved number ($B-L$), so we put $C_4 = 0$. One can show that two other eigenvalues k_1 and k_2 have positive real part and the third one k_3 is real and negative. The latter corresponds to a growing exponent as $x \rightarrow -\infty$ and is therefore not consistent with the boundary conditions. Hence, $C_3 = 0$. All three nonzero roots can be found analytically. They are solutions of the cubic equation

$$D_B D_L k^3 - v(D_L + D_B)k^2 - (D_B \Gamma + \frac{3}{2}D_L \Gamma - v^2)k + \frac{5}{2}v\Gamma = 0. \quad (5.7)$$

We shall write down here the relevant roots (k_1 and k_2) in two limiting cases, when the dimensionless quantity $3D_B \Gamma/v^2$ is small or large.

(i) $3D_B \Gamma/v^2 \ll 1$. Then

$$k_1 = \frac{v}{D_B} \left(1 + \frac{3\Gamma D_B}{2v^2} \right), \quad (5.8)$$

$$k_2 = \frac{v}{D_L} \left(1 + \frac{\Gamma D_L}{v^2} \right), \quad (5.9)$$

$$\xi_1 = \begin{pmatrix} 1 \\ \frac{3\Gamma D_B^2}{2v^2 D_L} \end{pmatrix}, \quad \xi_2 = \begin{pmatrix} -\frac{\Gamma D_L}{v^2} \\ 1 \end{pmatrix}. \quad (5.10)$$

(ii) $3D_B \Gamma/v^2 \gg 1$. Then

$$k_1 = \frac{5v}{3D_L}, \quad (5.11)$$

$$k_2 = \sqrt{\frac{3\Gamma}{2D_B}} + \frac{v}{2D_B}, \quad (5.12)$$

$$\xi_1 = \begin{pmatrix} 1 \\ -\frac{3}{2} \end{pmatrix}, \quad \xi_2 = \begin{pmatrix} 1 \\ \frac{D_B}{D_L} \left(1 - \frac{v\sqrt{2}}{\sqrt{3\Gamma D_B}} \right) \end{pmatrix}. \quad (5.13)$$

In these expressions we have approximated $D_L \gg D_B$, since leptons do not have strong interactions.

In order to define matching conditions at $x = 0$, one has to find the total currents for baryonic and leptonic number at $x = 0$. Let us denote the densities of baryonic and leptonic numbers next to the domain wall, in the unbroken phase, by B_- and L_- . Then, in the absence of CP -violating effects, the baryonic and leptonic currents flowing through the wall toward positive x would be, respectively,

$$j = \kappa(B_- - B_+) - \frac{1}{2} \left(D_B \frac{\partial(B_+ + B_-)}{\partial x} - v(B_+ + B_-) \right) \quad (5.14)$$

and

$$l = \kappa(L_- - L_+) - \frac{1}{2} \left(D_L \frac{\partial(L_+ + L_-)}{\partial x} - v(L_+ + L_-) \right). \quad (5.15)$$

The factor κ connects the density in a box to the current flowing through one side of the box. Essentially all quarks are relativistic, including those which are responsible for our effect which have small momentum perpendicular to the domain wall, because even these typically have large parallel momenta. Thus we have simply

$$\kappa = \frac{\int_0^{\frac{\pi}{2}} \cos \theta d \cos \theta}{\int_0^{\pi} d \cos \theta} = \frac{1}{4}. \quad (5.16)$$

In addition to the above currents arising from nonuniformities in particle densities, there is an additional contribution to the baryonic current due to the CP violation present in the interaction of quarks scattering from the bubble wall, denoted J_{CP} . There is no such contribution to the leptonic current, since CP is conserved in the leptonic sector due to the masslessness of the neutrinos. Altogether we have then, for the baryonic and leptonic currents,

$$J_B = j + J_{CP}, \quad J_L = l. \quad (5.17)$$

Current continuity implies that the currents through the wall are equal to those in the broken phase where there is no B or L violation. The currents in the broken phase are just due to the bulk transport of the charge densities with velocity v , so that

$$J_B = vB_+, \quad J_L = vL_+. \quad (5.18)$$

Next equate the currents flowing into the unbroken phase to the total rate of quantum number nonconservation due to sphaleron transitions:

$$-vB_+ = -vL_+ = \int_{-\infty}^0 \Gamma \left(\frac{3}{2}n_B + n_L \right), \quad (5.19)$$

which in turn satisfies

$$\begin{aligned} \int_{-\infty}^0 \Gamma \left(\frac{3}{2}n_B + n_L \right) &= D_B \frac{\partial B_-}{\partial x} - vB_- \\ &= D_L \frac{\partial L_-}{\partial x} - vL_- \end{aligned} \quad (5.20)$$

because we require a static solution to (5.3).

From Eqs. (5.18)–(5.20) we learn $\frac{\partial L_-}{\partial x} = -v(L_+ - L_-)/D_L$, which when combined with Eqs. (5.15), (5.17), and (5.18) implies $\frac{\partial L_-}{\partial x} = 0$. Thus $L_+ = L_-$ and $\frac{C_2}{C_1} = -\frac{\xi_{21} k_1}{\xi_{22} k_2}$. Similarly $B_+ - B_- = J_{CP}/\kappa$; when combined with $B_+ = L_+$ this gives an equation relating C_1 and C_2 to J_{CP}/κ . Thus the baryonic number density inside the bubble

$$B_+ = \frac{3}{5\kappa} J_{CP} f_{\text{sph}}(\rho), \quad (5.21)$$

with $\kappa \sim 1/4$ [Eq. (5.16)], $\rho = \frac{3D_{\text{eff}}\Gamma}{v^3}$ and

$$f_{\text{sph}}(\rho) = \frac{5}{3} \frac{k_2 - k_1}{k_2(1 - \xi_{11}/\xi_{21}) - k_1(1 - \xi_{12}/\xi_{22})}. \quad (5.22)$$

ξ is the matrix whose first and second columns are the eigenvectors corresponding to eigenvalues k_1, k_2 , respectively, defined by Eq. (5.6). For $\rho \gg 1$, $f_{\text{sph}}(\rho) = 1$ and for $\rho \ll 1$, $f_{\text{sph}}(\rho) = \frac{5}{6}\rho$. The physical importance of ρ is clear, since it represents the typical number of sphaleron transitions to which a quark is exposed between the time it enters the unbroken phase and the characteristic time at which the bubble of low temperature phase envelops it. Baryonic number density vanishes when baryon-number violation is effectively turned off, i.e., $\rho \rightarrow 0$. It also vanishes in thermal equilibrium, as required, since $J_{CP} = 0$ when $v = 0$. B_+ is the net baryon number density in the low temperature phase which, when divided by entropy, gives the desired asymmetry, n_B/s .

We remind the reader that the relation of Eq. (5.21) is valid in a quasiequilibrium approximation, and provides a lower limit for a more general situation. For instance, if all the quarks were carried along in front of the wall, the sphaleron rate would not matter at all, as long as it is large compared to the expansion rate of the Universe.

The next sections are devoted to determining J_{CP} .

VI. FERMIONIC EXCITATIONS IN THE HOT PLASMA AND CP VIOLATION

At zero temperature and omitting loop effects, the interaction of quarks with a (neutral) domain wall would be C and CP conserving.¹⁷ Indeed, the Lagrangian \mathcal{L} [see Eq. (2.1)] is CP and C invariant for any x dependent Higgs VEV of the form

$$\phi = (0, v(x)), \quad (6.1)$$

if all the gauge fields are zero. In other words, the separation of any C -odd or CP -odd quantum number is not possible in this approximation.

An even more general statement is true: as long as the Lagrangian for quarks has the form

$$\mathcal{L} = i\bar{L} \not{D}L + i\bar{R} \not{D}R + \bar{L}M(x)R + \text{H.c.}, \quad (6.2)$$

where $M(x)$ is an arbitrary mass matrix and the operator \mathcal{D} is the same for L and R terms, C is not violated. Since C relates the left quark to the right antiquark, the

reflection coefficients will be the same for left quark as for right antiquark and separation of baryonic number (which is odd under C) is not possible. However chiral currents such as axial quark number, $\bar{\Psi}\gamma_\mu\gamma_5\Psi$, are C even but CP odd, so that they *can* be produced by this Lagrangian, as long as it violates CP . Several extensions of the standard model have been developed in Refs. [31–33] making use of this fact to produce a BAU in the electroweak phase transition.

The case of *nonzero* temperatures is quite different. In the high temperature plasma, quarks and antiquarks interact incessantly. Each flavor and chirality of quark has a distinct interaction with the Higgs particles in the heat bath, lifting the degeneracy between them. Interactions with $SU(2)$ gauge bosons further split L and R chiralities, and even their common interaction with gluons is dynamically important since it affects their propagation. As is well known, it is essential to work in the correct basis of particle states. In standard perturbation theory one simply takes the quadratic part of the Lagrangian and finds particle states for it. At zero temperatures and densities this usually is successful for theories with small coupling constants, since higher order corrections are small. Fermion masses, for instance, receive corrections of the form $f^2 m_f$, where f is a Yukawa coupling constant. The high order correction are small if $f \ll 1$. However, at high enough temperatures and densities, naive perturbation theory fails even for theories with small couplings. The reason is that at high temperatures an additional dimensionful parameter appears, namely the temperature T itself. Corrections to masses can be large when the product of Yukawa coupling and temperature is comparable to the zero temperature mass. In more physical language this means that the particles appearing in the tree Lagrangian are not the actual particle excitations of the problem under consideration. There are many examples known from condensed matter and statistical physics in which particle excitations have little in common with the fundamental particles: phonons, sound waves, plasmon excitations, etc.

In order to find physical excitations one usually constructs the effective Lagrangian for the theory incorporating high temperature and/or high density effects, and then determines a better set of fields for doing perturbation theory. This problem is not very well-defined mathematically, since it is not clear precisely what the word “better” means. In practice, one usually calculates all mass operators of the theory and constructs fields corresponding to the poles of “exact” propagators (usually defined as an infinite sum of some subset of graphs). One gets in this way the properties of one-particle excitations of the medium and can consider the interactions between them, which will be, hopefully, weak enough. Of course, if one would be able to solve the problem exactly, the choice of variables would not matter at all. However, since we are confined to using perturbation theory for most problems, the starting approximation is very important.

Although we can solve the quantum mechanical problem of quarks scattering from the domain wall of Higgs VEV without the use of perturbation theory, we still

¹⁷The reason that loop corrections modify the assertion that C is not violated is that they involve interactions of the quarks with charged as well as neutral components of the Higgs doublet. Furthermore, the EW gauge interaction distinguishes between L and R in the covariant derivative, providing yet another source of C violation.

must be careful in our choice of particle states, in order to be able to ignore the (most significant) interactions of the particles with the heat bath during the course of their propagation through the domain wall. That is, we must determine what happens with the *fermionic excitations of the plasma* when they go through the domain wall. First, we have to define them far from the domain wall: outside the bubble, where the symmetry is unbroken, and inside, where it is broken.

Quite an extensive literature exists on the fermionic excitations in a hot plasma. For the reader's convenience we will partially summarize what is known about them from the literature, and then describe some additional properties which, as far as we know, are not discussed in the literature elsewhere. We work to one-loop accuracy in the quasiparticle propagators. This has the physical consequence of neglecting inelastic scattering of the quasiparticles, which may not be an adequate description of the problem, but is at least a first step. Improving this approximation is quite nontrivial for a number of reasons. For further discussion see Sec. XD.

A. Unbroken phase

Fermionic excitations correspond to the poles of quark propagators at high temperature. For a review see, e.g., Ref. [65]. We work in Minkowski space and use the following convention for the tree level Dirac operators:

$$\Sigma_{L,R}^0 = \omega \pm \vec{\sigma} \cdot \vec{p} \quad (6.3)$$

with $\omega > 0$ for particles and $\omega < 0$ for antiparticles, σ_i are the usual Pauli matrices. Then, in high temperature approximation (ω and $|p| \ll T$) the one loop fermionic mass operator in the gauge basis for the unbroken symmetry phase is [66, 67]

$$\Sigma_{L,R}^u(\omega, \vec{p})$$

$$= \Omega_{L,R}^2 \left\{ \pm \frac{\vec{\sigma} \cdot \vec{p}}{p^2} \left[1 - F\left(\frac{\omega}{p}\right) \right] - \frac{1}{\omega} F\left(\frac{\omega}{p}\right) \right\}, \quad (6.4)$$

where

$$F(x) = \frac{x}{2} \left[\ln\left(\frac{x+1}{x-1}\right) \right]. \quad (6.5)$$

Note that Lorentz invariance is broken because the plasma rest frame provides a preferred frame. For the left quarks,

$$\Omega_L^2 = \frac{2\pi\alpha_s T^2}{3} + \frac{3\pi\alpha_W T^2}{8} \left(1 + \frac{\sin^2 \theta_W}{27} + \frac{1}{3} \frac{(M_u^2 + KM_d^2 K^\dagger)}{M_W^2} \right). \quad (6.6)$$

For the right quarks with charge $+2/3$,

$$\Omega_R^2 = \frac{2\pi\alpha_s T^2}{3} + \pi\alpha_W T^2 \frac{2\sin^2 \theta_W}{9} + \frac{\pi\alpha_W}{8} M_u^2 \frac{T^2}{M_W^2}, \quad (6.7)$$

and for the right quarks with charge $-1/3$,

$$\Omega_R^2 = \frac{2\pi\alpha_s T^2}{3} + \frac{\pi\alpha_W T^2 \sin^2 \theta_W}{2 \cdot 9} + \frac{\pi\alpha_W}{8} M_d^2 \frac{T^2}{M_W^2}, \quad (6.8)$$

where the first and the second terms come from the gluon and weak gauge boson corrections, respectively, and the last term comes from Higgs boson exchange.

An important point is that in spite of the fact that the vacuum expectation value of the Higgs field is zero, particle excitations in the unbroken phase are some specific mixture of the initial fields. The physical fermionic fields (denoted by the bold letters) are three component spinors in flavor space,

$$\mathbf{L} = O \Psi_{Q_L}, \quad \mathbf{U} = \Psi_{U_R}, \quad \mathbf{D} = \Psi_{D_R}, \quad (6.9)$$

where the unitary matrix O diagonalizes the matrix Ω_L^2 :

$$O \Omega_L^2 O^\dagger \equiv \omega_L^2 = \text{diag}. \quad (6.10)$$

Since $M_u \gg M_d$ the matrix O is close to one. In the right sector the mixing is absent and we will use the notation

$$\Omega_R = \omega_{U,D}. \quad (6.11)$$

We use ω_0 to represent any one of the $\omega_{L,R}$. The dispersion relation for physical excitations has the form

$$\left(\left[\omega - \frac{\omega_0^2}{\omega} F\left(\frac{\omega}{p}\right) \right]^2 - \left\{ p + \frac{\omega_0^2}{p} \left[1 - F\left(\frac{\omega}{p}\right) \right] \right\}^2 \right) = 0. \quad (6.12)$$

For each chirality, there are two solutions to this dispersion relation. For small momenta the spectra are

$$\omega^2(p)_\pm = \omega_0^2 \left(1 \pm \frac{2}{3} \frac{p}{\omega_0} + \frac{7}{8} \frac{p^2}{\omega_0^2} + \dots \right), \quad (6.13)$$

while for high momenta, $p \gg \omega_0$, we have

$$\omega^2(p)_+ = p^2 + 2\omega_0^2 - \frac{\omega_0^4}{p^2} \ln \frac{p^2}{\omega_0^2}, \quad (6.14)$$

$$\omega^2(p)_- = p^2 \left[1 + 4 \exp\left(-2\frac{p^2}{\omega_0^2} - 1\right) \right].$$

The dependence of energy on p is shown in Figs. 1 and 2 for the strange and bottom quarks, in the approximation of neglecting mixing.¹⁸ Unlike the situation at zero temperature, the eigenstates are split due to their differing interaction with Higgs particles in the plasma, even when the VEV vanishes. Moreover at every energy there are two distinct collective excitations having different momenta. This phenomenon is analogous to photon excitations in the plasma: in addition to the usual transverse

¹⁸There is no visible difference between the strange and down quark dispersion relations on the scale of these figures, but it is nonvanishing.

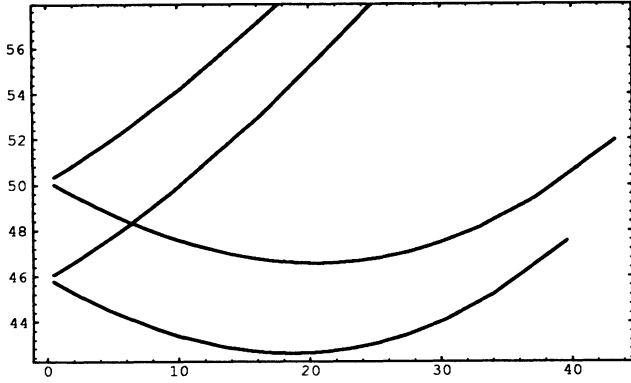


FIG. 1. Dispersion relation for s quarks in the unbroken phase, neglecting mixing. The figure is essentially identical for the broken phase, except for the neighborhood of the crossing.

excitations, a longitudinal one also occurs. We will call the mode labeled + (−) normal (abnormal), respectively. Note the mass gap which these solutions exhibit. It does not contradict the chiral invariance of the underlying Lagrangian, but is connected with the breaking of Lorentz invariance at nonzero temperatures [66, 67]. Higher order corrections to these dispersion relations have been studied in a number of papers [68, 69]. It was shown in [68] that the abnormal branch is actually unstable at momenta $p > gT$.

The knowledge of the Dirac operator allows us to construct the effective Lagrangian for the fermionic excitations in the plasma. Let us take for definiteness left chiral fermions and consider one fermionic flavor.¹⁹ Then, the effective Lagrangian is

$$\mathcal{L}_{\text{eff}} = L^\dagger(\Sigma_L^0 + \Sigma_L^4)L. \quad (6.15)$$

To become more familiar with the properties of the various excitations, let us study them first for small mo-

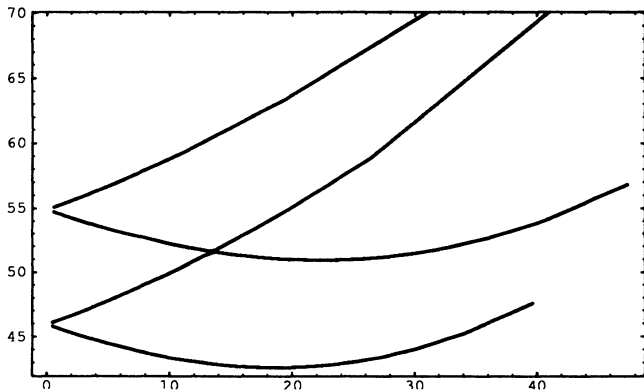


FIG. 2. Dispersion relation for b quarks in the unbroken phase, neglecting mixing.

¹⁹The treatment of right chiral fermions and multiple flavors is completely analogous.

menta p . As we shall see later, reflection amplitudes for particles are most substantial in this kinematic range. At small momenta [see Eq. (6.13)] the energies of the fermions are close to the mass gap, ω_0 . Expanding the Dirac operator for small p and small $\omega - \omega_0$ one obtains a linearized version of the Lagrangian:

$$\mathcal{L}_{\text{eff}} = 2iL^\dagger(\partial_0 - \frac{1}{3}\vec{\partial}\vec{\sigma} + i\omega_0)L. \quad (6.16)$$

One can define in the usual way creation and annihilation operators for the normal (a_n^\dagger, a_n) and abnormal (a_a^\dagger, a_a) excitations, so that the part of the field L which annihilates particles can be decomposed as²⁰

$$L(x) = \frac{1}{\sqrt{2}} \int \frac{d^3k}{(2\pi)^3} [a_n^i(k)e^{-i\omega_+ t + ikx} u_i + a_a^i(k)e^{-i\omega_- t + ikx} v_i], \quad (6.17)$$

here the two-component spinors u and v obey the equations

$$(|k| + \vec{k} \cdot \vec{\sigma})u = 0, \quad (|k| - \vec{k} \cdot \vec{\sigma})v = 0, \quad (6.18)$$

and

$$\omega_\pm = \omega_0 \pm \frac{1}{3}|k|, \quad (6.19)$$

$$\{a(k), a^\dagger(k')\}_+ = (2\pi)^3 \delta(k - k').$$

From (6.18) one can see that the two branches have different relations between their chirality and their helicity. For the normal branch the chirality and helicity are equal while for the abnormal branch the helicity is opposite to the chirality.

In the same way one can construct the effective Lagrangian for the right chiral excitations. We do not write the corresponding equations for this case; they can be derived from the equations for the left particles using ω_0 corresponding to right quarks.

The direction of the group velocity of the abnormal excitation is opposite to the direction of \vec{k} , since from Eq. (6.13) the group velocities of the two branches ($v = \frac{\partial\omega}{\partial k}$) are

$$\vec{v}_+ = \frac{\vec{k}}{3|k|}, \quad \vec{v}_- = -\frac{\vec{k}}{3|k|}. \quad (6.20)$$

It is interesting and physically important that for both branches the magnitude of the group velocity $\rightarrow 1/3$ as the momentum vanishes. For large momentum, $k > \omega_0$, the group velocities of both branches $\rightarrow 1$, as can be found from Eq. (6.14).

The left baryonic current is

$$J^0 = \int \frac{d^3k}{(2\pi)^3} (a_n^\dagger a_n + a_a^\dagger a_a), \quad (6.21)$$

²⁰The part for creation of antiparticles is obtained by expanding the Lagrangian for small $\omega + \omega_0$.

$$J^i = \int \frac{d^3k}{(2\pi)^3} \frac{k^i}{3|k|} (a_n^\dagger a_n - a_a^\dagger a_a). \quad (6.22)$$

The minus sign in front of the abnormal mode contribution reflects the fact that the abnormal excitation moves in the opposite direction to \vec{k} .

We need to transform between the plasma rest frame and the wall rest frame.²¹ $(\omega(k), \vec{k})$ is a four-vector, so that the dispersion relation in the moving frame is easily obtained from the invariance of $(\omega(k), \vec{k}) \cdot (1, v)\gamma$. Denoting the wall rest frame variables by $(\omega(k), \vec{k})$ and the plasma-rest-frame energy by $\bar{\omega}$, we have $\bar{\omega} = \gamma(\omega - \vec{k} \cdot \vec{v})$, where \vec{v} is the velocity of the plasma with respect to the wall. Since the phase space volume is a Lorentz invariant, if we denote the Fermi distribution in the plasma rest frame by $n_F(\bar{\omega})$, then in the rest frame of the wall, where the plasma moves with velocity v normal to the wall, the number distribution is $n_F(\omega - \vec{k} \cdot \vec{v})$. Thus in the wall-rest-frame, particles with momenta in the direction of the plasma have a higher density than if the plasma were at rest with respect to the wall, as expected intuitively.

To give a simple example of the frame dependence of the dispersion relation, let us work in linear approximation so the plasma-rest-frame dispersion relation is given by Eq. (6.19), and let v be nonrelativistic. This gives

$$(\omega - vk_t) = \omega_0 \pm \frac{1}{3} \sqrt{k_\perp^2 + (k_t - v\omega)^2} \quad (6.23)$$

where k_t is the component of the momentum parallel to v (i.e., perpendicular to the domain wall) in the wall rest frame, and k_\perp is the orthogonal component. From here one obtains the dependence $\omega = \omega(k_\perp, k_t, v)$. Continuing with this simple example, and taking $k_\perp = 0$, one finds the relationship between ω and k in the wall rest frame, for the normal and abnormal excitations, respectively:

$$\omega_{n,a} = \omega_0 \left(1 \mp \frac{1}{3}v \right) \pm \frac{k_t}{3} \left(1 \pm \frac{2v}{3} \right). \quad (6.24)$$

From the definition of the current (6.22) and these considerations, we have for the flux factor in nonrelativistic

$$\int \frac{d^3k}{(2\pi)^3} \frac{n_F(\epsilon_F)}{\epsilon_F} \left\{ \frac{\pm \vec{\sigma} \cdot \vec{p}}{p^2} \left[1 - F \left(\frac{\epsilon_F \omega}{|p||k|} \right) \right] - \frac{1}{\omega} F \left(\frac{\epsilon_F \omega}{|p||k|} \right) \right\} + \int \frac{d^3k}{(2\pi)^3} \frac{n_B(\epsilon_B)}{\epsilon_B} \left\{ \frac{\pm \vec{\sigma} \cdot \vec{p}}{p^2} \left[1 - F \left(\frac{\epsilon_B \omega}{|p||k|} \right) \right] - \frac{1}{\omega} F \left(\frac{\epsilon_B \omega}{|p||k|} \right) \right\} \quad (6.30)$$

where the $+$ sign is for left fermions and $-$ for right ones, n_B and n_F are Bose and Fermi distributions, and

approximation, but now for a general dispersion relation and not just the linearized version:

$$\int \frac{d^3k}{(2\pi)^3} n_F \left(\frac{\omega - vk_t}{T} \right) \frac{\partial \omega}{\partial k_t}. \quad (6.25)$$

The formal expressions for the left fermionic current in terms of the effective fields will be

$$J_L^0 = L^\dagger \left(1 + \frac{\partial \Sigma_L^u}{\partial \omega} \right) L, \quad (6.26)$$

$$J_L^i = L^\dagger \left(\sigma_i + \frac{\partial \Sigma_L^u}{\partial p_i} \right) L, \quad (6.27)$$

and analogous relations for the right baryonic current.

B. Broken phase

In order to determine the properties of the fermionic excitations in the broken phase one has to calculate the Dirac operator, which now will be a matrix in the space of right and left fields. In the one loop high temperature approximation the Dirac operator is

$$\begin{pmatrix} \Sigma_L^0 + \Sigma_L^b & M \\ M^\dagger & \Sigma_R^0 + \Sigma_R^b \end{pmatrix}. \quad (6.28)$$

The mass term M is proportional to the scalar field VEV, and depends on whether one is considering the charge $+\frac{2}{3}(U)$ or $-\frac{1}{3}(D)$ sector:

$$M_U = \frac{2g_w M_u}{M_W} \phi, \quad M_D = \frac{2g_w K M_d}{M_W} \phi. \quad (6.29)$$

In high temperature approximation, one-loop corrections to the off-diagonal mass term describing left-right transitions, M , vanish.

In the broken phase electroweak gauge bosons and quarks have non-zero mass already in tree approximation so the one-loop contribution to the Dirac operators, $\Sigma_{L,R}^b$, of any diagram has the generic form

$\epsilon_{B,F}^2 = k^2 + m_{B,F}^2$ with $m_{B,F}$ denoting the appropriate bosonic or fermionic mass.

In comparison with the unbroken case, the Dirac operator in the broken phase has additional corrections of the type m_B/T and $m_F^2/T^2 \ln(T/m_F)$. Corrections of the first type do not influence quark mixing in the broken phase and are numerically small in comparison with the leading flavor independent terms. They reduce the W^\pm , Z^0 , and Higgs contribution to $\omega_{L,R}^2$ compared to the

²¹We thank G. Baym for pointing out an error in our original discussion of the following, and for calling our attention to Ref. [70], where a detailed discussion of the Lorentz transformation properties of quasiparticles can be found.

unbroken phase, causing the coefficient of the $\alpha_W \partial/\partial t$ term in Σ to be multiplied by the factor $1 - \frac{4M_B}{\pi T}$, where M_B is the relevant boson's mass at temperature T . The coefficient of the $\alpha_W \partial/\partial x$ term in Σ^u also receives a cor-

rection, however it is less important than the correction to the coefficient of ω since p/ω is $\sim 1/8$. Thus the net effect of these corrections can be described by replacing Eq. (6.6) for Ω_L^2 by

$$\Omega_L^{b,2} \approx \frac{2\pi\alpha_s T^2}{3} + \frac{3\pi\alpha_W T^2}{8} \left[\left(1 - \frac{4M_W}{\pi T}\right) + \frac{\sin^2 \theta_W}{27} + \frac{1}{3} \frac{(M_u^2 + KM_d^2 K^\dagger)}{M_W^2} \left(1 - \frac{4M_H}{\pi T}\right) \right]. \quad (6.31)$$

We have discarded the correction to the $\sin^2 \theta_W$ term because the correction is suppressed by an additional factor of $\sin^2 \theta_W$ since the photon does not get a mass. The difference between ω_R and ω_R^b can be discarded because the Higgs boson and EW gauge boson contributions there are totally insignificant [except for the splitting between b_R and s_R where the splitting will be reduced by the factor $(1 - \frac{4M_H}{\pi T})$]. Except where specifically noted, corrections due to the difference between ω_L^b and ω_L^u are not included in the results reported in this paper.²²

Fermionic mass corrections in the diagram with a *gluon*

loop are comparable in magnitude to the corrections coming from loops containing Higgs boson exchange, which are responsible for the VEV-independent splittings between eigenstates. [See Eq. (6.6).] Thus they must be taken into account and a good approximation to the Dirac operator in the broken phase is

$$\Sigma_{L,R}^b = \Sigma_{L,R}^u + \delta\Sigma_{L,R}, \quad (6.32)$$

with

$$\begin{aligned} \delta\Sigma_{L,R} = & \frac{16\pi\alpha_s}{3} \int \frac{d^3k}{(2\pi)^3} \frac{n_F(\epsilon_k)}{\epsilon_k} \left\{ \pm \frac{\vec{\sigma} \cdot \vec{p}}{p^2} \left[1 - F \left(\frac{\epsilon_k \omega}{|p||k|} \right) \right] - \frac{1}{\omega} F \left(\frac{\epsilon_k \omega}{|p||k|} \right) \right\} \\ & - \frac{16\pi\alpha_s}{3} \int \frac{d^3k}{(2\pi)^3} \frac{n_F(|k|)}{|k|} \left\{ \pm \frac{\vec{\sigma} \cdot \vec{p}}{p^2} \left[1 - F \left(\frac{\omega}{|p|} \right) \right] - \frac{1}{\omega} F \left(\frac{\omega}{|p|} \right) \right\}, \end{aligned} \quad (6.33)$$

where for the left sector we have

$$\epsilon_k^2 = k^2 + M_u^2 + KM_d^2 K^\dagger. \quad (6.34)$$

For right quarks with charge $+2/3$, $\epsilon_k^2 = k^2 + M_u^2$, and for right quarks with charge $-1/3$, $\epsilon_k^2 = k^2 + M_d^2$.

For sufficiently small momenta, $|p| \ll \omega$, and small fermionic masses, $m_F \ll T$, this becomes

$$\delta\Sigma_{L,R} = \frac{2\alpha_s m_F^2}{3\pi\omega^2} \left\{ \pm \left[\ln \left(\frac{\pi T}{m_F} \right) - \gamma - \frac{1}{2} \right] \vec{\sigma} \cdot \vec{p} + \left[\ln \left(\frac{\pi T}{m_F} \right) - \gamma + \frac{1}{2} \right] \omega \right\}, \quad (6.35)$$

where $\gamma = 0.577$ is Euler's constant. The expansion in small fermionic masses is a poor approximation for the top quark, and the integral (6.33) should be calculated precisely. Numerical integration shows that the change due to including a nonzero value of the top-quark mass in the diagram with a gluon loop is about 10% of the contribution of the diagram with the Higgs boson loop, and, therefore, can be ignored. This is not the case for the light quarks where the Higgs boson contribution is much smaller than in the heavy-quark sector. For example, a nonzero charmed quark mass in the diagram with a gluon loop induces a *negative* correction to ω_0 in the broken phase, which is numerically about factor 2.5 times

larger than the corresponding diagram with Higgs boson exchange.

Finding the physical eigenstates is more complicated in the broken phase than it was for the unbroken phase. Even ignoring mixing between different generations (for a discussion of mixing in the broken phase see Appendix F), the dispersion relation is a quite complicated function of ω and p :

$$\det \begin{pmatrix} \Sigma_L^0 + \Sigma_L^b & M \\ M^\dagger & \Sigma_R^0 + \Sigma_R^b \end{pmatrix} = 0. \quad (6.36)$$

As an example Fig. 3 shows the dependence of ω on p for a b quark in the broken phase, neglecting mixing. For low momentum or small VEV, ϕ , there is a one-to-one correspondence of the normal and abnormal branches

²²These corrections were not included in the original version of this work.

in the broken and unbroken phases. In particular, the remarks regarding the group velocity of the excitations apply to the broken sector also.

It is worthwhile studying the properties of the

$$\mathcal{L}_{\text{eff}} = 2iL^\dagger(\partial_0 - \frac{1}{3}\vec{\partial}\vec{\sigma} + i\omega_L)L + 2iR^\dagger(\partial_0 + \frac{1}{3}\vec{\partial}\vec{\sigma} + i\omega_R)R + L^\dagger MR + \text{H.c.} \quad (6.37)$$

Now, left and right chiralities are mixed through the mass term. (We continue to denote by $\omega_{L,R}$ the different ω_0 's corresponding to the L and R interactions, as in the previous section.) This Lagrangian describes four different particle excitations with the dispersion relations

$$\omega = \frac{\omega_L + \omega_R}{2} \pm \sqrt{\frac{M^2}{4} + \left(\frac{\omega_L - \omega_R}{2} \pm \frac{|k|}{3}\right)^2}. \quad (6.38)$$

In the absence of the Higgs-boson-induced mass term, the correspondence of the signs in Eq. (6.38) to the various particle excitations is as follows for $|k| < \frac{3}{2}(\omega_L - \omega_R)$: $(+, +) \leftrightarrow L$, normal; $(+, -) \leftrightarrow L$, abnormal; $(-, -) \leftrightarrow R$, normal; $(-, +) \leftrightarrow R$, abnormal. Note that in the unbroken phase there is a coincidence in the left abnormal and right normal branch at momentum energy $= \frac{3}{2}(\omega_L - \omega_R), \frac{1}{2}(\omega_L + \omega_R)$. At larger $|k|$ the correspondence between signs in Eq. (6.38) and the excitations is changed and $(-, -) \leftrightarrow L$, abnormal; $(+, -) \leftrightarrow R$, normal, so that the levels cross. This level crossing in the unbroken phase persists even if one takes into account higher order perturbative corrections, since no transitions between $SU(2)$ doublet L and $SU(2)$ singlet R are allowed due to the unbroken gauge invariance. In the broken phase the Higgs boson condensate is nonzero, and these levels do not cross.²³

With the use of the dispersion relations one can define the contribution of the particles in the broken phase to the baryonic current as well as to the total momentum of the media, following the procedure of the previous section.

C. Full effective Lagrangian

Equation (6.28) allows one to write down an effective Lagrangian for the fermions in the background of the x -dependent scalar field. It has the form

$$\mathcal{L}_{\text{eff}} = L^\dagger[\Sigma_L^0 + \Sigma_L^b(x)]L + R^\dagger[\Sigma_R^0 + \Sigma_R^b(x)]R + \mathcal{L}_Y(x), \quad (6.39)$$

where the x dependence in the Σ 's comes from the x -

²³However it is possible that off-diagonal terms in the Dirac operator are produced by nonperturbative effects, even in the unbroken phase. If true, the dispersion relation in the unbroken phase would more closely resemble that of the broken phase and in particular the level crossing would be removed. This is discussed in Appendix E.

fermionic excitations in the broken phase for small momenta p . In complete analogy with the unbroken case one can write a linearized effective Lagrangian, again taking for simplicity the one flavor case:

dependent masses of quarks in loop corrections to the propagator, as discussed in the previous section.

This effective Lagrangian has an important property: it does not conserve C and CP symmetry, nor parity, provided the Higgs field is x dependent. As noted previously, this would not be the case if thermal effects, namely, the W^\pm, Z^0 , and Higgs loop corrections to the fermionic mass operator, were neglected. Moreover, because of the fact that left and right mass operators are different, the interaction of left-handed particles with the domain wall is not the same as the interaction of right-handed antiparticles. Thus, separation of C - and CP -odd quantum numbers is potentially possible, in contrast to the zero temperature case. Of course, the CP -violating properties of this Lagrangian are the same as that for the initial electroweak Lagrangian, so that if (with three generations) there is a degeneracy in the up or down sectors or some of the mixing angles are zero there exists a transformation removing all complexities in the kinetic terms and mass matrix simultaneously, and \mathcal{L}_{eff} would be CP conserving. This however is not the case in nature.

With the help of this effective Lagrangian one can determine the conserved baryonic current related to the problem. The current with components

$$J_B^\mu = J_L^\mu + J_R^\mu \quad (6.40)$$

is conserved, where the left and right baryonic currents are defined as in Eq. (6.27).

Having fixed the relevant properties of the quasiparticle excitations in the hot plasma we can turn now to the question of their scattering on the domain wall.

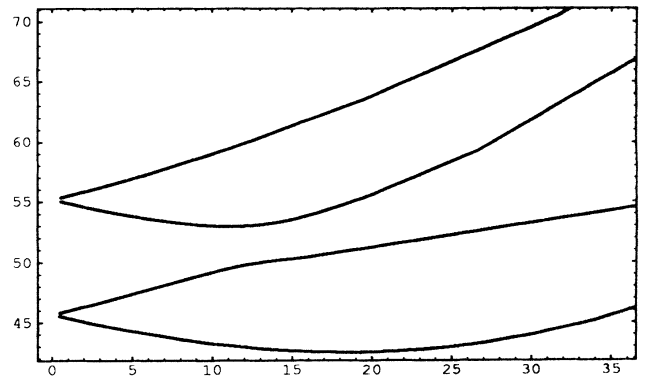


FIG. 3. Dispersion relation for b quarks in the broken phase, for zero CKM angles.

VII. QUARK SCATTERING FROM DOMAIN WALLS

A. Preliminaries

As we have argued in Sec. IV we expect the most interesting part of phase space to be that in which the s quark is reflected from the domain wall. Let us identify the momenta for which this occurs. We begin with a static domain wall, and discuss the moving domain wall later on.

There are two conserved quantities in the interaction of the quark with the domain wall, namely, the energy, ω , and the component of the momentum parallel to the domain wall. For definiteness we will first consider particles incident from the unbroken phase. Let us consider the case when the total momentum is perpendicular to the domain wall (the discussion of the more general case is contained in appendix E). Then (see Figs. 1 and 4) at any energy²⁴ $\omega > \omega_L = 0.502 T$, there are 4 s -quark excitations with different momenta, namely, the left and right normal and abnormal excitations. At energies $\omega_L > \omega > \omega_L^{\min}$ (the minimum value of the energy of the left abnormal branch) the normal left chiral excitation is absent and there are just three types of s -quark excitations: R_n , R_a , and L_a ; however, for each value of the energy there are actually two distinct L_a excitations having different momenta. In the unbroken phase, $\omega_L^{\min} = 0.463 T$. In the range $\omega_R = 0.459 T < \omega < \omega_L^{\min}$ there are just two excitations, R_n and R_a , while in the range $\omega_R^{\min} < \omega < \omega_R$ there is only a single type of excitation, the right abnormal one, with however two distinct momentum states for each energy. As will be seen below (Sec. VII F), in order to compute the total baryonic current in the one-dimensional (1d) problem it is sufficient

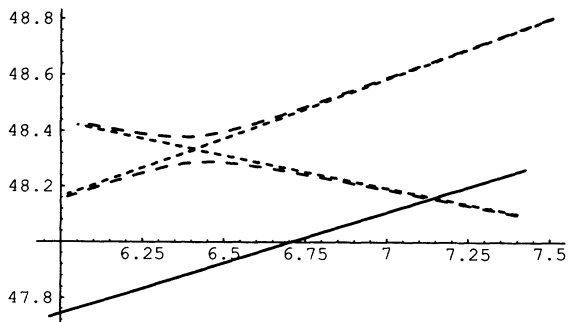


FIG. 4. Dispersion relation for d (short-dashed), s (long-dashed), and b (solid) quarks in the broken phase, focusing on the region of total reflection of the d and s . It is the R_n branch of the b which is visible in this region. CKM angles have been set to zero.

²⁴Quoted numbers in this section are to clarify the discussion and thus correspond to the figures, which do not include mixing – thus they do not correspond precisely to the results of the real calculation where mixing is included.

to determine the reflection coefficients for quarks (and, of course, antiquarks) incident from the unbroken phase, which become L upon reflection, since all other contributions can be obtained from these. Consistent with angular momentum conservation, we have the following possibilities: (i) $\omega > \omega_L$: $R_a \rightarrow L_a$, $R_n \rightarrow L_a$, $R_a \rightarrow L_n$, $R_n \rightarrow L_n$; (ii) $\omega_L^{\min} < \omega < \omega_L$: $R_n \rightarrow L_a$, $R_a \rightarrow L_a$; (iii) for $\omega < \omega_L^{\min}$ no processes involving left chiral particles are possible.

The interaction of the s quark with the domain wall is strongest when it is totally reflected. To find this region of ω , consider the dispersion curves in the broken phase. Because of the small value of the s -quark mass in comparison with temperature, they look almost the same as the dispersion curves in the unbroken phase, shown in Fig. 1, except for a shift in ω_L^b relative to ω_L^u . The only qualitative difference is the absence of the intersection of the right normal branch with the left abnormal one near $\omega = \frac{1}{2}(\omega_L + \omega_R)$, $p = \frac{3}{2}(\omega_L - \omega_R) \sim 6$ GeV. This region is shown “close up” in Fig. 4. Hence, for

$$\frac{1}{2}(\omega_L + \omega_R - m_s) < \omega < \frac{1}{2}(\omega_L + \omega_R + m_s) \quad (7.1)$$

instead of four solutions to the s -quark dispersion relations (as in the unbroken phase) we have in the broken phase only two, which we can designate left and right abnormal branches, with momenta about 40 GeV. Since chirality is not conserved in the presence of the Higgs-induced mass, the labeling of these states is just a matter of convention, which we fix by analogy with the zero-mass case.

Let us consider first what happens in the broken phase if we send, say, a right normal s or \bar{s} from the unbroken phase toward the domain wall, with energy just above the interval (7.1), case (ii). Helicity is conserved in transmission, so two transmitted waves are possible: R_n , with practically the same momentum as the incident R_n , and another, L_a , with a much higher momentum, ~ 40 GeV. The transmission probability for production of the high momentum mode (L_a) is semiclassically exponentially suppressed by the factor²⁵ $\exp(\pi p/a)$, so that one can neglect this process. Therefore, only the right normal excitation will be transmitted to the broken phase when a right normal excitation is incident. For the same reason the reflection probability for producing a left abnormal state from an incident R_a is exponentially suppressed, since in this case the reflected particle has large momentum in comparison with the momentum of the incident particle. In other words, only the reflection process $R_n \rightarrow L_a$ and the transmission process $R_n \rightarrow R_n$ have non-negligible amplitudes. If the energy is well above (7.1) the reflection coefficient will for all cases be small, since then the s -quark mass can be neglected.

Thus we can deduce that in the interval of energies (7.1), the reflection coefficient for an incident R_n s quark is essentially unity. This is because in this energy range there is no physical R_n excitation of the s quark in the

²⁵ a is the inverse wall thickness.

broken phase, so that the transmission process $R_n \rightarrow R_n$ is not allowed, while at the same time the transmission coefficient for producing the high momentum L_a excitation, and the reflection coefficient for $R_a \rightarrow L_a$, are still exponentially suppressed. This is the part of phase space where one can expect to have a substantial contribution to the left chiral current, due to an asymmetry in the reflection coefficients for s, \bar{s} which can be significantly different from the asymmetry in reflection coefficients for d, \bar{d} as long as the d quark is not also totally reflected. Thus to be precise, the energy range of interest is

$$\frac{1}{2}(\omega_L^b + \omega_R^b - m_s) < \omega < \frac{1}{2}(\omega_L^b + \omega_R^b - m_d), \quad (7.2)$$

$$\frac{1}{2}(\omega_L^b + \omega_R^b + m_d) < \omega < \frac{1}{2}(\omega_L^b + \omega_R^b + m_s).$$

Another region in which the reflection coefficients can be large, and thus produce a net quark-antiquark asymmetry, occurs at a slightly lower energy where there is a coincidence of solutions to the dispersion relation for s_L or d_L and b_R excitations, as can be seen from Fig. 4. Because of off-diagonal pieces in the matrix M [see Eq. (6.28)], especially $m_b \sin \theta_{23}$ which mixes b and s , these levels actually repel in the broken phase, producing another region of total reflection in which an (abnormal) s_L incident from the unbroken phase is reflected to a (normal) b_R or vice versa. This phenomenon produces the lower energy region of nonvanishing asymmetry which will be evident in the figures of Sec. IX.

The momentum of the s and d quarks in both these energy ranges is small compared with ω_L and ω_R . This allows one to expand fermionic self-energies with respect to momentum and keep only the first term in p . Thus the scattering can be described in terms of first order differential equations, as will be discussed next.

B. Basic equations

In Sec. VI we derived the effective Dirac equation describing the interaction of quark excitations with the scalar field. Let the scalar field of the domain wall be

$$\phi = \phi_0 f(vt - r), \quad (7.3)$$

where ϕ_0 is the vacuum expectation value of the Higgs field inside the bubble at $T = T_c$, v is the velocity of the bubble wall, and r is the bubble radius. Letting $t = 0$ at the moment of bubble formation at $r = 0$, $f = 0$ for negative argument and $f = 1$ for positive argument larger than the wall thickness. For sufficiently large bubbles, the domain wall can be considered as planar and perpendicular to, say, the x_3 axis, and in the rest frame of the wall we have the Higgs VEV:

$$\phi(x) = \phi_0 F(x_3) \quad \text{with} \quad F(-\infty) = 0, \quad F(+\infty) = 1. \quad (7.4)$$

We will consider the scattering problem in the rest frame of the wall. In order to solve the problem of reflection from the domain wall one has to specify boundary conditions. Particles incident from the unbroken phase and particles transmitted to the broken phase have a

wave function proportional to

$$\exp(-i\omega t + i\vec{k} \cdot \vec{x}), \quad (7.5)$$

with $\omega > 0$ and $\frac{\partial \omega}{\partial k_3} > 0$, while reflected particles have a wave function proportional to

$$\exp(-i\omega t + i\vec{k} \cdot \vec{x}), \quad (7.6)$$

with $\omega > 0$ and $\frac{\partial \omega}{\partial k_3} < 0$. The conditions on $\frac{\partial \omega}{\partial k_3}$ guarantee that the direction of the group velocity has the correct sign.

The equations for antiparticles can be derived from those for particles by CP conjugation. They differ from the equations for particles only in one place: everywhere the CKM matrix K appears, it should be replaced by its complex conjugate K^* . The boundary conditions for antiparticles are the same as for particles.

The Dirac operator (6.28) is highly nonlocal in space and time and it is extremely difficult to solve the Dirac equation as it stands. For a domain wall at rest the nonlocality in time does not matter very much, since energy is conserved so that every time derivative can be eliminated by $\frac{\partial}{\partial t} \rightarrow -i\omega$. The same applies to derivatives with respect to the coordinates parallel to the domain wall, since the momentum parallel to the wall is conserved: $\frac{\partial}{\partial x_2} \rightarrow ik_2$, $\frac{\partial}{\partial x_1} \rightarrow ik_1$. However, the dependence of the equation on x_3 is still nontrivial. The following physical consideration simplifies the problem substantially. It is clear that scattering amplitudes should depend strongly only on k_3 , being the component of the momentum of the particle normal to the bubble surface. As we argued in the discussion of CP violation, we are particularly concerned to treat reliably the regime of energy in which the s quark is reflected but the d is not. We shall see that in this regime the perpendicular momenta are small compared to ω , the energy, so that we can expand the fermionic kinetic term operator with respect to k_3 and take into account only the first term. (Improvement of this approximation is discussed in Appendix H.) This results in a first order differential equation which can be solved. This kind of approximation is not good at all for the up quark sector due to the large value of the top mass. However, as we have argued in the previous section and shall confirm below, the magnitude of CP -violating effects in the up-quark sector is not important.

In this paper we solve the scattering problem only for the case when the momenta of the fermions are normal to the bubble wall. This simplifies the problem significantly while giving results which are at least qualitatively applicable. A discussion of the formalism for the general case is given in Appendix E. We will return to the quality of this approximation in the discussion of uncertainties in Sec. X. Henceforth we consider the one-dimensional scattering problem and denote the coordinate normal to the wall, previously called x_3 , simply by x .

The system of equations describing the reflection of fermions from the domain wall is then

$$\begin{pmatrix} \omega(1 + \alpha_L + \beta_L) + i \frac{\partial}{\partial x}(1 + \alpha_L) & \mathcal{M}_{U,D} \\ \mathcal{M}_{U,D}^\dagger & \omega(1 + \alpha_R + \beta_R) - i \frac{\partial}{\partial x}(1 + \alpha_R) \end{pmatrix} \begin{pmatrix} L \\ R \end{pmatrix} = 0, \quad (7.7)$$

where L and R correspond to up and down components of two-dimensional Weyl spinors which have 3 flavor components. In the plasma rest frame, and neglecting for the moment corrections due to mass insertions in one-loop diagrams, the 3×3 diagonal matrices α and β are defined as

$$\alpha_{L,U,D} = \frac{1}{2} \beta_{L,U,D} = -\frac{1}{3} \frac{\omega_{L,U,D}^2}{\omega^2} \quad (7.8)$$

and

$$\mathcal{M}_{U,D} = O M_{U,D}, \quad (7.9)$$

with $\omega_{L,U,D}$, $M_{U,D}$ and O as defined in Sec. VI. As in that section, we use the subscript R to generically denote the relevant U or D subscript for the right chiral states. Expressions for finite plasma velocity are given in Appendix C. Aside from a small (but important) correction due to W^\pm and Higgs boson masses, and quark mass insertions in a gluon loop, discussed in Sec. VIB, the above expressions for α and β are valid in the broken as well as unbroken phases. For the quantitative calculations reported below we use the exact expressions including the change in α and β in going from unbroken to broken phases.

These equations correspond to left chirality particles incident from the unbroken phase (right particles are reflected in this case) and right chirality particles incident from the broken phase (with left particles reflected). If the sign of the $i \frac{\partial}{\partial x}$ term is reversed one gets the complementary cases. The treatment of both equations is similar, so we will deal in this section with one equation only, in the down quark sector to be concrete.

We introduce new variables

$$\Psi = R^{-1} \begin{pmatrix} L \\ R \end{pmatrix}, \quad (7.10)$$

where R is a diagonal matrix

$$R = \begin{pmatrix} R_{LL} & 0 \\ 0 & R_{RR} \end{pmatrix}, \quad (7.11)$$

$$R_{LL} = (1 + \alpha_L)^{-1}, \quad R_{RR} = -(1 + \alpha_R)^{-1}.$$

In terms of these new variables the equations can be rewritten in the convenient form

$$\frac{\partial}{\partial x} \Psi = iDR\Psi, \quad (7.12)$$

where the Hermitian matrix D is defined by

$$D = \begin{pmatrix} \omega(1 + \alpha_L + \beta_L) & \mathcal{M} \\ \mathcal{M}^\dagger & \omega(1 + \alpha_R + \beta_R) \end{pmatrix}. \quad (7.13)$$

The expression for the baryonic current [see Eq. (6.27)] in terms of these new variables is simply

$$J^B = \Psi^\dagger R \Psi. \quad (7.14)$$

Consider first the asymptotics of the solutions at $x \rightarrow -\infty$ and $x \rightarrow +\infty$. We can write

$$\Psi(x \rightarrow \pm\infty) \rightarrow e(\pm\infty) \exp[ip(\pm\infty)x] \Psi_\pm, \quad (7.15)$$

where $p(\pm\infty)$ are the eigenvalues of the matrix $D(\pm\infty)R$ and $e(\pm\infty)$ is the matrix whose columns are the eigenvectors of $D(\pm\infty)R$:

$$DR e = e p. \quad (7.16)$$

One can introduce also a scattering matrix (which is determined by solving the Dirac equation) mapping the incident onto the outgoing wave function:

$$\Psi_+ = V \Psi_- \quad (7.17)$$

First we note that at $x \rightarrow -\infty$ all eigenvalues of DR are real and are given by

$$p_i(-\infty) \equiv p_L^u = \omega \frac{1 + \alpha_L + \beta_L}{1 + \alpha_L}, \quad i \leq 3, \quad (7.18)$$

$$p_i(-\infty) \equiv p_R^u = -\omega \frac{1 + \alpha_R + \beta_R}{1 + \alpha_R}, \quad i > 3. \quad (7.19)$$

The first three of these correspond to left chiral incident particles and the last three to reflected right chiral outgoing particles.²⁶

We cannot write the corresponding analytic expressions for the particle momenta in the broken phase in closed form due to the mixing of the quark generations. We denote them as

$$p_i(+\infty) = p_L^b, \quad i \leq 3, \quad p_i(+\infty) = p_R^b, \quad i > 3. \quad (7.20)$$

These momenta are not necessarily real due to the fact that the matrix DR is not Hermitian. Complex eigenvalues appear in complex conjugate pairs (see Appendix A). Physically, a pair of complex conjugate eigenvalues corresponds to complete reflection of some particular quark flavor eigenstate.

Let us order the particle momenta in the broken phase in such a way that the first three correspond to propagating modes with positive group velocity or to non-propagating modes with positive imaginary part (this will produce an exponentially decaying wave function) and the last three have negative group velocity or negative imaginary part.

²⁶Since $\alpha_{L,R}$ and $\beta_{L,R}$ are negative and proportional to $\frac{1}{\omega^2}$, for small enough ω the sign of the momenta will change, but not the group velocity. Thus our asymptotic behavior is correct for all ω .

C. Reflection and transmission coefficients

It is not difficult to relate the scattering matrix V to the reflection and transmission amplitudes. The wave function corresponding to the reflection (and transmission) of a left particle incident from the unbroken phase of, say, the first flavor, has the form, at $x \rightarrow -\infty$,

$$\Psi_- = \begin{pmatrix} 1 \\ 0 \\ 0 \\ r_{11}^u \\ r_{21}^u \\ r_{31}^u \end{pmatrix} \quad (7.21)$$

and, at $x \rightarrow +\infty$,

$$\Psi_+ = \begin{pmatrix} t_{11}^u \\ t_{21}^u \\ t_{31}^u \\ 0 \\ 0 \\ 0 \end{pmatrix} \quad (7.22)$$

where r^u and t^u are the reflection and transmission coefficients to be determined. The overall phase is irrelevant to us, since we use in the end only the magnitudes of r_{ij} and t_{ij} .

The wave functions for right-handed particles of the first flavor, incident from the broken phase, have the asymptotic behavior, again dropping an irrelevant phase:

$$\Psi_- = \begin{pmatrix} 0 \\ 0 \\ 0 \\ t_{11}^b \\ t_{21}^b \\ t_{31}^b \end{pmatrix}, \quad x \rightarrow -\infty \quad (7.23)$$

$$\Psi_+ = \begin{pmatrix} r_{11}^b \\ r_{21}^b \\ r_{31}^b \\ 1 \\ 0 \\ 0 \end{pmatrix}, \quad x \rightarrow +\infty \quad (7.24)$$

where r^b and t^b are the reflection and transmission coefficients for the particles incident from the broken phase. Note that the labeling of which flavor is "first," etc., is arbitrary and not related between broken and unbroken phases, except in the limit of no mixing.

If we denote

$$V = \begin{pmatrix} V_{LL} & V_{LR} \\ V_{RL} & V_{RR} \end{pmatrix} \quad (7.25)$$

then the reflection and transmission coefficients are

$$r^u = -V_{RR}^{-1}V_{RL}, \quad t^u = V_{LL} - V_{LR}V_{RR}^{-1}V_{RL}, \quad (7.26)$$

$$r^b = V_{LR}V_{RR}^{-1}, \quad t^b = V_{RR}^{-1}. \quad (7.27)$$

The determination of the scattering matrix V is dis-

cussed in Appendixes A and G. Let us denote the various reflection coefficients of interest as follows: $(r_{LR}^u)_{ij}$ is the reflection coefficient for left particle of flavor j incident from the unbroken phase, which becomes upon reflection a right particle of flavor i . r_{RL}^b is the reflection coefficient matrix for right particles incident from the broken phase, etc. Thus, for instance, the r^u given in the equation above would be more precisely denoted as r_{LR}^u .

D. CPT properties of amplitudes

CPT-invariance puts a number of constraints on the reflection and transmission amplitudes. To find them, let us write all the equations we have for our problem.

(1) For left particles incident from the unbroken phase we have

$$\frac{\partial}{\partial x}\Psi_1 = iDR\Psi_1. \quad (7.28)$$

(2) Left (chirality) antiparticles obey

$$\frac{\partial}{\partial x}\Psi_2 = iD^*R\Psi_2. \quad (7.29)$$

(3) Right particles obey

$$\frac{\partial}{\partial x}\Psi_3 = -iDR\Psi_3. \quad (7.30)$$

(4) Right (chirality) antiparticles obey

$$\frac{\partial}{\partial x}\Psi_4 = -iD^*R\Psi_4. \quad (7.31)$$

One can see that Eqs. (7.28) and (7.31) as well as (7.29) and (7.30) are related by complex conjugation. Therefore, the reflection and transmission coefficients for, say, left incident particles are related to those for right incident antiparticles. Let us find this relation.

As we noted in the previous subsection, and develop in detail in Appendix A, the solution to Eq. (7.28) can be written in the form

$$\Psi_1 = eEV\Psi_0, \quad (7.32)$$

where Ψ_0 is some constant vector and E is a diagonal matrix whose entries are $\exp[i \int p dx]$. Evidently, then,

$$\Psi_4 = e^*E^*V^*\Psi_0^*. \quad (7.33)$$

However in this expression at $x \rightarrow -\infty$, the first three exponentials in E correspond to waves going from right to left while the last three correspond to the incident right antiparticles. To make the calculation of the reflection coefficients transparent, we wish to return to our convention in which the first three describe (now antiparticle) waves going from left to right. Therefore we introduce the matrix T , with $T^2 = 1$, of 0's and 1's which reshuffle the positions of the eigenstates relabeling the eigenvalues in the broken phase in the following way:

$$\Psi_4 = e^*T^2E^*T^2V^*T^2\Psi_0^*, \quad T p T = p^*. \quad (7.34)$$

Then, when $x \rightarrow +\infty$ the last three exponentials in TE^*T will correspond to the waves transmitted to the

broken phase, as desired. If some of the particles undergo complete reflection from the domain wall then $T \neq 1$. If we denote

$$\begin{pmatrix} \bar{V}_{LL} & \bar{V}_{LR} \\ \bar{V}_{RL} & \bar{V}_{RR} \end{pmatrix} \equiv TV^*, \quad (7.35)$$

we see that the reflection coefficients for right chirality antiparticles incident from the unbroken phase are determined by the same V which determined the reflection coefficients of L particles incident from the unbroken phase:

$$\bar{r}_{RL}^u = -\bar{V}_{LL}^{-1}\bar{V}_{LR}, \quad \bar{t}^u = \bar{V}_{RR} - \bar{V}_{RL}\bar{V}_{LL}^{-1}\bar{V}_{LR}, \quad (7.36)$$

$$\bar{r}^b = \bar{V}_{RL}\bar{V}_{LL}^{-1}, \quad \bar{t}^b = \bar{V}_{LL}^{-1}. \quad (7.37)$$

This means, in particular, that there is no need to separately solve all four initial equations; one can solve first two of them and CPT will fix all other matrix elements.

E. Unitarity constraints

From any of the equations one finds the general statement that the ‘‘probability’’ current (coinciding in our case with baryonic current) is conserved: namely,

$$\frac{d}{dx} \Psi^\dagger R \Psi = 0. \quad (7.38)$$

From here one can find a number of useful relations between reflection and transmission amplitudes. In particular, the following relation holds true at $x \rightarrow +\infty$:

$$V^\dagger E^* e^\dagger \text{Re} E V = V^\dagger R^b V = R, \quad (7.39)$$

where the matrix R^b is defined by

$$R^b = e^\dagger \text{Re}. \quad (7.40)$$

It is a diagonal matrix when there is no total reflection

and contains nondiagonal pieces when some of the eigenvalues are complex. From here one finds

$$(t^u)^\dagger R_{LL}^b t^u - (r^u)^\dagger R_{RR} r^u = R_{LL}, \quad (7.41)$$

$$(r^b)^\dagger R_{LL}^b r^b - (t^b)^\dagger R_{RR} t^b = -R_{RR}^b, \quad (7.42)$$

which reflects the fact that one can calculate the baryonic current either from transmission or from reflection coefficients.

Combining CPT symmetry and unitarity one finds the following relations between reflection and transmission coefficients:

$$|(r_{LR}^u)^{ij}|^2 R_{RR}^{ii} / R_{LL}^{jj} = |(\bar{r}_{RL}^u)^{ji}|^2 R_{LL}^{ii} / R_{RR}^{jj}, \quad (7.43)$$

$$\begin{aligned} & |(r_{LR}^b)^{ij}|^2 (R_{RR}^b)^{ii} / (R_{LL}^b)^{jj} \\ &= |(\bar{r}_{RL}^b)^{ji}|^2 (R_{LL}^b)^{ii} / (R_{RR}^b)^{jj}. \end{aligned} \quad (7.44)$$

These relations guarantee the vanishing of any C - and CP -odd currents through the domain wall in thermal equilibrium, as will be seen when they are used in the explicit expressions for currents given in the next section.

F. Baryonic current in terms of reflection coefficients

One can show (see Appendix D) that the thermal averages of the currents of interest are, for the one dimensional problem:

(1) If we send toward the domain wall an equal number of left quarks and antiquarks from the unbroken phase, with the distribution of quasiparticle momenta given by the Fermi distribution in the unbroken phase, their contribution to the net baryonic current is

$$\langle J_{LR}^u \rangle = \int \frac{d\omega}{2\pi} \text{Tr} \left\{ n_F(\omega, v)_{uL} (R_{LL})^{-1} [(r_{LR}^u)^\dagger R_{RR} r_{LR}^u - (\bar{r}_{LR}^u)^\dagger R_{RR} \bar{r}_{LR}^u] \right\}, \quad (7.45)$$

where the \bar{r} 's are the reflection coefficients computed with $K \rightarrow K^*$.

(2) The contribution of right quarks and antiquarks incident from the unbroken phase is

$$\langle J_{RL}^u \rangle = \int \frac{d\omega}{2\pi} \text{Tr} \left\{ n_F(\omega, v)_{uR} (R_{RR})^{-1} [(r_{RL}^u)^\dagger R_{LL} r_{RL}^u - (\bar{r}_{RL}^u)^\dagger R_{LL} \bar{r}_{RL}^u] \right\}. \quad (7.46)$$

(3) ‘‘Left’’ particles incident from the broken phase, now using the equilibrium momentum distributions appropriate to the broken phase, contribute

$$\langle J_{LR}^b \rangle = - \int \frac{d\omega}{2\pi} \text{Tr} \left\{ n_F(\omega, v)_{bL} (R_{LL}^b)^{-1} [(r_{LR}^b)^\dagger R_{RR}^b r_{LR}^b - (\bar{r}_{LR}^b)^\dagger R_{RR}^b \bar{r}_{LR}^b] \right\}. \quad (7.47)$$

(4) ‘‘Right’’ particles incident from the broken phase contribute

$$\langle J_{RL}^b \rangle = - \int \frac{d\omega}{2\pi} \text{Tr} \left\{ n_F(\omega, v)_{bR} (R_{RR}^b)^{-1} [(r_{RL}^b)^\dagger R_{LL}^b r_{RL}^b - (\bar{r}_{RL}^b)^\dagger R_{LL}^b \bar{r}_{RL}^b] \right\}. \quad (7.48)$$

Here $n_F(\omega, v)_{uL, uR, bL, bR}$ are the distributions of the particles in the rest frame of the wall defined in Appendix D. Note that only propagating modes in the broken phase contribute to the asymmetry, so that the trace in Eqs. (7.47) and (7.48) is taken only over eigenstates having real p_L^b and p_R^b .

The total CP -noninvariant component of the baryonic current through the surface is given by

$$\langle J^B \rangle = \langle J_{LR}^u + J_{RL}^u + J_{LR}^b + J_{RL}^b \rangle. \quad (7.49)$$

It is the same in the broken and unbroken phases, since baryonic number is conserved in the interaction with the scalar field. Left and right fermionic currents are not conserved, and cannot be defined in the broken phase. In the unbroken phase they are equal to

$$\langle J^L \rangle = \langle J_{RL}^u + J_{LR}^b \rangle \quad (7.50)$$

and

$$\langle J^R \rangle = \langle J_{LR}^u + J_{RL}^b \rangle. \quad (7.51)$$

QCD sphaleron transitions violate chirality, so that on time scales long compared to $\Gamma_{\text{QCD, sph}}^{-1} \sim 100/T$ these currents are not separately conserved, even in the unbroken phase.

In thermal equilibrium with $v = 0$, all distributions of the particles have the standard form $n_F(\omega) = [\exp(\omega/T) + 1]^{-1}$. In this limit, using²⁷ Eqs. (7.44),

$$\begin{aligned} \langle J_{RL}^u \rangle &= -\langle J_{LR}^u \rangle = -\langle J_{LR}^b \rangle = \langle J_{RL}^b \rangle = \int \frac{d\omega}{2\pi} \Delta(\omega) n_F(\omega) \\ &\simeq \frac{n_F(\bar{\omega})}{2\pi} \Delta_{\text{int}}, \end{aligned} \quad (7.52)$$

where

$$\Delta(\omega) = \text{Tr}\{(R_{RR})^{-1}[(r_{RL}^u)^\dagger R_{LL} r_{RL}^u - (\bar{r}_{RL}^u)^\dagger R_{LL} \bar{r}_{RL}^u]\}, \quad (7.53)$$

thus all C - and CP -odd currents vanish due to the CPT and unitarity relations between different amplitudes given in Eqs. (7.44), as expected.

The main quantity of interest for us is $\Delta(\omega)$, so in the next section we turn to the problem of finding the reflection coefficients. If we are satisfied with the linear term at small v , we can use the differential equation for $v = 0$. J_{CP} will be nonzero due to the difference between Fermi distributions for the particles incident from broken and unbroken phases, when $v \neq 0$. In fact, however, keeping the v dependence in the differential equation (see Appendix C) is quantitatively significant for v 's in the expected range, $v > 0.1$, as is reported in Sec. IX where we parametrize the velocity dependence of Δ_{int} which

enters J_{CP}^L as $\Delta_{\text{int}}(v) \equiv \Delta_0(1 + \zeta v)$. In Appendix C it is shown that for J_{CP}^R , $\Delta_{\text{int}}(-v)$ enters.

At small but nonzero plasma velocity v in the wall rest frame, we saw in Sec. VIA that

$$n_F(\omega, v) = \frac{1}{\exp[\frac{\omega}{T}(1 - \frac{kv}{\omega})] + 1}. \quad (7.54)$$

For the various contributions to the current enumerated in Eqs. (7.45)–(7.48), we encounter different k 's. For instance, for J_{RL}^u , $k \equiv k_R^u$ is the momentum of the R quasiparticle incident from the unbroken phase. The main contribution in this region comes from s_R or b_R being reflected to s_L or d_L . The flavor dependence of the R -quasiparticle momenta can be neglected as it is a higher order effect, so k is just the momentum of the right normal branch²⁸ at $\bar{\omega} = \frac{1}{2}(\omega_L^b + \omega_R)$, which from Eq. (6.19) is $k_R^u \equiv \frac{3}{2}(\omega_L^b - \omega_R)$. For J_{RL}^b we have right normal branch excitations incident from the broken phase. Thus k for this case has the opposite sign as for J_{RL}^u . Moreover since the right branch does not shift in going from broken to unbroken phase, the magnitude of k is the same as in the previous case, so $k = -k_R^u$. For J_{LR}^u and J_{LR}^b the incident excitation is left abnormal. As we saw in Sec. VIA the abnormal branches have k opposite in sign to the group velocity, which must be positive for particles incident from the unbroken phase and negative for particles incident from the broken phase. Thus for J_{LR}^b we have $k = +k_L^b$. Since total reflection occurs at the value of $\bar{\omega}$ for which levels cross in the broken phase, $k_L^b = k_R^b$. Similarly, for J_{LR}^u we have $k = -k_L^u$, where $k_L^u \equiv 3(\omega_L^u - \bar{\omega})$. Neglecting the shift in going from the unbroken to broken phase for the average of ω_L and ω_R compared to the shift in that difference, we have from Sec. VIB that $(\omega_L^b - \omega_R) = (1 - \frac{4M_W}{\pi T})(\omega_L^u - \omega_R)$, so that $k_L^u = \frac{3}{2}(\omega_L^u - \omega_R)(1 + \frac{4M_W}{\pi T})$. Combining the above with Eq. (7.52) gives

$$\begin{aligned} J_{CP} &= \frac{\Delta_{\text{int}}}{2\pi} [n_F(\bar{\omega} - k_R^u v_u) - n_F(\bar{\omega} + k_L^u v_u) \\ &\quad + n_F(\bar{\omega} + k_R^u v_b) - n_F(\bar{\omega} - k_L^u v_b)], \end{aligned} \quad (7.55)$$

where the terms come in order from J_{RL}^u , J_{LR}^u , J_{RL}^b , and J_{LR}^b and v_u , $v_b \geq 0$ are the velocities of the plasma in the wall rest frame in the unbroken and broken phases. In general the temperature differs slightly in going through the wall and that can be taken into account if quantitatively relevant. If the actual distribution functions are not those of thermal equilibrium, say because the wall carries along particles in front of it, then the true distributions may be substituted for the equilibrium distributions we have assumed.

For the quasiequilibrium assumption of equal temperatures and equal velocities, we can make the small velocity expansion of Eq. (7.55). In this case, contributions from J_{RL}^u and J_{RL}^b cancel to leading order in the flavor dependence of the fluxes, leaving

²⁷Since the range of ω for which $\Delta(\omega)$ is nonzero is very narrow and n_F does not change significantly in this range, we take it out of the integral and evaluate it at the central value of ω : $\bar{\omega}$.

²⁸Recall that there is no need to distinguish between ω_R^u and ω_R^b .

$$J_{CP} = \frac{\Delta_{\text{int}}}{2\pi} n_F(\bar{\omega}) [1 - n_F(\bar{\omega})] (k_L^u - k_R^u) v. \quad (7.56)$$

Inserting the expressions obtained above for k_R^u and k_L^u , and using $(\omega_L^u - \omega_R) \approx \frac{3\pi\alpha_W T^2}{16\bar{\omega}}$, gives

$$J_{CP} = \frac{\Delta_{\text{int}}}{2\pi} n_F(\bar{\omega}) [1 - n_F(\bar{\omega})] \frac{9\alpha_W T}{4\bar{\omega}} v. \quad (7.57)$$

We can also consider, as an extreme alternative, the case when the distribution functions vanish in the broken phase, corresponding to all quarks (in the relevant energy range) being swept along by the wall. Now the v dependence of Δ_{int} (see Appendix C) is of the same order as the v dependence from the fluxes. Taking $\Delta_{\text{int}}(v) = \Delta_0(1 + \zeta v)$, we find

$$\begin{aligned} J_{CP} &= \frac{1}{2\pi} [n_F(\bar{\omega} - k_R^u v_u) \Delta_{\text{int}}(v) - n_F(\bar{\omega} + k_L^u v_u) \Delta_{\text{int}}(-v)] \\ &\approx \frac{\Delta_0}{2\pi} n_F(\bar{\omega}) \left(2\zeta + [1 - n_F(\bar{\omega})] \frac{3(\omega_L^u - \omega_R)}{\bar{\omega}} \right) v, \end{aligned} \quad (7.58)$$

again having expanded for small v .

VIII. SOME ANALYTICAL RESULTS

Some properties of the fermions' reflection from the domain wall can be studied analytically. Namely, the case without fermionic mixing allows an analytical solution for some specific profiles of the domain wall, while the real case with mixing can be solved perturbatively in a thin wall approximation.

A. No mixing

If mixing between different quark flavors is absent and the kinetic term is independent of the VEV,²⁹ then the quark scattering problem simplifies significantly. We have just two differential equations for the scattering problem, which can be transformed to the equation for a hypergeometrical function for some profiles of the domain wall. For instance, for

$$F^2(x) = \frac{1}{1 + \exp(-ax)} \quad (8.1)$$

the problem can be converted to one which is solved in, e.g., Ref. [71]. We do not go to the details of the derivation and only present the result. The differential

equations describing the scattering of the fermion on the domain wall can be written as

$$\left(p_L^u + i \frac{\partial}{\partial x} \right) L - M_R R = 0, \quad (8.2)$$

$$M_L L + \left(p_R^u + i \frac{\partial}{\partial x} \right) R = 0,$$

where $M_{L,R} = M/(1 + \alpha_{L,R})$, and $p_{L,R}^u$ are as defined in Eqs. (7.18) and (7.19). M in this expression is the Higgs-induced mass in the broken phase, $\equiv M_{T=0} \left(\frac{\text{VEV}(T)}{\text{VEV}(T=0)} \right)$. Introduce

$$\bar{\omega} \equiv \frac{\omega}{2} \left(\frac{1 + \alpha_L + \beta_L}{1 + \alpha_L} + \frac{1 + \alpha_R + \beta_R}{1 + \alpha_R} \right) \equiv \frac{p_L^u - p_R^u}{2} \quad (8.3)$$

and

$$B \equiv \bar{\omega}^2 - \frac{M^2}{(1 + \alpha_R)(1 + \alpha_L)}. \quad (8.4)$$

There are two solutions to this differential equation. They are

$$L_1(x) = \exp \left[i \left(\frac{(p_R^u + p_L^u)}{2} + \sqrt{B} \right) x \right] F \left(\frac{1}{2} - \frac{i}{a}(\bar{\omega} + \sqrt{B}), \frac{i}{a}(\bar{\omega} - \sqrt{B}), 1 - \frac{2i}{a}\sqrt{B}; -e^{-ax} \right) \quad (8.5)$$

and

$$L_2(x) = \exp \left[i \left(\frac{(p_R^u + p_L^u)}{2} - \sqrt{B} \right) x \right] F \left(\frac{1}{2} - \frac{i}{a}(\bar{\omega} - \sqrt{B}), \frac{i}{a}(\bar{\omega} + \sqrt{B}), 1 + \frac{2i}{a}\sqrt{B}; -e^{-ax} \right). \quad (8.6)$$

²⁹That is, $\alpha_{L,R}$ and $\beta_{L,R}$ are x independent, as is the case when mass corrections to loops in the broken phase are dropped.

The right-handed component of the wave function corresponding to these solutions is given by

$$R_j(x) = \frac{1}{M_R} \left(p_L^u + i \frac{\partial}{\partial x} \right) L_j(x). \quad (8.7)$$

Here $F(\alpha, \beta, \gamma; z)$ is the usual hypergeometric function, whose asymptotic behavior fixes the reflection coefficients. The result can be cast into the form

$$|r_{L \rightarrow R}|^2 = \left(\frac{1 + \alpha_R}{1 + \alpha_L} \right) \gamma(\omega), \quad (8.8)$$

$$|r_{R \rightarrow L}|^2 = \left(\frac{1 + \alpha_L}{1 + \alpha_R} \right) \gamma(\omega), \quad (8.9)$$

with

$$\gamma(\omega) = \frac{\sinh 2\pi(\bar{\omega} - \sqrt{B})/a}{\sinh 2\pi(\bar{\omega} + \sqrt{B})/a} \quad (8.10)$$

for $B > 0$, and $\gamma = 1$ for $B < 0$.

If the energy of the fermion is much higher than the barrier height, then

$$|r_{L \rightarrow R}|^2 = \frac{2\pi M^2}{(1 + \alpha_L)^2 a \bar{\omega}} \exp\left(-\frac{2\pi \bar{\omega}}{a}\right). \quad (8.11)$$

As expected, reflection from the domain wall is suppressed by the semiclassical exponent in this case. Note that this dependence of the amplitude on M can be interpreted as reflecting the perturbative coupling of the fermion to the Higgs potential. On the other hand, in the energy region where total reflection occurs ($B < 0$) the amplitudes are of order 1. In this energy regime perturbation theory in Yukawa coupling constants does not work.

Complete reflection of some flavor corresponds to the case when $B < 0$. With $m_t = 150$ GeV, $m_c = 1.6$ GeV, $m_u = 5$ MeV, $m_b = 5$ GeV, $m_s = 0.15$ GeV, and $m_d = 10$ MeV, $T = 100$ GeV, and the temperature-dependent Higgs VEV such that $m_W(T_c) = 50$ GeV, i.e., $\text{VEV} = 150$ GeV, the regions of total reflection (ignoring flavor mixing) are (1) for the t quark, $\omega < 117.764$ GeV, (2) for the c quark, $47.892 < \omega < 48.886$ GeV, (3) for the u quark, $47.384 < \omega < 48.387$ GeV, (4) for the b quark, $49.491 < \omega < 52.531$ GeV, (5) for the s quark, $48.146 < \omega < 48.237$ GeV, and (6) for the d quark, $48.188 < \omega < 48.194$ GeV.

It is interesting to note that, contrary to expectations based on the zero-temperature dispersion relation, the regions of complete reflection are in general limited by some minimal and maximum values of energies. The reason is the peculiar dispersion relation of the thermal excitations in the hot plasma: as p is increased from $p = 0$, the energy of the abnormal branch initially decreases with increasing momentum, as shown in Figs. 1 and 2. We also note that the region of d -quark reflection lies inside the region of s reflection, and u quark reflection lies inside the region of c reflection. The interesting region of ω is shown in Fig. 4. As we shall see in the section on numerical results, the region of ω in which the momentum of b_R is nearly degenerate with that of s_L or d_L also produces

total reflection, with a b_R incident from the unbroken phase being reflected as an s_L .

The consideration of this subsection confirms that the interesting part of phase space is the region where reflection is substantial. Consideration of the thin wall approximation, with CP effects taken into account, allows one to be even more specific.

B. Thin wall approximation

Many properties of the fermionic interaction with the domain wall can be seen already in thin wall approximation. In this subsection we will suppose that the function F in Eq. (7.4) has the step form

$$F(x) = \theta(x). \quad (8.12)$$

Now the solution of the Dirac equation for all $x < 0$ is

$$\Psi = \exp(ip^u x) \Psi_0, \quad (8.13)$$

and, for $x > 0$,

$$\Psi = e \exp(ip^b x) V \Psi_0. \quad (8.14)$$

We will suppose that the matrix of eigenvectors and eigenvalues are known in both the unbroken and broken phases and that the first three eigenvalues in the broken phase correspond to the transmitted waves, as has been our convention. The aim is to determine the scattering matrix, V . The wave function is continuous at $x = 0$, giving the very simple relation

$$V = e^{-1}. \quad (8.15)$$

The reflection coefficients, which are determined by V [see Eqs. (7.26) and (7.27)], can therefore be expressed via the $x \rightarrow +\infty$ eigenvalue matrices; e.g., for incident L quark by using $Ve = 1$ we find

$$r^u = e_{RL}(e_{LL})^{-1}, \quad r^b = -(e_{LL})^{-1}e_{LR}. \quad (8.16)$$

Now let us consider the propagation of the antiparticles. The corresponding equation for them is

$$\frac{\partial}{\partial x} \Psi = iD^* R \Psi, \quad (8.17)$$

with their eigenvalue problem in the broken phase giving

$$D^* R \bar{e} = \bar{e} \bar{p}^b. \quad (8.18)$$

As demonstrated in Appendix A, one can prove that the set of p^b and \bar{p}^b are the same. This is fundamentally a CPT theorem result. We choose a basis in such a way that $p^b = \bar{p}^b$.

With these simple relations we can investigate in which ranges of energy CP -violating effects can be important. Suppose first that all particle modes can propagate in the broken phase. This means that all eigenvalues are real in the broken phase. Making then a complex conjugation of Eq. (8.18) and comparing to Eq. (7.16) one finds that

$$\bar{e} = e^* \quad (8.19)$$

and, therefore, $\bar{V} = V^*$. This means that reflection co-

efficients for particles are precisely the same as those for antiparticles. Therefore, in thin wall approximation, one cannot expect any CP -violation effects in this region of the phase space.

The other extreme case is also quite simple. Suppose that all eigenvalues are complex so that all fermions are completely reflected from the domain wall. Clearly no separation of baryonic number can occur here.

Now, let one fermionic flavor be reflected while all others are transmitted. This means, that, e.g., p_1^b and p_4^b are complex and $p_1^b = (p_4^b)^*$, $\text{Im}p_1^b > 0$ (by our convention). Then, complex conjugation of Eq. (7.16) for particles does not give (8.18). Instead, we get

$$\bar{e} = e^*T, \quad (8.20)$$

where

$$T^2 = 1, \quad TpT = p^*, \quad T \neq 1. \quad (8.21)$$

So we have

$$\bar{V} = TV^*, \quad (8.22)$$

and reflection coefficients for particles and antiparticles are different [see (8.16)]. The same conclusion is true also for the case when two quark flavors are reflected.

It would be nice to have an analytical expression for the asymmetry covering the whole range of quark masses and mixing angles. Unfortunately, it does not generally exist even for the case of the thin wall. Since we have [Eq. (8.15)] $V = e^{-1}$, simply finding the eigenvectors in the broken phase is sufficient to solve the problem. However doing this requires finding analytically the roots of a sixth

order polynomial, which is not generally possible as is well known. However we can proceed perturbatively in the mixing and obtain some useful insight.

Rather than deal with the 6×6 matrix e , we derive an equation for the reflection coefficient r^u , a 3×3 matrix. From the eigenvalue equation [Eq. (7.16)] in the broken phase, $DRe = e p^b$, one can show³⁰

$$p_L^u e_{LL} + \mathcal{M} R_{RR} e_{RL} = e_{LL} p_L^b, \quad (8.23)$$

$$\mathcal{M}^\dagger R_{LL} e_{LL} + p_R^u e_{RL} = e_{RL} p_L^b. \quad (8.24)$$

Now, multiply Eq. (8.23) by the matrix e_{LL}^{-1} from the right and Eq. (8.24) by e_{RL}^{-1} from the left. Then insert p_L^b defined by the second equation into the first equation. The result of these transformations is

$$p_L^u + \mathcal{M} R_{RR} e_{RL} e_{LL}^{-1} = e_{LL} e_{RL}^{-1} \mathcal{M}^\dagger R_{LL} + e_{LL} e_{RL}^{-1} p_R^u e_{RL} e_{LL}^{-1}. \quad (8.25)$$

Then, using the fact [Eq. (8.16)] that the matrix r of reflection coefficients for R particles incident from the unbroken phase can be written $r = e_{RL} e_{LL}^{-1}$, we arrive at

$$r p_L^u - p_R^u r + r \mathcal{M} R_{RR} r = \mathcal{M}^\dagger R_{LL}. \quad (8.26)$$

We will solve this equation perturbatively. Let us start first from the case without mixing. The eigenvalue problem for one flavor, using the linear Dirac equation since p is small, can be written (see Sec. VII) as

$$\det \begin{pmatrix} \omega(1 + \alpha_L + \beta_L) - p(1 + \alpha_L) & -M \\ M & \omega(1 + \alpha_R + \beta_R) + p(1 + \alpha_R) \end{pmatrix} = 0 \quad (8.27)$$

The solution, using the notation defined in the previous subsection, is

$$p_\pm = \bar{\omega} \pm \sqrt{\bar{B}}. \quad (8.28)$$

The reflection coefficient for $R \rightarrow L$ with no mixing is

$$r_0 = \frac{1 + \alpha_R}{M} (\bar{\omega} \pm \sqrt{\bar{B}}), \quad (8.29)$$

with the root chosen so that $r \rightarrow 0$ when $M \rightarrow 0$.

The physical case with mixing can be solved by perturbation theory in mixing angles. Equation (8.26) provides an ideal recursion procedure for that. For regions of ω with flavor-diagonal total reflection one writes $r = r_0 + \delta r$, $\mathcal{M} = M + \delta M$, where δM is the nondiagonal part of the mass matrix \mathcal{M} , and defines δr order by order in mixing angles. The expansion parameters are roughly

$$\frac{(\delta M)_{ij}}{d_{kl}}, \quad (8.30)$$

where

$$d_{kl} = (p_L^u)_k - (p_R^u)_l + (r_0 M R_{RR})_{kk} + (r_0 M R_{RR})_{ll}. \quad (8.31)$$

The procedure is straightforward, and the calculation can be done with the use of MATHEMATICA or MAPLE. For the region of ω with off-diagonal $b_R - s_L$ reflection, one first rotates the basis and the equations become more complicated, but present no fundamental problem. \bar{r} is obtained in the same way as r with $\delta_{CP} \rightarrow -\delta_{CP}$. Since in regions of total reflection r_0 is complex [see Eq. (8.29)], $r \neq \bar{r}$. A nonzero asymmetry first appears in the third order of perturbation theory, as expected, since mixing

³⁰These results are for the case that the kinetic term is VEV independent, i.e., $\omega_L^b = \omega_L^u$. More generally, the $p_{L,R}^u$ which appear should be replaced by $\tilde{p}_{L,R}^b$, the broken phase momenta for $\mathcal{M} = 0$.

between all three generations is essential.

The full expressions are too lengthy to be quoted here; however, if we make further approximations, valid for $p/\omega \ll 1$, we can obtain a more compact result as follows. We present here the result of the computation of the asymmetry in the region where only the s quark is reflected. We shall work in the approximation in which the velocity of the domain wall is equal to zero and mass corrections to the left-left and right-right transitions in the broken phase are neglected. Modifications of the result for more realistic cases is discussed later. Recall that the quantity Δ in which we are interested is defined by Eq. (7.53). It is convenient to redefine reflection coefficients in the following way:

$$r = \tilde{r} K^\dagger O^\dagger R_{LL}. \quad (8.32)$$

In terms of \tilde{r} , Eq. (8.26) for the reflection coefficients is

$$\tilde{r} K^\dagger O^\dagger p_L^u O K - p_R^u \tilde{r} + \tilde{r} K^\dagger O^\dagger R_{LL} O K M R_{RR} \tilde{r} = M^\dagger, \quad (8.33)$$

where M is the diagonal down quark mass matrix at T_c (recall that $\mathcal{M} = OKM$ for the charge $-1/3$ sector). The expression for Δ is a bit more complicated in this basis and contains the matrices K and O . There are two nondiagonal entries in Eq. (8.33). Namely, the second term on the left contains the momenta of charge $-1/3$ quarks in the unbroken phase rotated by the matrices O and K , and the last term contains the rotated matrix R_{LL} . Now let us take advantage of the fact that reflection of the s -quark occurs at small incident particle momenta, so that an expansion with respect to p/ω_0 can be used. In zeroth order in this expansion, $R_{LL} = -R_{RR} = 3/2$, and

$$\Delta = \frac{9}{4} \text{Tr}[\tilde{r}^\dagger \tilde{r} - \tilde{r}^\dagger \tilde{r}]. \quad (8.34)$$

One perturbs in the nondiagonal pieces of $K^\dagger O^\dagger p_L^u O K$, which are to a good approximation

$$-\frac{3\pi\alpha_W T^2}{16} \frac{K^\dagger M_u^2 K}{\omega M_W^2}. \quad (8.35)$$

In the limit $m_b, m_s \ll \omega$, $m_d = 0$, $r_{33} m_b \gg m_s$, and $p_L^u - p_R^u$ for the b quark $\ll m_b$ (which are actually quite good approximations as long as $m_t \sim 150$ GeV) the expression simplifies to

$$\Delta(\omega) = -2 \left(\frac{\pi\alpha_W T^2}{8\omega M_W^2} \right)^3 \frac{m_t^4 m_c^2 s_{12} s_{23} s_{13} \sin\delta_{CP}}{m_b^2 m_s} \text{Im}(r_s), \quad (8.36)$$

where all masses are taken at high temperature and r_s is the reflection coefficient for the strange quark given by Eq. (8.29).

The dependence of this result on quark masses has a simple physical interpretation. Let us work in the basis of \tilde{r} , where the bubble wall presents a diagonal barrier, i.e., the basis of zero temperature physical quarks. The main contribution to the amplitude for $s \rightarrow s$, i.e., the contribution which is present even when mixing angles are zero,

we call r_s . When there is total reflection the reflection coefficient has unit magnitude but a nontrivial phase, so $r_s = e^{i\delta_r}$. However the incident s quark actually is a mixture of the broken phase eigenstates which we could call d_b, s_b, b_b . Thus there are additional contributions to the amplitude for $s \rightarrow s$ coming from ‘‘paths’’ in which another quark is present as an intermediate state. CP violation is first encountered when one considers paths such that, for instance, the b_b component of the s reflects, and is projected back onto the s via a d . Thus we have an amplitude which is of the form

$$e^{i\delta_r} + A_{(s \text{ in } b)} r_b A_{(b \text{ in } d)} A_{(d \text{ in } s)}. \quad (8.37)$$

The path in which an intermediate d is reflected makes a negligible contribution as long as the d is not totally reflected, since then $r_d \sim m_d$ and is thus very small compared to r_b . Note that as long as the b is not totally reflected, r_b is purely real. From standard perturbation theory, the amplitudes $A_{(i \text{ in } j)}$ are just the relevant mixings divided by the level separations. Thus from Eq. (8.35) we have, e.g., $A_{(d \text{ in } s)} \sim \frac{-3\pi\alpha_W T^2}{16\omega M_W^2} m_c^2 s_{12}$, divided by the level separation, m_s . From $A_{(s \text{ in } b)} \cdot A_{(b \text{ in } d)}$ we have $(\frac{-3\pi\alpha_W T^2}{16\omega M_W^2})^2 m_t^4 s_{23} s_{13} e^{i\delta_{CP}}$, divided by the 2-3 and 1-3 level splittings. Some care must be taken to determine them, using Eqs. (8.35), but one finds $\frac{r_b}{d_{23} d_{31}} \sim 1/m_b^2$, which is anyway the naive guess when the momentum of the bottom quark is small. Therefore the relevant portion of the amplitude for s quark reflection is

$$\sim e^{i\delta_r} + c \left(\frac{3\pi\alpha_W T^2}{16\omega M_W^2} \right)^3 \frac{m_c^2 m_t^4 s_{23} s_{13} s_{12}}{m_s m_b^2} e^{i\delta_{CP}}, \quad (8.38)$$

where c is a constant of order 1. Taking the absolute value squared of this, minus the corresponding quantity with $\delta_{CP} \rightarrow -\delta_{CP}$ for the antiparticles, then produces the form seen in the actual analytic result above. Of course to get the overall coefficient and do the sum over flavors requires the real calculation outlined earlier in this section.

This heuristic derivation is useful for realizing that the quark masses which appear in the denominator of (8.36) are just the usual level-splitting denominators in perturbation theory. It shows us that as long as the levels are split by $m_s \neq m_d$, so that there is a region in which the s but not the d quark is totally reflected, the asymmetry is actually enhanced by a near-degeneracy in the levels, since that increases the intergenerational mixing which is essential to the asymmetry. Clearly, when the masses of the b and s quarks go to zero, perturbation theory breaks down and Eq. (8.36) does not hold. Furthermore, we see from yet another point of view how the total reflection of one or two quark eigenstates is crucial to obtain a nonvanishing asymmetry: had there been no total reflection, the only phase in (8.38) would have been the CP violating phase δ_{CP} , and there would be no asymmetry in rates, as is familiar from B physics, where the necessary interference is between a CP violating phase and a strong interaction final state phase shift. In the case at hand, the only source of a phase shift to interfere with

the CP violating phase is the phase shift which develops when the reflection is total, as is evident from Eq. (8.29). The resultant asymmetry is proportional to the product $\sin \delta_{CP} \sin \delta_r$, and the shape of the upper peak we will see in the numerical results reflects the shape of the function $\sin \delta_r \equiv \text{Im}(r_s)$ as the reflection phase shift moves from 0 to π .

Taking into account the mass corrections to the left-left part of the Dirac operator, discussed in Sec. VIB, requires one to replace m_c^2 in Eq. (8.36) with

$$m_c^2 \rightarrow -m_c^2 \left[\frac{16\alpha_s M_W^2}{3\pi^2 \alpha_W T^2} \left(\ln \frac{\pi T}{m_c} - \gamma + \frac{1}{2} \right) - 1 \right]. \quad (8.39)$$

This is because the dispersion relation, when modified for this correction, can be rewritten in its original form with that substitution. The correction due to bosonic masses in the broken phase can be incorporated by replacing α_W in Eq. (8.36) with $\alpha_W(1 - \frac{4M_W}{\pi T})$.

For nonzero but small velocities the result increases by a factor $[(1 - v/3)(1 + v)]^3$ for J_{RL}^u and J_{LR}^b while for J_{LR}^u and J_{RL}^b the same factor appears with $v \rightarrow -v$, due to the velocity dependence of the coefficients $\alpha_{L,R}$ and $\beta_{L,R}$ (see Appendix C). For physical quark masses, the analytic result presented here reproduces the exact numerical result in the region of the upper peak for which Eq. (8.36) is applicable, to about factor-of-2 accuracy. Keeping terms of order p/ω is necessary to do better than this.

The total asymmetry also includes a contribution at a slightly lower energy from $b \rightarrow s$ reflection which is comparable in magnitude to this contribution and of the opposite sign. Thus as parameters change, the sign of the total predicted asymmetry can change as shall be seen in the next section, and for a quantitative description we must do the full calculation.

We see that the asymmetry in the up-quark sector is suppressed by a factor of roughly $\frac{m_s^2 m_c^2}{m_t^2 m_b^2} \sim 10^{-11}$ and is therefore numerically unimportant, as argued heuristically in Sec. II.

IX. NUMERICAL RESULTS FOR Δ

The analytic results of the previous section are helpful for our comprehension, but we wish to go beyond a perturbative expansion in the mixing, in particular not to miss level-crossing phenomena, and also to investigate the dependence of the result on wall thickness. This must be done numerically.

In this section we present the results of our full computation of the baryonic asymmetry current. We solve numerically the one-dimensional quantum mechanical scattering problem for the thermal Dirac equation (6.28) using the methods described in Appendixes A and B. We neglect the shift in the broken phase kinetic term due to mass corrections for thermal W^\pm and Higgs boson. The differential equation is solved twice, once using K and once using K^* . As described in Secs. VIIC and VIID, this enables us to determine all the reflection and

transmission coefficients which we need, for particles and antiparticles of both chiralities, incident from either the broken or unbroken phase. We can then determine the various contributions to the baryonic current, using the formulae of Sec. VIIF. In this section we present our results for this current.

We take as our ‘‘canonical’’ values of parameters: $m_t = 150$ GeV, $m_c = 1.6$ GeV, $m_u = 0.005$ GeV, $m_b = 5$ GeV, $m_s = 0.15$ GeV, $m_d = 0.01$ GeV, $s_{12} = 0.22$, $s_{23} = 0.05$, $s_{13} = 0.007$, $\sin(\delta_{CP}) = 1$, $M_W(T_c) = 50$ GeV, $T_c = 100$ GeV,³¹ and inverse wall thickness [see Eq. (8.1)] $a = T/10$. Our result is proportional to $\sin \delta_{CP}$. As we shall illustrate with a series of figures, the total asymmetry current depends sensitively on some quantities, and little on others. Figures 5–8 shows $\Delta(\omega)$ as a function of ω in the range of ω for which the total asymmetry is non-negligible, for several choices of masses and mixing angles.

For the canonical values of the masses and mixings, the region of total reflection of the s , found in the section on analytical results, is $\omega = 48.15 - 48.24$ GeV. This can be seen to coincide with the region of the upper pair of peaks in Fig. 5. The ‘‘notch’’ between them, from $\omega = 48.188 - 48.194$ GeV, is the region in which both the s and d is totally reflected. As can be seen from Fig. 4 and was discussed in Sec. VII, the broad peak of opposite sign at lower ω corresponds to a region of ω in which

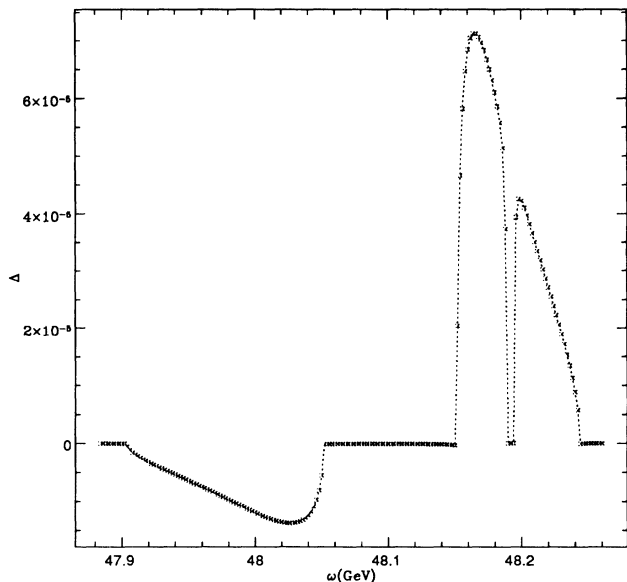


FIG. 5. Dependence of Δ on ω , in GeV, for the ‘‘canonical’’ choices of masses and mixing angles, and wall velocity $v = 0$.

³¹While T_c and $M_W(T_c)$ are not precisely known, from (8.36) one sees that it is the ratio $M_W(T_c)/T_c$ which is important. This ratio is constrained to be near 1/2 from the requirement that the sphaleron rate in the low temperature phase is sufficiently suppressed.

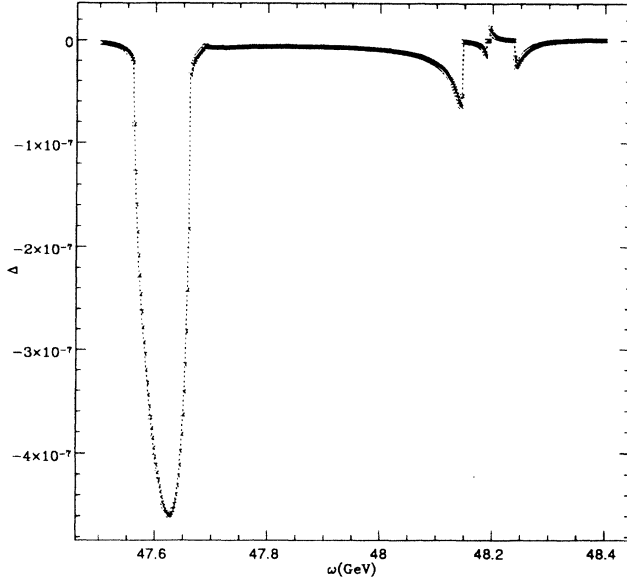


FIG. 6. Dependence of Δ on ω , in GeV, for $m_t = 90$ GeV and the “canonical” choices for the other masses and the mixing angles, and $v = 0$.

the momentum of the b_{Rn} becomes degenerate with the momentum of the $s_{L\alpha}$ or $d_{L\alpha}$ somewhere in its traversal of the bubble wall, inducing resonant level crossing and total reflection to an s or d quark.

The interpretations we have given above of the peaks are borne out by their dependence on the quark masses and CKM parameters, as seen by comparing the various figures to one another. The width and positions of the upper peaks are very insensitive to changes in the mixing angles, or to changes in any masses other than m_s or m_d . By contrast, the position, width, and shape of the lower peak is very sensitive to the mixing angles and m_t .

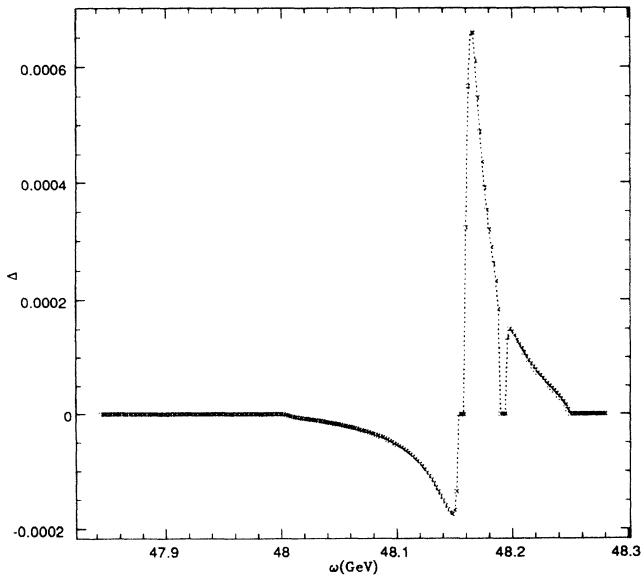


FIG. 7. Dependence of Δ on ω , in GeV, for $m_t = 210$ GeV and the “canonical” choices for the other masses and the mixing angles, and $v = 0$.

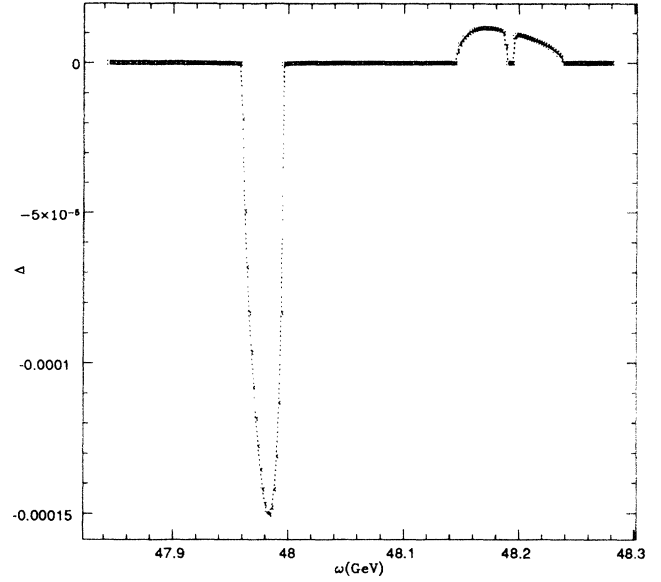


FIG. 8. Dependence of Δ on ω , in GeV, for $\theta_{23} = 0.01$ and the “canonical” choices for the masses and other mixing angles, and $v = 0$.

The height of the upper peaks is given to within $\sim 30\%$ by the thin wall analytic expression (8.36), and varies qualitatively correctly as the relevant masses and mixings are varied.

In the regions between the peaks, the asymmetry is less than $\sim 10^{-12}$, consistent with zero given our numerical precision. This confirms our expectation that the asymmetry is negligible except in a region in which either the s or the d , but not both, is totally reflected.

The character of the lower peak is sensitive to the top mass and the intergenerational mixing, particularly³² θ_{23} . Moreover it has the opposite sign and the same order of magnitude as the upper peaks. Thus as m_t and θ_{23} are varied, the sign of the total asymmetry, integrated over ω , can change. This can be seen by comparing Figs. 5, 6, 7, and 8. The integrated asymmetry, Δ is shown in Fig. 9, over the range $90 < m_t < 250$ GeV. For $m_t = 90$ GeV, the sign of the asymmetry current is negative, then changes to positive [for positive $\sin(\delta_{CP})$] for larger m_t . Its magnitude increases by a factor of 4 in going from $m_t = 150 \rightarrow 210$ GeV, and decreases by a factor of 2 (50) in going from $m_t = 150 \rightarrow 130$ (110) GeV. Figure 10 shows the sensitivity of the integrated asymmetry to θ_{23} , which is far from “perturbative” in the physically interesting region, due to growth of the lower peak. On the other hand, for values of $\sin(\theta_{13}) \lesssim .01$, the baryonic current is linear in $\sin(\theta_{13})$, so we give no figures for that.

³²One can crudely estimate its width and location in analogy to the argument used for the upper peak, as follows. Since it occurs on account of the level crossing of the s_L and b_R dispersion curves, one can approximately use Eq. (7.1) replacing the mass of the s quark with the mixing-induced contribution of the b quark, so that the width of the peak is $\sim m_b \sin(\theta_{23})$.

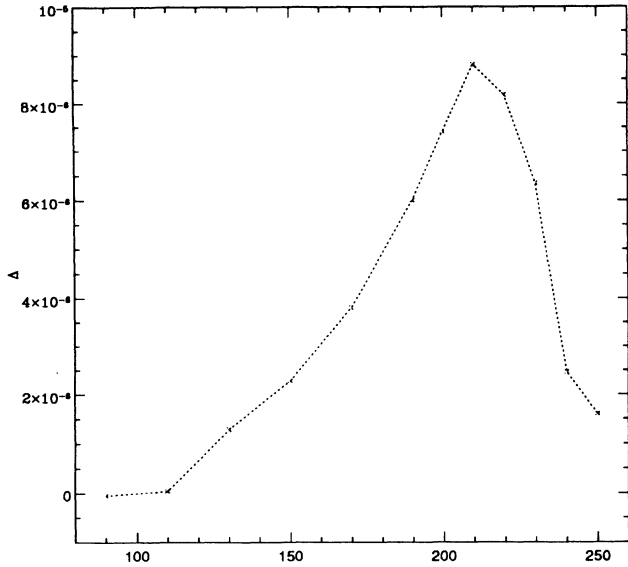


FIG. 9. Dependence of Δ_{int} (in GeV) on $m_t(T=0)$, in GeV.

We have checked that when charge $+2/3$ sector masses are made degenerate, e.g., $m_u \rightarrow m_c$, the asymmetry also vanishes. This occurs through a reduction in the size of the asymmetry for all ω .³³ When $m_d \rightarrow m_s$ the notch between the upper peaks grows until there is nothing left, with the magnitude of the asymmetry inside the peaks

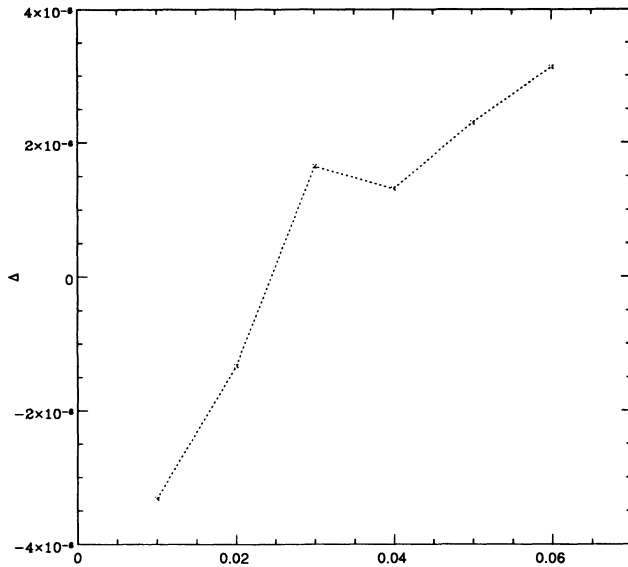


FIG. 10. Dependence of Δ_{int} (in GeV) on $\sin(\theta_{23})$.

³³If m_u is varied from 0.005 to 1.4 GeV the asymmetry decreases by a factor of 6, although neither a linear nor quadratic dependence on mass differences provides a perfect fit over this entire mass region, as is not very surprising.

staying approximately constant and the magnitude of the negative peak vanishing like $m_s^2 - m_d^2$. We give also, in Fig. 11, the dependence of the total asymmetry on m_b , mainly for its conceptual interest, since the value is well enough known to not be a major source of uncertainty. It is interesting however that had the bottom mass been 2 GeV lower, CKM CP violation would have been insufficient to account for the BAU in this mechanism, at least for 3 generations.

An important result, shown in Fig. 12, is the relative insensitivity of the asymmetry current to a , the inverse thickness of the wall, for wall thickness up to $\sim (20 \text{ GeV})^{-1}$, and then strong increase for large wall thickness. As previously noted, the result does not vanish for zero wall thickness. Furthermore, as could have been anticipated, the positions of the peaks are independent of a . A thick wall enhances the asymmetry, although the quantum mechanical approach becomes invalid when the wall thickness is greater than the quasiparticle scattering length.

Modifying the expressions for $\alpha_{L,R}$ and $\beta_{L,R}$ to correspond to their finite velocity expressions, given in Appendix C, we can rerun the program to have an idea of the dynamical effect of finite wall velocity. The left baryonic asymmetry increases as v is increased, as shown in Fig. 13. Using the linear approximation to the dispersion relation, the asymmetry reaches a maximum at $v = 0.25$, where Δ_{int} is a factor of 4 greater than at $v = 0$. We cannot trust the results of the linear approximation for larger v , because the value of p/ω corresponding to the region of total reflection increases rapidly for $v \gtrsim 0.25$, with $p/\omega \gtrsim 0.4$ for $v \gtrsim 0.3$. However blindly using the small p/ω and high- T approximation formulas, even outside the region where they can be trusted, suggests that Δ_{int} may not continue to increase, and may even decrease, for $v > 0.3$. Thus although the figure suggests that Δ_{int} will

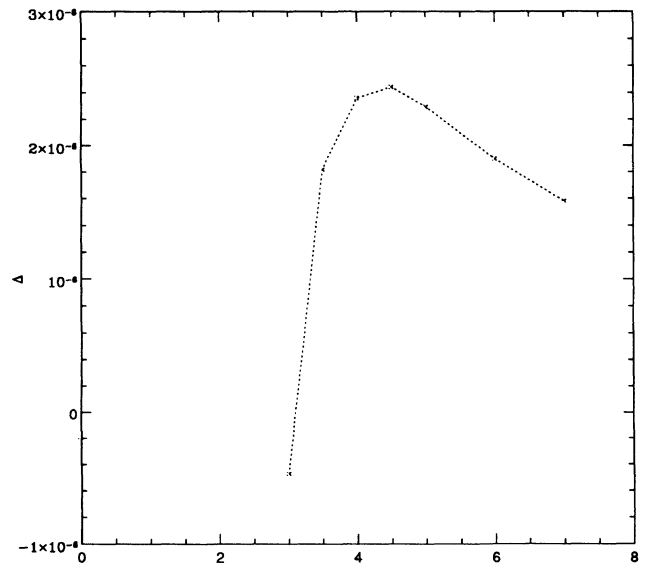


FIG. 11. Dependence of Δ_{int} (in GeV) on $m_b(T=0)$, in GeV.

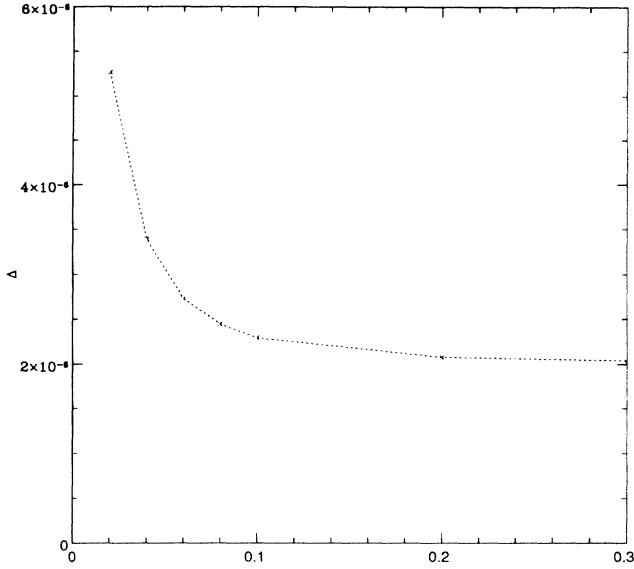


FIG. 12. Dependence of Δ_{int} (in GeV) on inverse wall thickness a , in units of $T = 100$ GeV, other parameters having their canonical values.

continue rising for larger v , that may be misleading and further work is necessary to know what actually happens for larger v . For $v \lesssim 0.25$ we can use the linear approximation $\Delta_{\text{int}}(v) = \Delta_0(1 + \zeta v)$ with $\Delta_0 = 2.3 \times 10^{-6}$ GeV and $\zeta = 12$. We remind the reader that for nonzero v , J_{CP}^R is determined by the usual equations but with Δ determined using $-v$ (see Appendix C).

As noted in Appendix E, a remnant of GIM cancellation between the asymmetry for $s(\bar{s})_R \rightarrow d(\bar{d})_L$ and that for $s(\bar{s})_R \rightarrow s(\bar{s})_L$ suppresses the total asymmetry by a factor $\sim 10^2$ – 10^3 in comparison to the asymmetries in individual flavor channels. Figure 14 demonstrates

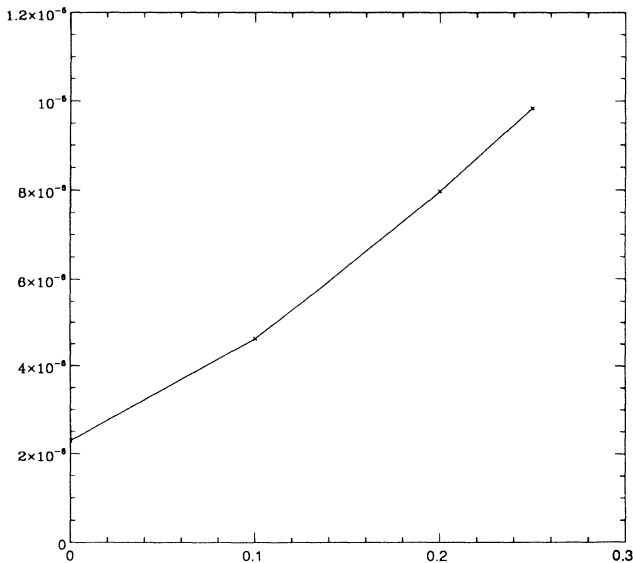


FIG. 13. Dependence of Δ_{int} (in GeV) on wall velocity, other parameters having their canonical values.

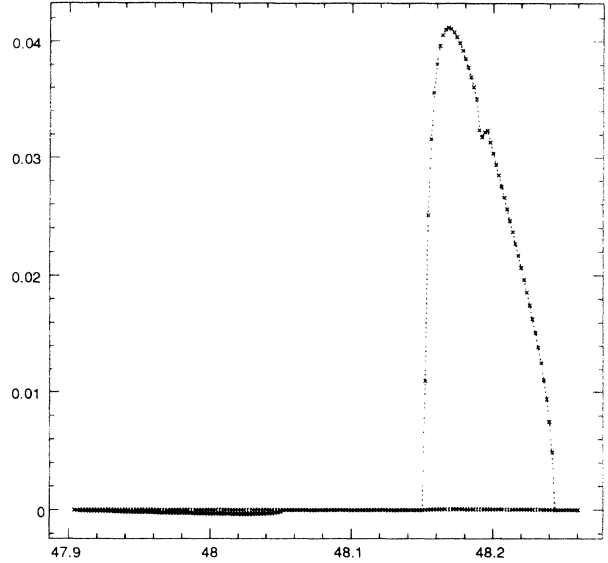


FIG. 14. Dependence of Δ on ω , in GeV, for the individual reflection $s_R \rightarrow d_L$. Also shown is the sum of this asymmetry and that for $s_R \rightarrow s_L$, which is practically equal and opposite, so that the sum is 2–3 orders of magnitude less than the individual asymmetries.

this point, for “canonical” masses, mixing and $v = 0$, by showing the individual $s_R \rightarrow d_L$ vs $\bar{s}_R \rightarrow \bar{d}_L$ asymmetry, and the sum of it plus the $s_R \rightarrow s_L$ asymmetry. If there is some mechanism which we have not incorporated in this calculation which lifts this degeneracy, e.g., by a flavor-dependent modification of flux factors, then the result could be 2–3 orders of magnitude larger than we find.

The quantitative results presented in this section raise some interesting questions. Firstly, how does the sensitivity to m_t and m_b arise, given that the heavy quarks might be expected to decouple from the scattering of the light quarks? Since at least three generations are required for there to be CP violation, it is clear that they cannot decouple altogether, but one would like to understand the mechanism through which they exert their influence. Secondly, how do the properties of the charge $+2/3$ quarks manage to affect the CP violation in the scattering of the charge $-1/3$ quarks? For instance we could have removed the KM phase from the charge $-1/3$ sector and put it in the charge $+2/3$ sector, where one might have thought that it could not affect the scattering of the charge $-1/3$ quarks at all, and would have transferred the effect to the $+2/3$ reflection coefficients, which on account of the larger splitting between c and u might have produced a bigger effect. Of course this does not happen, since the physics must be independent of the convention as to which sector contains the KM phase. Moreover an appropriate measurement at the time of the EW phase transition could have determined that the baryonic asymmetry was in the charge $-1/3$ sector. Similarly, it must

be³⁴ the case that if two quarks of the charge $+2/3$ sector were degenerate in mass, the asymmetry in the reflection coefficients in the charge $-1/3$ sector would disappear. But how do these consistency requirements on the scattering get enforced? Appendixes F, G, and H, are devoted to developing the technology necessary to answer these questions. Using those techniques one can see that heavy quarks do not participate significantly in the scattering, but do participate in the fixing of the eigenstates, and play their crucial role this way. The independence of the convention as to which charge sector contains the KM phase arises because it is the *change* in the relative phases of the eigenstates when the bubble wall is traversed which matters, and this is independent of convention. It is nonvanishing in the charge $+2/3$ sector, just much smaller than for the charge $-1/3$ sector. Likewise, the masses of the charge $+2/3$ quarks play a role in fixing the charge $-1/3$ eigenstates, both in the broken and unbroken phases.

X. PREDICTION FOR n_B/s AND DISCUSSION OF UNCERTAINTIES

A. Prediction

In Eq. (5.21) we found the relation between the left-baryonic current and the ultimate baryon number density in the low-temperature phase: $n_B = \frac{12}{5} J_{CP} f_{\text{sph}}(\rho)$, in quasistatic approximation. We have given in the previous section our results for Δ_{int} , which determines this current, in the one-dimensional problem. From it, we might attempt to estimate the current corresponding to the full 3D problem. As explained in Appendix E, this cannot be done reliably. Instead we divide the one-dimensional current by the one-dimensional entropy corresponding to the known particle content at the temperature of the EW phase transition:

$$s_{1-d} = \frac{73\pi T}{3} = 76.44T, \quad (10.1)$$

and insert a factor f_{3d} as a reminder of this source of uncertainty.

The results for Δ_{int} shown in the figures of the previous section must be multiplied by $\sin \delta_{CP}$. We can reexpress $\sin \delta_{CP}$ in terms of $J \equiv \sin(\theta_{12}) \sin(\theta_{13}) \sin(\theta_{23}) \sin(\delta_{CP})$, in order to reduce the overall uncertainty due to CKM angles and phase, since this combination is relatively better constrained than the individual angles and phase. The “one-sigma” range on J , $(1.4-5.0) \times 10^{-5}$, obtained from a global fit [59] to data, allows us to replace $\sin \delta_{CP}$ in Δ_{int} by

$$\left(\frac{J}{0.22 \times 0.05 \times 0.007} \right) = (0.2 - 0.7). \quad (10.2)$$

We have seen that the final asymmetry is sensitive to

the asymmetry in the fluxes from broken and unbroken phases, and have considered two extreme models of this. In the first, the only deviation from perfect equilibrium comes from the nonzero velocity of the plasma with respect to the bubble wall, taking it and the temperature to be the same on both sides. In this case, using Eq. (7.57) to find J_{CP} from Δ_{int} and taking $m_t = 150$ GeV, and otherwise “canonical” values as defined in the previous section, we obtain, to leading order in v ,

$$\begin{aligned} n_B/s &\approx \frac{3}{73\pi} J_{CP} \frac{12}{5} f_{\text{sph}} f_{3D} \\ &= (2-8) 10^{-5} \frac{\Delta_0}{\bar{\omega}} v f_{\text{sph}} f_{3D} \\ &= (1-4) \times 10^{-12} v. \end{aligned} \quad (10.3)$$

For the other extreme of no flux from the broken phase, we use Eq. (7.58) to determine J_{CP} from Δ_{int} and find

$$n_B/s \approx (3-9) \times 10^{-10} v f_{\text{sph}}(\rho) f_{3D}. \quad (10.4)$$

The range in the parentheses reflects the uncertainty in J , the product of sines of CKM angles. Letting m_t be 135 (180) GeV multiplies the above results by about $2/3$ (2). We shall discuss other sources of uncertainty below.

First, however, let us note that comparison with the observed asymmetry, $n_B/s \sim (4-6) \times 10^{-11}$, is quite encouraging. Not only is the magnitude in the right ballpark, the sign is correct as well.³⁵ This is highly non-trivial, given the intricate dependence of $\Delta(\omega)$ on quark masses and mixing angles as discussed in Sec. IX. However until a number of uncertainties in our calculation and in the theory of the electroweak phase transition are removed, and quasiparticle behavior in that environment is better understood, this result can only be taken as indicative that minimal standard model physics can be responsible for the observed baryon excess of the universe. We now turn to a discussion of the factors f_{sph} and f_{3D} , and a critique of the calculation which we have done to obtain Δ_{int} .

B. Sphaleron efficiency factor, $f_{\text{sph}}(\rho)$

The sphaleron efficiency factor $f_{\text{sph}}(\rho)$ depends a lot on whether the wall perturbs the fermionic distribution functions in its vicinity. Recall that if the quasiequilibrium approximation employed in Sec. V is valid,

³⁵To be precise, only the sign of the product $B \sin \delta_{CP}$ is actually measured at present, where B connects quark matrix elements to hadronic matrix elements for the K meson. If it is positive as is generally believed to be the case, then J is positive and our prediction has the same sign as observation, namely, a baryonic, not antibaryonic excess. Fortunately, the sign of $\sin \delta_{CP}$ can be separately determined experimentally, given the correct set of measurements [72].

³⁴And, we checked, it is.

$f_{\text{sph}}(\rho) = 1$ when $\rho \equiv \frac{3D_B\Gamma}{v^2} \gg 1$, while for $\rho \ll 1$, $f_{\text{sph}}(\rho) = \frac{5}{6}\rho$. In order to estimate ρ we need rather detailed knowledge of the high temperature environment: the sphaleron rate, velocity of the domain wall, and, to estimate D_B , the mean free path of the quasiparticles.

Assuming the wall does not disturb the quark distribution functions, which is correct for walls thicker than a typical mean free path, the rate of sphaleron transitions in the unbroken phase directly enters the expression for the final baryonic asymmetry through the function $f_{\text{sph}}(\rho)$, with $\rho = \frac{3D_B\Gamma}{v^2}$ and³⁶ $\Gamma = 9\Gamma_{\text{sp}}/T^3$. Only two estimates of the sphaleron rate in the unbroken phase have been made [73–75] so far. In the first, an attempt was made to analytically compute the rate of sphaleron transitions, taking some sphaleronlike configuration (namely, the standard instanton in $A_0 = 0$ gauge at $t = 0$) with a fixed size and half integer topological number, and then integrating over the size of this configuration. This yielded the estimate [73]:

$$\Gamma_{\text{sph}} \sim 20(\alpha_W T)^4 \sim 2 \times 10^{-5} T^4. \quad (10.5)$$

It is not clear how reliable the analytical calculation is, since the corrections to it are not under control.³⁷

In Refs. [74, 75], lattice simulations of the sphaleron transitions were performed. A lower limit was found to be³⁸

$$\Gamma_{\text{sph}} \gtrsim 0.45(\alpha_W T)^4. \quad (10.6)$$

The actual sphaleron rate may be much larger than this lower limit, and to find it with better accuracy much larger lattices and larger values of the lattice coupling β_G must be used. In addition to the usual lattice artifacts (finite spacing and finite-size effects) which make it difficult to accurately estimate the sphaleron rate on available computers, there is also a subtle problem connected with the renormalization of the Debye screening mass in three dimensions. This problem, however, is not supposed to affect the main conclusion of Ref. [75].³⁹ We shall take $\Gamma_{\text{sph}} = 10^{-5 \pm 1} T^4$ for our estimates below, although given the many uncertainties and inadequacies of the existing estimates, the actual value may well wind up outside this range.

The parameter ρ also depends on the velocity of the bubble wall which has about one order of magnitude uncertainty [60, 40, 41, 61] $v \sim 0.1 - 0.9$, and on the quark diffusion constant, D_B , which has never been calculated. Roughly speaking, D_B is the quark mean free path which has been estimated to be $\lambda \sim 4/T$ [40, 41] based on strong interaction scattering cross sections. Another sim-

ilar estimate of the mean free path comes from the calculation of the damping rates of the quasiparticles [68, 69], $\lambda \sim (0.15g_s^2 T)^{-1} = 5/T$. Yet another estimate can be had by taking the viscosity of a 5-flavor quark-gluon plasma as determined in [79] and dividing by the typical energy density. This gives $\lambda \sim 4/T$. In Appendix I we discuss the specific case of relatively low momentum quasiparticles and include the effect of Debye screening. We conclude that $D_B \sim (3 - 5)/T$ and $\lambda \sim (4 - 25)/T$.

Combining the above results gives

$$\rho \sim 10^{-3 \pm 1}/v^2. \quad (10.7)$$

As can be seen, one can get either no suppression of the baryonic asymmetry, or 4 orders of magnitude of suppression. In the latter case, MSM baryogenesis seems practically impossible, unless there is a fourth family of quarks. Clearly, a more precise determination of the sphaleron rate in the unbroken phase is of crucial importance.

We also recall to the reader that our derivation (Sec. V) of the relation $n_B = \frac{12}{5} J_{CP} f_{\text{sph}}(\rho)$ assumed almost-equilibrium conditions, while in fact if the domain wall is much thinner than a typical mean free path this may be a poor approximation. In the extreme case that quarks in front of the wall are at rest with respect to it, with a void immediately behind the wall, then one has simply $n_B = J_{CP}/\kappa$, from the definition of κ ($\sim 1/4$, see Sec. V). In this case the sphaleron rate only needs to be greater than the expansion rate of the Universe to do the necessary job. While we do not advocate this extreme example as a good description, it does serve to emphasize the necessity of understanding how the bubble wall affects the quark distribution functions in its neighborhood, in order to determine the magnitude of the final asymmetry. Clearly, a treatment which goes beyond the quasistatic approximation is needed.

To summarize this section we have seen that it is reasonable to suppose that there is no significant suppression from $f_{\text{sph}}(\rho)$. However there could instead be a huge suppression. We can take $10^{-4} < f_{\text{sph}} \leq 1$. From Appendix I we have also seen that the effective collision length of the relevant quasiparticles may be as large $\sim 25/T$, although a value as small as $4/T$ cannot be ruled out.

C. 3D versus 1D prediction, f_{3D}

We have developed the technical tools for carrying out the quantum mechanical (QM) scattering problem for arbitrary p_{\parallel} (see Appendix E), but this calculation is substantially more work, and requires solving other problems first. The contribution coming from the region of $p_{\parallel} \gtrsim p_{\perp}$ is much more sensitive to the issue of the asymmetry in the fluxes than is the small p_{\parallel} contribution, because the velocity perpendicular to the wall is much smaller in this case. In addition, we should improve our approximation methods, especially the high- T expansion, in order to obtain a valid Dirac operator for large momentum particles and to deal with large velocities of the plasma with respect to the wall rest frame.

Even if the Dirac operator we have obtained here were valid under the more extreme circumstances encountered

³⁶See Sec. V.

³⁷Estimates of the prefactor for the sphaleron rate in the broken phase differ by many orders of magnitude [76–78].

³⁸The values of κ in Table 4 of Ref. [75] must be multiplied by the factor 4.4, due to an arithmetic mistake in Eq. (50), which should be replaced by $N(t) = 0.01\kappa \frac{N^3}{\beta_G^3}$.

³⁹J. Ambjorn and M. E. Shaposhnikov (in preparation).

in the full 3D problem, it would be difficult to reliably deduce even the order of magnitude of the 3D result, from the 1D results obtained so far. This is because the level crossing structure is quite different in the two cases, and one needs $R - R$ and $L - L$ reflection amplitudes as well as the $L - R$ and $R - L$ amplitudes required in the 1D case. These complications appear as likely to give an enhanced result as a decreased result since, for instance, the residual GIM cancellation mentioned in Sec. IX seems to be lifted for at least some of the kinematic regions relevant to large⁴⁰ $p_{||}$. Therefore for the time being we must retain the uncertainty factor f_{3D} , which we believe is in the range⁴¹ $\sim (10^{-3} - 10^{+3})$.

D. Other uncertainties in the calculation of J_{CP}

One source of uncertainty is the calculation of the thermal Dirac operator in Sec. VI. We used and even extended the state-of-the-art calculations of the quark propagator, which are done in 1-loop, high-temperature expansion. However one can think of various effects which are clearly physically important and which are not included in this approximation. Simply going to higher-loop approximation and to higher order in mass insertions could make a quantitative difference in the predictions, given their strong sensitivity to the small splittings between eigenstates. Moreover, lattice studies suggest that nonperturbative effects may be very important. We can expect that these effects could also modify the propagation of the fermionic quasiparticles and their inclusion could modify the result for Δ_{int} , although we have not identified any effect of this sort which would modify the

⁴⁰When $p_{||} = 0$, with the approximations of the present work, the degeneracy between the momenta in the unbroken phase of s_L and d_L is almost perfect: $(p_s - p_d)/(p_s + p_d) \sim 10^{-3}$, due to the dominance of the thermal inertia when p is small. This degeneracy in the flux factors determines the extent of GIM compensation between the individual asymmetries in the final result, causing the $p_{||} = 0$ asymmetry summed over flavors to be $\sim 10^{-3}$ times a typical individual asymmetry. A number of effects might lift this, either associated with the full treatment of large $p_{||}$, or coming from nonperturbative effects on the propagation which we have not taken into account. In our numerical study of the one-dimensional system (see Sec. IX), the asymmetries in the individual processes are found to be quite large, of the order of 10^{-1} for $v = 0.25$. Thus the net contribution could be 2–3 orders of magnitude larger than when the cancellation mentioned occurs. To minimize the proliferation of symbols, this possible source of enhancement will be included in f_{3D} , even though it may also appear in a more complete treatment of the 1D problem.

⁴¹In the first preprint version of this paper we had not yet included the effects of QCD-sphaleron-induced $L - R$ transitions, nor the effects of mass corrections to bosonic propagators in the broken phase. When these are included, the naive estimates of f_{3D} which we attempted then break down, and must simply be discarded. See Appendix E for details.

result by more than numerical factors of order 1.

Related to working to lowest nontrivial order in coupling constants in obtaining the quasiparticle propagator, is our purely quantum-mechanical approach to fermion scattering from the domain wall. This neglects non-diffractive collisions of the fermions on the particles in the plasma which occur while they are scattering from the domain wall in the Higgs VEV. While this effect is technically of a higher order (2-loop), we must ask whether it is physically unimportant or not. One can neglect the influence of these processes, provided the effective collision length λ_{inel} of the quarks in the plasma is much larger than the bubble wall thickness a^{-1} and smaller than the imaginary part of the momenta of totally reflected particles, in the broken phase.

The first requirement, that the quasiparticles can scatter through the wall without having a collision, depends on the wall thickness. Because of uncertainties in the effective potential, the wall thickness is poorly known. For instance, using a perturbative calculation of the effective potential yields a wall thickness of $(10 - 40)/T$ [61, 40, 41], while recent work including nonperturbative effects in the unbroken phase indicates that the wall may be much thinner than this, $\sim 1/T$ [44]. Evidently, if the wall is as thin as the latter estimate, our calculation is valid, but if its thickness is $40/T$, our calculation can only be considered an indication of the possible order of magnitude of the asymmetry. For a thick domain wall, a better approximation to the problem would be consideration of the plasma in the background of a (slowly) varying uniform scalar field.

The second requirement for the validity of our quantum mechanical approach, $\text{Im}(p_t)\lambda$ large compared to 1, arises because we specify boundary conditions at infinity in which the coefficient of the growing exponential is set to zero while the falling exponential is kept. This is not physically sensible if there is a collision at a distance λ from the wall, with $\text{Im}(p_t)\lambda$ not large compared to one. From the discussion in Sec. VIII, one can see that in the region of s -quark total reflection, $\text{Im}(p_t) \sim m_s$ so that for this region at least, the condition is not met. This is an aspect of the present calculation which must be improved before the result can be considered quantitatively reliable. However if it is the flavor-decoherence length, $\lambda_{FD} \sim \frac{\alpha_s M_W^2}{\alpha_W m_c^2} \lambda_{inel}$, which proves to be the relevant quantity, there may be no problem with our method since $m_s \lambda_{FD} \sim 200$. Unfortunately, improving the calculation to systematically include these effects seems quite nontrivial, since one must also include at this order emission and reabsorption of thermal quanta during the scattering itself. We have not found a convincing method for estimating the consequences of these effects. Since they are formally of a higher order in α_s , including them may not qualitatively change the conclusions.

E. Effect of a fourth generation

Presently feasible experimental measurements are generally insensitive to a possible fourth generation of quarks, unless there is a large difference between the t'

and b' masses.⁴² This is not the case for the baryon asymmetry produced in the MSM. If there is another generation, then the relevant GIM cancellation will be between the second-most-degenerate pair of generations, namely, the second and third generations. Then the s - b degeneracy will limit the magnitude of the CP violation. Taking the analytic thin-wall result of Eq. (8.36) as a guide, suggests an enhancement over the 3-generation prediction by a factor

$$\sim \left(\frac{m_{t'}}{m_t}\right)^4 \left(\frac{m_t}{m_c}\right)^2 \left(\frac{m_b}{m_{b'}}\right)^2 \frac{s_{23}s_{24}s_{34}}{s_{12}s_{23}s_{13}}, \quad (10.8)$$

where we used the fact that $\Delta(\omega)$ is nonzero over a range $\sim m_s(m_b)$ in the two cases, respectively, and replaced all CP -violating sines by 1. For $\frac{m_{t'}}{m_{b'}} = 10$, and taking the ratios of the sines of the mixing angles to be ~ 1 , this produces an enhancement by a factor $\sim 10^3$. It would appear to be unnatural for the contribution of a fourth generation to be very much less than this, at least given our present inability to account for quark masses and mixings, so that we can consider three-generation results to be a lower bound on the baryonic asymmetry produced in the MSM. If refinements in the theory of MSM baryogenesis significantly lower the prediction in comparison to observation, it could signal the existence of a hitherto-unsuspected fourth generation.

XI. CONCLUSION

We have shown that the baryonic asymmetry of the Universe may be a natural consequence of the CP violation present in the minimal standard model. Within our present treatment of this problem we have found that the MSM prediction is very sensitive to quark masses and mixings, for instance, changing sign for $m_t < 110$ GeV and increasing by a factor of 8 when m_t increases from 130 \rightarrow 210 GeV and for $m_t = 150$ GeV and a plausible choice of wall velocity ($v = 0.25$) we found

$$n_B/s \sim (0.1 - 10) \times 10^{-11} v f_{\text{sph}} f_{3D}.$$

The range reflects the experimental uncertainty in J , the product of sines of CKM angles, and in the asymmetry in the flux factors. Varying m_t from 135 to 180 GeV would introduce a factor $\frac{2}{3}$ to 2. The greatest uncertainties in this prediction come from dynamical aspects of the electroweak phase transition which are still unclear. To remove the uncertainty from the flux factor requires knowing the quark distributions in the vicinity of the wall, specifically, understanding how the passage of the wall affects these distributions. The sphaleron conversion efficiency, f_{sph} , is 1 if the rate of sphaleron transitions in the unbroken phase is large compared to the typical time the quarks remain in the unbroken phase before being overtaken by the expanding bubble of low temperature

phase. While f_{sph} may be 1, it could also be as small as 10^{-4} , in which case the known CP violation of the MSM is inadequate to explain the observed BAU. f_{3D} is very hard to estimate. We believe it lies between $10^{-3} - 10^{+3}$; it also depends sensitively on the flux asymmetry.

While the present result can be considered only a preliminary indication of the true prediction, the possible consistency in magnitude with the observed $n_B/s \sim (4 - 6) \times 10^{-11}$ is encouraging. The sign of the prediction is very sensitive to quark masses and mixing angles, but is correct when these quantities lie in their experimentally allowed ranges. Many of the uncertainties which affect the magnitude of the final asymmetry, such as the sphaleron efficiency and the effect of the bubble wall on the quark distributions in its neighborhood, and our simplified quantum-mechanical treatment neglecting inelastic effects, do not affect the sign of the prediction. Thus it is heartening that the prediction of the sign is correct, because this is likely to not change as the calculation is improved.

In any scenario of electroweak baryogenesis the Higgs potential must be such that it produces a strongly first order phase transition, and such that sphaleron transitions after the phase transition are suppressed. When non-perturbative effects are better understood in the MSM, this should imply a firm upper bound on the Higgs boson mass [80, 44]. In addition to the LEP experimental lower bound, there is a theoretical lower bound resulting from requiring the $T = 0$ vacuum to be stable, which for a MSM Higgs boson is actually more stringent:

$$m_H > 75 + 1.64(m_t - 140), \quad (11.1)$$

in GeV, for $130 < m_t < 150$ GeV [81]. Combining the theoretical bounds will either exclude, or precisely predict, the mass of the MSM Higgs boson, if the minimal standard model with no extensions whatever can be responsible for the baryonic asymmetry of the Universe.

If the upper bound from requiring the sphaleron rate in the low temperature phase to be small enough is violated, it does not mean that electroweak baryogenesis must be rejected or that the mechanism we have developed in this paper cannot be responsible for the BAU. It could instead indicate, for instance, that the Higgs sector is more complicated than in the MSM, so that the upper bound on the Higgs boson mass is relaxed. The real test, eventually, of whether the phenomenon we have discussed is responsible for the observed baryonic asymmetry of the Universe, will be in its quantitative comparison with the measured sign and magnitude of the BAU. Once the dynamical aspects of the EW phase transition are well enough understood, this can be done.

Our work underlines the importance of a reliable and precise observational determination of n_B/γ , which fixes $n_B/s \approx \frac{1}{7} n_B/n_\gamma$. The most recent comprehensive analysis [82] quotes the range $2.8 \times 10^{-10} < n_B/n_\gamma < 4.0 \times 10^{-10}$. However many aspects of the determinations of the primordial abundances are complex and controversial, and the true uncertainty may be larger than reflected in these error bars. For instance, if the primordial ${}^4\text{He}$ abundance, Y_p , proved to be 0.228 ± 0.005 as claimed in Ref. [83], i.e., below the big bang nucle-

⁴²Of course a fourth generation neutrino must be heavy enough to not have influenced too much the Z^0 width.

osynthesis (BBN) “lower limit” of 0.236, some change in determinations of D and $D+^3\text{He}$ or in the simple, homogeneous BBN theory would be necessary for self-consistency, since we know now that there are three light neutrinos. Such changes could cause the prediction for n_B/s to move outside the $(4-6) \times 10^{-11}$ range. For instance, using only $Y_P = 0.228 \pm 0.005$ and three neutrinos would lead to [82] $n_B/s = 2 \times 10^{-11}$.

If the minimal standard model is responsible for baryogenesis, we will be able to use a well-determined value for n_B/s to quantitatively test our understanding of the dynamics of the electroweak phase transition. This could eventually be as powerful a test of our dynamical understanding, as nucleosynthesis has been for later stages of cosmology. Conversely, anticipating the day when the physics of the electroweak phase transition can be considered understood, one can even imagine being able to constrain the particle content, masses and mixing of the MSM on account of the sensitivity of the BAU to these quantities. As noted in Sec. X, a fourth generation would characteristically increase the asymmetry by a large factor in comparison to the 3-generation prediction. Just as the theory of nucleosynthesis, combined with measurement of the relative abundances of primordial nuclei, led to the correct conclusion that there are three light neutrinos, we may one day be able to rule out the existence of a fourth generation, or infer properties it must have, by comparing the observed baryonic asymmetry to the predicted one.

ACKNOWLEDGMENTS

The research of G.R.F. was supported in part by Grant No. NSF-PHY-91-21039. We have benefited from stimulating, provocative, and useful discussions with many colleagues, especially J. Ambjørn, G. Baym, A. Cohen, E. Farhi, J.-M. Frere, B. Gavela, S. Khlebnikov, R. Kolb, P. Langacker, A. Linde, L. McLerran, Y. Nir, J. Orloff, O. Pene, J. Reppy, A. Ringwald, J. Sellwood, S. Shenker, I. Tkachev, M. Turner, and L. Wolfenstein. The contributions of A. Terrano were particularly important.

APPENDIX A: THE SOLUTION OF THE DIRAC EQUATION

In spite of the fact that the problem of finding the reflection coefficients can be given a transparent formulation, as discussed in Sec. VII, it is not so easy to solve. In this appendix we will describe a method suitable for high accuracy numerical solution.

First we note that the problem we want to solve is a problem with boundary conditions rather than a Cauchy problem. We should be able to separate incoming and outgoing waves, exponentially rising and decaying functions. There are many different scales, and there is no way to separate them looking at the numerical solution for the wave function.

The linear character of the differential equations is very helpful. The following trick converts the boundary condition problem to the Cauchy problem. Let us look for

solutions of Eq. (7.12) in the form

$$\Psi(z) = e(z)E(z)V(z)\Psi_0, \quad (\text{A1})$$

where Ψ_0 is a constant vector, e is a matrix constructed from the eigenvectors of the matrix $D(z)R$,

$$D(z)Re(z) = e(z)p(z), \quad (\text{A2})$$

$p(z)$ is a diagonal matrix of eigenvalues of the matrix $D(z)R$,

$$E = \exp\left(i \int_{z_0}^z dz p(z)\right), \quad (\text{A3})$$

and z_0 is some arbitrary point. Here z is a complex variable.

We shall suppose that $F(z)$ is an analytic function of the complex variable z in some region of the complex z plane including the real axis. Most numerical studies we have done are based on the following choice of the domain wall profile:

$$F^2 = \frac{1}{1 + \exp(-ax)}. \quad (\text{A4})$$

There is no serious motivation of this particular choice of the domain wall structure. It resembles, however, some basic features of the expected behavior of the scalar field near the domain wall. Namely, when $x \rightarrow \infty$,

$$F \rightarrow 1 - \frac{1}{2} \exp(-ax), \quad (\text{A5})$$

so that the parameter a can be identified with the effective Higgs boson mass in the broken phase, while, for $x \rightarrow -\infty$,

$$F \rightarrow \exp(-a|x|/2), \quad (\text{A6})$$

incorporating the expectation that the effective Higgs boson mass in the unbroken phase is generally smaller than in the broken phase. The other advantage of this choice is that, for it, we can find the reflection and transmission coefficients analytically for the case without mixing (see Sec. VIII) and compare them with the numerical solution, checking in this way the correctness of the numerical calculations.

In order to get an equation for V let us consider in more detail the properties of eigenvectors and eigenvalues of the matrix $D(x)R$ on the real axis. One can show that for any real x the set of eigenvalues p obeys the following properties. We have either 6 real eigenvalues or 4 real eigenvalues and 1 complex conjugate pair or 2 real eigenvalues and two conjugate complex pairs or 3 conjugate complex pairs.

The proof. The equation for determining the eigenvalues of the matrix DR can be written in the form $\det(DR - p) = 0$, where p here is any one of the eigenvalues, not a matrix. It can also be written in the form $\det(RDR - Rp) = 0$, since $\det R \neq 0$. The equation for the complex conjugate of the eigenvalue has the same form, due to the Hermiticity of the matrices RDR and R : $\det(RDR - Rp^*) = 0$. Therefore the set $\{p\}$ coincides with the set $\{p^*\}$, proving the statement.

This fact has a transparent physical meaning: if all

eigenvalues are real, all particle states can propagate in the background of the scalar field $\phi(x)$, while if two eigenvalues are complex then those states cannot propagate, etc. From this result one can derive the following orthogonality conditions for the eigenvectors. Let us denote by e_i the eigenvectors of the matrix DR , and define the matrix $e = (e_1, \dots, e_6)$. It is easy to see that if $p_i \neq p_j^*$, $i \neq j$, the vectors e_i and e_j are orthogonal in the following sense:

$$e_j^\dagger Re_i = 0. \quad (\text{A7})$$

Therefore, if $e_i^\dagger Re_i \neq 0$, then p_i is real and given by

$$p_i = \frac{e_i^\dagger RDR e_i}{e_i^\dagger Re_i}. \quad (\text{A8})$$

If, for some i and j , $p_i = p_j^*$, then $e_i^\dagger Re_i = 0$ and $e_j^\dagger Re_j = 0$. However, generally speaking, $e_i^\dagger Re_j \neq 0$.

It is convenient to introduce also another eigenvalue matrix f obeying the equation on the complex axis

$$fRD = \tilde{p}f. \quad (\text{A9})$$

One can easily see that eigenvalues defined by Eqs. (A2) and (A9) are the same. To prove it, we notice that the eigenvalues of the problem Eq. (A2) can be found from the equation

$$\det(DR - pI) = 0, \quad (\text{A10})$$

and the eigenvalues of the other one from the equation

$$\det(RD - \tilde{p}I) = 0. \quad (\text{A11})$$

Taking into account the fact that $\det R \neq 0$, one sees that the roots of (A10) and (A11) are the same. Therefore, one can choose a basis in which the matrices p and \tilde{p} are identical. The important property of the matrices f and e which motivates the introduction of f is that they are orthogonal everywhere in the complex plane in the sense that

$$fRe = \text{diagonal matrix}. \quad (\text{A12})$$

This follows from the relation

$$pfRe = fRep. \quad (\text{A13})$$

A convenient normalization is

$$fRe = R. \quad (\text{A14})$$

On the real axis, where the operator D is Hermitian, f and e can be related as

$$f = Te^\dagger, \quad (\text{A15})$$

where

$$T^2 = 1, \quad Tp^*T = p. \quad (\text{A16})$$

Then, the equation for V has the form

$$\frac{\partial V}{\partial z} = -(RE)^{-1}fR\frac{\partial e}{\partial z}EV. \quad (\text{A17})$$

One can also find the equations for the evolution of eigenvectors and eigenvalues:

$$\frac{dp_i}{dz} = \frac{1}{R_{ii}} \left(fR \frac{dD}{dZ} Re \right)_{ii} \quad (\text{A18})$$

$$\frac{de}{dz} = eR^{-1}A, \quad \frac{df}{dz} = -AR^{-1}f, \quad (\text{A19})$$

where

$$A_{ii} = 0, \quad A_{ij} = -\frac{1}{p_i - p_j} \left(fR \frac{dD}{dZ} Re \right)_{ij}. \quad (\text{A20})$$

One can see that the matrix A is singular when $p_i - p_j = 0$; therefore the complex contour should be chosen in such a way that A is regular everywhere along it. The advantage of this formalism is that we have explicitly separated the waves corresponding to the different flavors and helicities. The other helpful feature is that these equations are local in the sense that the matrix V changes only in the vicinity of the domain wall, provided all $\text{Im } p_i(+\infty) < a/2$. In this case the exponential tail of the domain wall is stronger than the exponentially rising functions appearing in the complete reflection case. If some $\text{Im } p_i(+\infty) > a/2$, then the equation for V does contain an exponentially rising term and it is difficult to achieve high accuracy. The formalism for treating this case is described in Appendix G. It was necessary for the numerical analysis of the charge $+2/3$ sector in the region of momenta in which the c quark is totally reflected but the u is not.

It is easy to find the eigenvectors and eigenvalues of the operator DR far from the domain wall in the unbroken phase. Eigenvalues are given by (7.18) and (7.19) and the matrices e and f are just unit matrices.

It is convenient to choose the initial condition for the matrix V :

$$V(z_0) = 1. \quad (\text{A21})$$

Then, choosing z_0 to lie on the real axis and far from the domain wall ($z_0 \rightarrow -\infty$), if one can determine the asymptotic value of the matrix V for $z \rightarrow +\infty$ on the real axis, all reflection and transmission coefficients are determined as shown in Sec. VII.

Even in the case without total reflection it is useful to integrate the equation for V along a complex contour, due the physical phenomenon of level crossing. In spite of the fact that $\Psi(z)$ is an analytic function in the same region of the complex z plane as the potential is analytic, including the real axis, the matrix V has different analytical properties. For example, if at some z , some of the eigenvalues of the matrix DR are degenerate, the eigenvectors corresponding to those eigenvalues are not uniquely defined and, in general, are singular at this point. Furthermore, eigenvalues of the matrix DR have branch cut singularities on the real axis for the case of the complete reflection of some fermionic flavor. Therefore, the equation for V has singularities of various types at the points where p and e have singularities. Of course, these singularities would be canceled in the expression

for V , but this fact does not help when solving for V .

So, our strategy is to solve the equation for V on some contour in the complex plane of the variable z , lying in the region of analyticity of the function $F(z)$. The initial and final points of the contour lie on the real axis, far from the domain wall. For example, for the function F in Eq. (8.1), a suitable contour is

$$z = x - \frac{i}{b \cosh(cx)} \quad (\text{A22})$$

where $b > a/\pi$ to avoid singularities of the function F , and c is an arbitrary number. The function Ψ at the end point does not depend on the choice of contour, on account of the analyticity. However, the function V as well as the normalization of the eigenvectors can depend on the contour. Nevertheless, observables, such as the baryonic current, are, of course, contour independent (see below).

Suppose now that we have chosen some contour and have calculated at the end point the matrix V as well as the eigenvector matrix and eigenvalues, taking for definiteness the case of particles incident from the unbroken phase. In order to find the reflection amplitudes, we first must decide which eigenvalues correspond to acceptable boundary conditions and which must be excluded. For complex eigenvalues it is simple: the exponentially dying wave function ($\text{Im } p > 0$) can exist in the broken phase ($+\infty$), while the coefficient in front of the exponentially rising wave function ($\text{Im } p < 0$) must be equal to zero. The situation with propagating waves (real eigenvalues) is more complicated. In order to decide which one is allowed in the broken phase, one should calculate the group velocities corresponding to the various eigenvalues. Those with positive group velocities at $x \rightarrow +\infty$ are acceptable transmitted waves, while those with negative group velocities correspond to waves traveling in from $+\infty$ and must have zero coefficient in the solution. In the unbroken phase the sign of the group velocity corresponding to the eigenvalue p_i is the same as the sign of the matrix element:

$$(e^\dagger Re)_{ii}. \quad (\text{A23})$$

One can check that this is also true in the broken phase, at least when the mass of the fermion is not much larger than its momentum, which is the region of interest.

Having decided which waves are allowed in the broken phase, let us relabel the eigenvalues p in such a way that the first 3 eigenvalues at $+\infty$ correspond to transmitted waves. This relabeling causes columns of the matrix V , and rows of the matrix e , to be interchanged:

$$\Psi = eEV\Psi_0 = ePPEPPV\Psi_0, \quad (\text{A24})$$

where the matrix P with the property $P^2 = 1$ ‘‘reshuffles’’ the eigenvalues in the desired way. If we denote

$$PV = \begin{pmatrix} V_{LL} & V_{LR} \\ V_{RL} & V_{RR} \end{pmatrix}, \quad (\text{A25})$$

then the reflection coefficients are determined by Eqs. (7.26) and (7.27).

APPENDIX B: NUMERICAL INTEGRATION

Even taking an optimistic view that the asymmetry could be as large as $\sin(\theta_{12}) \sin(\theta_{13}) \sin(\theta_{23}) \sin(\delta_{CP}) \sim 10^{-4} - 10^{-5}$ in the most favorable regions of energy, it is clear that very precise calculations are required. Furthermore we wish to investigate the dependence of the result on many parameters including quark masses and mixing angles and the wall thickness, and we must determine the asymmetry as a function of energy with a fine grid spacing in order that the integrated asymmetry be accurately determined. Thus an integration method is required which is at the same time efficient and accurate.

We have used C++ as a programming language, in order that complex numbers and matrices could be treated as natural units while retaining the benefits of C. We adopted the Burlirsch-Stoer integration algorithm described in Ref. [84], although we wrote our own programs in order to use C++ functionality and the customized matrix manipulation procedures we required. The routines in Ref. [85] we mimicked were ODEINT, BSINT, MMID, and RZEXTR. The Burlirsch-Stoer method is well adapted to our situation: most of the nontrivial variation occurs in a range which is small compared to the full integration range, so that an adaptive stepsize is required, while rational function extrapolation enhances the precision in a minimal number of steps. We checked, by comparing our numerical results with the exact analytic solution for the case with no mixing (see Sec. VIII), that the actual precision of the numerical integration was what it was supposed to be, even when the precision was required to be 1 part in 10^{14} .

We require reflection coefficients to be known, typically, with an accuracy of one part in 10^8 , in order to be able to take differences between the quark and anti-quark sectors, sum up over all the flavors, and still have a result which is accurate to one part in a thousand or better. Depending on the energy and other parameters, we could achieve a final precision on the total asymmetry at each energy of one part per mil by running our integrations at a precision of $10^{-8} - 10^{-10}$. We verified that our results are independent of the precision of the integration, at this level, under these conditions.

An extremely important check of our results was to verify that they are independent of the complex contour chosen. We integrated along the complex contour

$$z = x - \frac{i}{b \cosh(cx)} \quad (\text{B1})$$

and varied b between 1 and 100 and c between 0 and 2. We also checked that the result does not change as the initial and final points of the integration, (x_{\min}, x_{\max}) , are varied.⁴³ For routine use we took $x_{\min} = -60/a$ and $x_{\max} = +30/a$, where a is the inverse wall thickness in

⁴³It is essential to begin and end the integration on the real axis, but the contributions of the segments between x_{\min} , x_{\max} and $z(x_{\min})$, $z(x_{\max})$ can be represented analytically.

GeV. When the mass and mixing parameters are such that there is level crossing, one cannot allow the contour to be too close to the real axis, or the kernel of the differential equation becomes singular. However even in these cases we verified that we could vary b and c each by factors of 5 without changing the final asymmetry by more than one part in a thousand, the typical precision of our numerical calculation for the overall result, as discussed above.

The continuity with ω of the asymmetry, shown in the figures of Sec. IX, testifies to the quality of the numerical

integration, since roundoff and many other types of errors would be uncorrelated in the runs at each different ω , and would therefore show up as jitter in the ω dependence.

APPENDIX C: VELOCITY DEPENDENCE OF THE REFLECTION COEFFICIENTS

The equation describing the reflection of left fermions (incident from the unbroken phase) from the moving domain wall, in the rest frame of the plasma, for small momenta of fermions is

$$\begin{pmatrix} \omega(1 + \alpha_L + \beta_L) + i\frac{\partial}{\partial x}(1 + \alpha_L) & \mathcal{M}[\gamma(x + vt)] \\ \mathcal{M}^\dagger[\gamma(x + vt)] & \omega(1 + \alpha_R + \beta_R) - i\frac{\partial}{\partial x}(1 + \alpha_R) \end{pmatrix} \begin{pmatrix} L \\ R \end{pmatrix} = 0, \quad (\text{C1})$$

where L and R correspond to the upper and lower components of two-dimensional Weyl spinors which have 3 flavor components. $\gamma = 1/\sqrt{1 - v^2}$, t is time and v is the velocity of the domain wall. Positive v corresponds to the wall propagating into the unbroken phase, as is the case physically. The 3×3 diagonal matrices α and β are defined to be

$$\alpha_{L,R} = \frac{1}{2}\beta_{L,R} = -\frac{1}{3}\frac{\omega_{L,R}^2}{\omega^2}. \quad (\text{C2})$$

Due to the explicit time dependence of the Higgs field, the energy ω in this equation is a time derivative: $\omega \rightarrow$

$i\partial/\partial t$, rather than a c number. It is more convenient to solve this equation in the rest frame of the domain wall, where the energy of the fermions interacting with the classical scalar field is conserved. In order to go to the rest frame of the wall one can make the standard Lorentz transformation of coordinates $x \rightarrow \gamma(x + vt)$, $t \rightarrow \gamma(t + vx)$ together with the transformation of spinor fields:

$$\begin{pmatrix} L \\ R \end{pmatrix} \rightarrow \begin{pmatrix} \Lambda_L & 0 \\ 0 & \Lambda_R \end{pmatrix} \begin{pmatrix} L \\ R \end{pmatrix}, \quad (\text{C3})$$

with $\Lambda_L = (\frac{1+v}{1-v})^{\frac{1}{4}}$, $\Lambda_R = (\frac{1-v}{1+v})^{\frac{1}{4}}$. Now, keeping only the linear term in space derivatives (which is correct for small enough momenta of incident fermions) one obtains the equation

$$\begin{pmatrix} \omega(1 + \tilde{\alpha}_L + \tilde{\beta}_L) + i\frac{\partial}{\partial x}(1 + \tilde{\alpha}_L) & \mathcal{M}(x) \\ \mathcal{M}^\dagger(x) & \omega(1 + \tilde{\alpha}_R + \tilde{\beta}_R) - i\frac{\partial}{\partial x}(1 + \tilde{\alpha}_R) \end{pmatrix} \begin{pmatrix} L \\ R \end{pmatrix} = 0 \quad (\text{C4})$$

with

$$\tilde{\alpha}_L = \alpha_L(1 - 3v - 2v^2)(1 - v), \quad (\text{C5})$$

$$\tilde{\beta}_L = 2\alpha_L(1 + v)^2(1 - v),$$

and

$$\tilde{\alpha}_R = \alpha_R(1 + 3v - 2v^2)(1 + v), \quad (\text{C6})$$

$$\tilde{\beta}_R = 2\alpha_R(1 - v)^2(1 + v).$$

The consideration of right particles incident from the unbroken phase goes along the same lines. Now, one can solve these equations by the methods described in

the paper and in the Appendixes. The only important difference is that the reflection coefficients entering J_{RL}^a and J_{LR}^b are obtained from the same equations with $v \rightarrow -v$. It is necessary to solve for V twice, with $D(v)$ and $D(-v)$ since when $v \neq 0$ parity relates the equation for right particles to the one for left particles with $v \rightarrow -v$, modifying Eqs. (7.28) and (7.30).

For the case of incident R particles (whose reflection contributes to the left baryonic current) and $v \gtrsim 0.4$, some momenta become so large that the techniques of Appendix G are required. One must also take care not to leave the regime of applicability of the approximations which have been made in obtaining Eqs. (C1), (C2), and (C4). For instance, a small p with respect to the wall, corresponding to s -quark reflection, may come from a plasma-rest-frame momentum which is large, for large enough v . In practice we can safely work to $v \sim 0.25$ with these approximations, for the case of interest.

APPENDIX D: FLUX FACTORS IN ONE DIMENSION

The calculation of the flux factors is a bit nontrivial in this scattering problem, since we deal with quasiparticles rather than particles. This means that we must take care regarding such things as wave function normalization, etc. Let us first fix these factors for left chiral particles incident from the unbroken phase. We recall that the current of interest is

$$j = \Psi^\dagger R \Psi. \quad (\text{D1})$$

This current is conserved ($\partial_x j = 0$) so that we can find it wherever it is most convenient, e.g., at $x \rightarrow -\infty$. If we send a quark of the first flavor toward the domain wall, then the initial wave function is given by

$$\Psi_- = \eta_1 \begin{pmatrix} 0 \\ 0 \\ r_{11}^u \\ r_{21}^u \\ r_{31}^u \end{pmatrix}, \quad (\text{D2})$$

where η_1 is the normalization factor to be determined later. Then the current is

$$j = |\eta_1|^2 [(R_{LL})_{11} + (r^\dagger R_{RR} r)_{11}]. \quad (\text{D3})$$

The normalization factor η should be chosen in such a way that we have just one particle in the initial state. To find it, let us consider the initial left flux in the unbroken phase. According to Eqs. (6.27) and (6.25) it is given, in the one-dimensional case we are considering, by

$$\int \frac{dk_1}{2\pi} \frac{1}{(R_{LL})_{11}} n_F. \quad (\text{D4})$$

Comparing (D4) and (D3) one finds $\eta_1 = 1/(R_{LL})_{11}$. Now, integrating the result (D4) with respect to the momentum of the initial fermion and changing the integration variable from dk_1 to $d\omega$ we arrive at Eq. (7.45).

The calculation of the flux factors in the broken phase is precisely the same, with the obvious substitution $R \rightarrow R^b$, and we do not present it here. This amounts to assuming that the distribution functions of the quarks in the broken phase are just the equilibrium thermal distribution functions of the broken phase. For a sufficiently slow bubble wall this is a good approximation.

We have found the flux factor for the one-dimensional problem. In the real three-dimensional problem, one

must integrate over the components of the momentum parallel to the surface. As is argued in Appendix E, the reflection coefficients may strongly depend on the parallel components of the momentum, and the solution of the exact equations is required. We do not attempt to solve here the problem of parallel motion. Instead, we will just use the one-dimensional entropy of the plasma when we estimate the final baryonic asymmetry.

APPENDIX E: PARALLEL MOMENTA

In the main body of the paper we deal with the case in which the momenta of the fermions are perpendicular to the domain wall. In this appendix we construct the formalism for the more general case and discuss the influence of parallel momenta on the asymmetry. Evidently, when $p_{||} \neq 0$ angular momentum can be conserved in the scattering while at the same time $L-L$ and $R-R$ reflection can occur, in addition to $L-R$ and $R-L$ reflections. Thus the matrix equations will be 12×12 instead of 6×6 . In the familiar situation without a plasma, one can Lorentz boost to a $p_{||} = 0$ frame where the problem can be reduced to one involving just $L-R$ and $R-L$ reflections. However Lorentz invariance is lost in the plasma, so that a trivial boost in the direction parallel to the domain wall does not produce the problem we have already solved and the additional $R-R$ and $L-L$ amplitudes are physically important.

The study of the new problem can be divided into steps. The first step is the construction of a formalism allowing one to compute the reflection coefficients in this more complicated case. The second step is the derivation of the general expressions for the asymmetry current, assuming that the reflection coefficients are known as a function of the energy and $p_{||}$. The third step is the kinematic analysis to determine in which part of phase space the asymmetry can be substantial. We do not proceed in this paper to the final step of actually computing the reflection coefficients for finite $p_{||}$ quantitatively.

Reflection coefficients. Here we will construct a transformation which allows the problem to be studied by the one-dimensional methods given above. We shall work in the approximation in which the component of the momentum perpendicular to the surface is small (the region relevant to CP violation), while the component of the momentum parallel to the wall is arbitrary. At first order in derivatives with respect to z , the coordinate normal to the wall, the Dirac equation is

$$K \Psi = \begin{pmatrix} \omega(1 + \alpha_L + \beta_L) + (i\sigma_3 \frac{\partial}{\partial z} - \vec{\sigma} \vec{p}_{||})(1 + \alpha_L) & \mathcal{M} \\ \mathcal{M}^\dagger & \omega(1 + \alpha_R + \beta_R) - (i\sigma_3 \frac{\partial}{\partial z} - \vec{\sigma} \vec{p}_{||})(1 + \alpha_R) \end{pmatrix} \begin{pmatrix} L \\ R \end{pmatrix} = 0, \quad (\text{E1})$$

where $p_{||}$ denotes the momentum parallel to the wall, i.e., transverse to z . Now although p_{\perp} is small, the total momentum need not be small so α and β cannot be simplified as in Eq. (7.8). We must use

$$\alpha_{L,R} = -\frac{\omega_{L,R}^2}{p^2} \left[1 - F\left(\frac{\omega}{p}\right) \right], \quad (\text{E2})$$

$$\beta_{L,R} = -\frac{\omega_{L,R}^2}{p^2} F\left(\frac{\omega}{p}\right). \quad (\text{E3})$$

Note that the spinors L, R here have 2 components for each of the three flavors. In the $p_{||} = 0$ case the equations decouple and we could reduce to a description in which L, R have just one component for each flavor. Here that will not be possible.

We want to find some transformation to the new variables in which this equation has a diagonal form in the unbroken phase, so we can apply the methods which have been already developed. In other words, we want to re-

move somehow the matrix $\vec{\sigma} \cdot \vec{p}_{||}$ from these equations. We introduce an analog of the spinor Lorentz transformation, which is different for the left and right sectors:

$$\Lambda K \Lambda \Psi' = 0, \quad \Psi' = \Lambda^{-1} \Psi, \quad (\text{E4})$$

$$\Lambda = \begin{pmatrix} \Lambda_L & 0 \\ 0 & \Lambda_R \end{pmatrix}, \quad (\text{E5})$$

where Λ_L and Λ_R are given by

$$\Lambda_L = \exp\left(\frac{1}{2}\vec{\sigma} \cdot \vec{n}\Theta_L\right), \quad \Lambda_R = \exp\left(\frac{1}{2}\vec{\sigma} \cdot \vec{n}\Theta_R\right), \quad (\text{E6})$$

Here $\vec{n} = \vec{p}_{||}/|p_{||}|$ is the direction of the momentum parallel to the wall, and Θ_L and Θ_R are matrices in flavor space to be determined. One finds

$$v_{L,R} = th\Theta_{L,R} = \mp \frac{p(1 + \alpha_{L,R})}{\omega(1 + \alpha_{L,R} + \beta_{L,R})}. \quad (\text{E7})$$

The equation in terms of the new variables is

$$K' \Psi' = \begin{pmatrix} \omega(1 + \alpha_L + \beta_L)/\gamma_L + i\sigma_3 \frac{\partial}{\partial x}(1 + \alpha_L) & \Lambda_L \mathcal{M} \Lambda_R \\ \Lambda_R \mathcal{M}^\dagger \Lambda_L & \omega(1 + \alpha_R + \beta_R)/\gamma_R - i\sigma_3 \frac{\partial}{\partial x}(1 + \alpha_R) \end{pmatrix} \begin{pmatrix} L \\ R \end{pmatrix} = 0, \quad (\text{E8})$$

where

$$\gamma_{L,R} = (1 - v_{L,R}^2)^{-1/2} = ch\Theta_{L,R}. \quad (\text{E9})$$

In a sense, $v_{L,R}$ is the velocity of the Lorentz boost, and $\gamma_{L,R}$ is the analog of the usual γ factor.

As we see in this more complicated case the equations for the upper and lower components of the two-dimensional (for each flavor) spinors L, R do not decouple and one must solve the complete system of 12 differential equations. (Note that for the vacuum case where α and β are zero the equations do decouple, as expected from Lorentz invariance.) To keep the analogy with the one-dimensional case it is convenient to “reshuffle” the rows and columns of the matrix K' in such a way that its first 6 rows correspond to particles moving from left to right and the other 6 to particles moving in the opposite direction. After this reshuffling, in full analogy with the

one-dimensional case, one can introduce matrices D and R ,

$$R = \begin{pmatrix} R_{++} & 0 \\ 0 & R_{--} \end{pmatrix} \quad (\text{E10})$$

so that the equation for nonzero $p_{||}$ has the form (7.12). We do not solve this equation in this paper.

Flux factors. Suppose that the reflection coefficients are determined from Eq. (E8) and are now functions of energy ω and parallel momentum $p_{||}$. Let us take for definiteness an initial particle in the unbroken phase of type i [i is the index according to Eq. (E8)] and compute the baryonic flux coming from its interaction with the domain wall. We denote the matrix of reflection coefficients by $r(p_{||}, \omega)_{ji}$ or r for short. Now, using the analysis of the one-dimensional case contained in Appendix D, one obtains, for the asymmetry current, summed over all final states,

$$\langle J \rangle = \int \frac{d\omega k_{||} dk_{\perp}}{(2\pi)^2} \text{tr} \{ n_F^i (R_{++}^{ii})^{-1} [(r)^\dagger R_{--} r - (\bar{r})^\dagger R_{--} \bar{r}] \}, \quad (\text{E11})$$

where \bar{r} denotes the matrix of antiparticle reflection coefficients, and n_F^i is the Fermi distribution for the incident particle as in Eq. (6.25). The same equation can be derived for particles incident from the broken phase.

Phase space analysis. We would like to determine in which regions of phase space the reflection of strange quarks can be substantial. To find this, one must deter-

mine the region of energies, ω , and momenta parallel to the surface, $p_{||}$, for which the s -quark excitations exist in the unbroken phase but not in the broken phase, or vice versa.

Consider first the case when the parallel momenta of the incident particles in the unbroken phase are large, $p_{||} \gg \omega_0$. For this region of phase space the dispersion

relations for normal quasiparticles have the same form as the familiar Lorentz-invariant dispersion relations for massive particles but with a modified effective mass. In the unbroken phase we have (Sec. VIA)

$$\omega^2 = |k|^2 + 2\omega_0^{u2}, \quad (\text{E12})$$

while in the broken phase we have

$$\omega^2 = |k|^2 + 2\omega_0^{b2} + m_s^2. \quad (\text{E13})$$

One can make a Lorentz boost in the direction parallel to the wall and remove $p_{||}$ from the problem, as done above. In this frame the dispersion relations are again (E12) and (E13) with the substitution $|k| \rightarrow k_t$ and $\omega^2 \rightarrow \omega^2/\gamma^2$. Since $\omega_L^u > \omega_L^b > \omega_R$, there are additional forbidden regions, depending on which chiralities are under consideration, which are not present for the $p_{||} = 0$ case analyzed previously, making it difficult to estimate the contribution from this region.⁴⁴

Let us turn now to consideration of the case $p_{||} \ll \omega_0$. We can ask what fraction of s quarks are totally reflected due to level crossing as was discussed for $p_{||} = 0$ in Sec. VII. The $L - R$ and $R - L$ level crossings occur for

$$|p| = \frac{3}{2}(\omega_L - \omega_R) \sim 6 \text{ GeV}. \quad (\text{E14})$$

Simple geometry gives the flux coming from particles satisfying this condition. If the reflection coefficients depend only weakly on $p_{||}$, then the contributions from $L - R$ and $R - L$ s -quark total reflections give $J_{3D} = \frac{1}{6\pi}|p|^2 J_{1D} \sim 5 \times 10^{-4} T^2 J_{1D}$. This provides a rough estimate of the minimal contribution of this region of phase space; however, we should not place much confidence in it as a real estimate. Studying the differential equation (E8), it is far from clear that we are justified in assuming a weak $p_{||}$ dependence of the Δ 's. Moreover neglect of the $L - L$ and $R - R$ scattering amplitudes cannot be justified, but their contribution cannot be determined without going much farther toward the solution of these equations than we have.

Range of validity of the Dirac operator. The actual values of ω_0 and T of interest are $\omega_0 \sim 50$ GeV and $T = 100$ GeV. From the dispersion relation (E12), one sees that the condition for the validity of the high-temperature expansion ($\omega^2 - |p|^2 \ll T^2$) is only marginally satisfied for the large $p_{||}$ relativistic kinematics. Thus the dispersion relation needs to be obtained in a more suitable approximation before one can accurately describe the physics of the 3D problem.

APPENDIX F: MIXING IN THE BROKEN PHASE

Our purpose in this appendix is to give the reader a feeling for the qualitative differences between the eigen-

states in the broken and unbroken phases, and especially for the effects of mixing. We will therefore restrict the discussion here to the case of $p \rightarrow 0$, and make a perturbative expansion in the scalar field VEV, ϕ , dropping quadratic terms. The mixing in the broken phase for the charge $-\frac{1}{3}$ sector is then described by the matrix O_D (D for down), where

$$O_D \left(\Omega_L^2 + \frac{16\alpha_s\phi^2}{9\alpha_W\sigma^2} K M_d^2 K^\dagger \right) O_D^\dagger = \bar{\omega}_L^{D2}, \quad (\text{F1})$$

where ω_L and ω_R are given in Eq. (6.10) and (6.11) above, and it is henceforth understood that when the notation R is used, one must substitute, e.g., ω_U or ω_D for ω_R , as appropriate. $\sigma = 246$ GeV is the zero temperature VEV. The particle eigenstates⁴⁵ are related to the initial fields by

$$D_L = O_D^\dagger \mathbf{D}_L, \quad D_R = -\frac{32g_s\phi}{3\sqrt{6}g_W^2\sigma} M_d K^\dagger O_D^\dagger \mathbf{D}_L \quad (\text{F2})$$

and

$$D_L = \frac{32g_s\phi}{3\sqrt{6}g_W^2\sigma} M_d \mathbf{D}_R, \quad D_R = \mathbf{D}_R. \quad (\text{F3})$$

The mass gap in the broken phase is $\bar{\omega}_L^{D2}$ for \mathbf{D}_L and

$$\bar{\omega}_D^2 = \Omega_D^2 - \frac{16\alpha_s\phi^2}{9\alpha_W\sigma^2} M_d^2 \quad (\text{F4})$$

for \mathbf{D}_R .

The equations for the up quarks can be written in the same way and we present them for completeness. The mixing in the up sector is described by the matrix O_U , where

$$O_U \left(\Omega_L^2 + \frac{16\alpha_s\phi^2}{9\alpha_W\sigma^2} M_u^2 \right) O_U^\dagger = \bar{\omega}_L^{U2}. \quad (\text{F5})$$

The particle eigenstates are related to the initial fields by

$$U_L = O_U^\dagger \mathbf{U}_L, \quad U_R = -\frac{32g_s\phi}{3\sqrt{6}g_W^2\sigma} M_u O_U^\dagger \mathbf{U}_L, \quad (\text{F6})$$

and

$$U_L = \frac{32g_s\phi}{3\sqrt{6}g_W^2\sigma} M_u \mathbf{U}_R, \quad U_R = \mathbf{U}_R. \quad (\text{F7})$$

The mass gap in the broken phase is $\bar{\omega}_L^{U2}$ for \mathbf{U}_L and

$$\bar{\omega}_U^2 = \Omega_U^2 - \frac{16\alpha_s\phi^2}{9\alpha_W\sigma^2} M_u^2 \quad (\text{F8})$$

for \mathbf{U}_R .

It is important to notice that the mixing matrices of quarks in the broken phase differ from the correspond-

⁴⁴In the original version of this paper we did not distinguish between broken and unbroken ω 's and thus this complication was overlooked.

⁴⁵Note that physical states in the broken phase do not carry any fixed chirality, so that subscripts L and R have nothing to do with actual chirality and are merely labels to distinguish the two distinct states.

ing matrices in the unbroken phase. Note also that the change of mixing between unbroken and broken phases in the down sector is considerably larger than in the up sector, due to the fact that masses of up quarks are larger than masses of down quarks. This reveals the mechanism by which degeneracy in one sector inhibits CP violation in the other, independently of the convention in which sector CKM phases occur. It is the reason that CP -violating effects are most profound for scattering in the down quark sector.

APPENDIX G: EQUATIONS IN TERMS OF OBSERVABLES

As we discussed in Appendix A, the equation for the scattering matrix does not contain exponentially rising terms only if the imaginary parts of the particle momenta in the broken phase are small enough: $|\text{Im}p_i| < a/2$. While this inequality holds for the charge $-1/3$ quarks for all energies, for zero wall velocity, it breaks down for the top quark, since its mass is quite large in the broken phase, and also for the charge $-1/3$ sector when the wall velocity becomes larger than ~ 0.4 . Therefore, under these circumstances the equations should be modified. The idea is quite simple. It is obvious that all physical reflection and transmission amplitudes must be perfectly finite independently of the top quark mass or wall velocity. In other words, if we would write equations for the scattering amplitudes themselves, there would be no exponentially large terms floating around.

Let us concentrate on the problem of left quark reflection and choose the contour in the complex plane for which at $x \rightarrow +\infty$ the first three eigenvalues of the matrix DR correspond to the transmitted wave. In particular, $\text{Im} p_i(+\infty) > 0$ for $i = 1, 2, 3$. We denote the eigenvectors by

$$p_L = p_i, \quad i = 1, 2, 3, \quad p_R = p_i, \quad i = 4, 5, 6. \quad (\text{G1})$$

In order to simplify the notation we write an equation for the scattering matrix V in the form

$$R_2 = \exp\left(-\text{Im} \int_{z_0}^z p_L dz\right) r^b \exp\left(\text{Im} \int_{z_0}^z p_R dz\right), \quad R_1 = r^u, \quad (\text{G10})$$

$$T_2 = t^b \exp\left(\text{Im} \int_{z_0}^z p_R dz\right), \quad T_1 = \exp\left(-\text{Im} \int_{z_0}^z p_L dz\right) T_2. \quad (\text{G11})$$

Now, the equations for these new variables do not contain any exponentially large terms at all due to our sign convention:

$$\frac{\partial R_1}{\partial z} = -T_2 \bar{\Omega}_{RL} T_1, \quad (\text{G12})$$

$$\frac{\partial T_1}{\partial z} = -\text{Im} p_L T_1 + \bar{\Omega}_{LL} T_1 - R_2 \bar{\Omega}_{RL} T_1, \quad (\text{G13})$$

$$\frac{\partial V}{\partial z} = \Omega V, \quad (\text{G2})$$

$$\Omega = -(RE)^{-1} f R \frac{\partial e}{\partial z} E, \quad (\text{G3})$$

$$\Omega = \begin{pmatrix} \Omega_{LL} & \Omega_{LR} \\ \Omega_{RL} & \Omega_{RR} \end{pmatrix}. \quad (\text{G4})$$

Some of the elements of the matrix Ω can be exponentially large. Using the equation for V and expressions for transmission and reflection coefficients through V [see Eqs. (7.26) and (7.27)] we get a set of nonlinear equations:

$$\frac{\partial r^u}{\partial z} = -t^b \Omega_{RL} t^u, \quad (\text{G5})$$

$$\frac{\partial t^u}{\partial z} = \Omega_{LL} t^u - r^b \Omega_{RL} t^u, \quad (\text{G6})$$

$$\frac{\partial r^b}{\partial z} = \Omega_{LL} r^b - r^b \Omega_{RR} + \Omega_{LR} - r^b \Omega_{RL} r^b, \quad (\text{G7})$$

$$\frac{\partial t^b}{\partial z} = -t^b \Omega_{RL} r^b - t^b \Omega_{RR}, \quad (\text{G8})$$

with initial conditions at $x \rightarrow \infty$

$$r^u = r^b = 0, \quad t^u = t^b = 1. \quad (\text{G9})$$

The important point is that not all of the reflection and transmission coefficients are observable. If, for instance, p_3 and p_6 are complex, we cannot have the third flavor in the broken phase since it cannot propagate there. In other words, only the quantities $(r^b)_{ij}$, $i, j = 1, 2$, $(t^b)_{ij}$, $j \neq 3$ and $(t^u)_{ij}$, $i \neq 3$ have direct physical meaning. We will not change physical quantities if we go to another set of matrices defined by

$$\frac{\partial R_2}{\partial z} = -\text{Im} p_L R_2 + R_2 \text{Im} p_R + \bar{\Omega}_{LL} R_2 - R_2 \bar{\Omega}_{RR} + \bar{\Omega}_{LR} - R_2 \bar{\Omega}_{RL} R_2, \quad (\text{G14})$$

$$\frac{\partial T_2}{\partial z} = +T_2 \text{Im} p_R - T_2 \bar{\Omega}_{RL} R_2 - T_2 \bar{\Omega}_{RR}, \quad (\text{G15})$$

where

$$\bar{\Omega} = -(RE')^{-1} f R \frac{\partial e}{\partial z} E', \quad (\text{G16})$$

$$E' = \exp \left(i \text{Re} \int_{z_0}^z p(z) dz \right).$$

We have checked that these equations give precisely the same values for the reflection coefficients as the scattering matrix formalism, which is a good check of the correctness of the numerical integration schemes. We also used them for scanning the up-quark case, but no significant asymmetry was found there. This was expected since for the up quark sector the change in mixing angles in going from the unbroken to the broken phase is substantially smaller than it is for the down sector.

The equations in this form are quite convenient and allow one to integrate out particles with momenta large compared with some typical scale. For example, for up-sector reflection one expects that an interesting effect can appear only near the c -reflection threshold, since at higher energies the momenta of the c and u quarks are nearly degenerate. Near the c threshold the momentum of the t quark is huge, and the approximate solution to Eqs. (G12)–(G15) is

$$(R_2)_{3i} = (R_2)_{i3} = (T_1)_{3i} = (T_2)_{i3} = 0, \quad (\text{G17})$$

with other equations unchanged. In this approximation the equations for physical reflection amplitudes do not contain either the momentum of the t quark nor the eigenvectors corresponding to it. Nevertheless, the t quark does not decouple completely since it influences the structure of other particle eigenstates through the mixing. Formally, the t quark must be taken into account at the stage at which one solves the equation to determine the eigenstates and eigenfunctions.

The same kind of procedure can also be used to integrate out the b quark. In the region of s -quark reflection, the momentum of the b quark is large compared with other particle momenta. In a sense, rapid oscillations of the wave function are equivalent to exponential suppression. This observation actually works quite well, as can be checked by solving the equations for reflection coefficients in terms of observables, throwing away the b quark as in Eq. (G17) but keeping it in the equations for e , f , and p . This procedure gives essentially the same result for the asymmetry as obtained by our standard procedure.

We can understand the strong dependence of the asymmetry on the top quark mass as follows. The mass of the top quark contributes to the mass gap of the left chiral b quark. Changing the top mass therefore changes the mixing among the charge $-1/3$ left chiral quarks, and thus influences the properties of the light flavors indirectly, through the mixing in the physical eigenstates.

APPENDIX H: QUADRATIC APPROXIMATION

In the low momentum approximation to which we confined ourselves in other sections, the relation between energy and momentum of the quasiparticles was unam-

biguous. For any fixed energy we had just one momentum corresponding to it. This fact is lost when one treats the dispersion relations exactly. For example, at second order in the momentum, the dispersion relation looks like

$$\omega = \omega_0 + \frac{1}{3}p + \frac{p^2}{3\omega_0}, \quad (\text{H1})$$

so that if $\omega > \frac{11}{12}\omega_0$, there are two solutions for the particle momenta. Physically, this means that there are two quasiparticle excitations degenerate in energy but not in momentum, one of which corresponds to the normal branch and the other to the abnormal one. If the energy is close to the mass gap, then the momentum of one of the excitations is small, and it is this excitation whose scattering off the domain wall we have considered. The other value of the momentum corresponds to the abnormal branch and is not small: $p \sim \omega_0$. If we leave aside the question of the stability of the abnormal excitations at such high momentum (in Refs. [68, 69] they are argued to be unstable), then the scattering problem is much more complicated than we had before. Instead of 3 possible initial and 3 possible final states, we have now 6 initial and 6 final states. The three additional states are the high momenta excitations corresponding to the abnormal branch. On the other hand, if $\omega < \frac{11}{12}\omega_0$, the momenta are complex so that particles with these energies cannot propagate even in the unbroken phase and their wave function must be zero everywhere. Actually, in the region of energies corresponding to s -quark total reflection, ω lies well below ω_L for the b quark, so that the b quark actually is absent in the initial states. (Note that this is not the case in linear approximation.)

As we discussed in Appendix G, particles with large momenta decouple from the low-momentum s and d quarks. This justifies the use of the linear approximation in the paper: in spite of the fact that we treat b -quark excitations in the wrong way, as having very short wavelength rather than zero amplitude, the b quark decouples from the equations for the scattering matrix in either case, so that it is immaterial which method we use. The influence of b -quark properties on the asymmetry is due to its effect in fixing the initial physical eigenstates in the light sector, which we do correctly no matter what approximation is used for the b quark in the differential equation. The linear approximation is much faster to numerically integrate, so that is our method of choice. We present, however, for the sake of completeness, the method which one can use for more complete analysis of the system. In particular it would be useful if one wished to study an intermediate range of momenta: large enough that linear approximation is inadequate, but small enough that the decoupling is not complete.

Let us expand the fermionic mass operators in the momentum, up to second order terms in p . The change $p \rightarrow i \frac{\partial}{\partial x}$ gives then an equation

$$\left(a_L \left(\frac{\partial}{\partial x} \right)^2 + b_L i \frac{\partial}{\partial x} + c_L \mathcal{M}^\dagger \right) \begin{pmatrix} L \\ R \end{pmatrix} = 0 \quad (\text{H2})$$

where

$$a_L = \frac{\omega_L^2}{3\omega^3}, \quad b_L = 1 - \frac{\omega_L^2}{3\omega^2}, \quad c_L = \omega \left(1 - \frac{\omega_L^2}{\omega^2} \right), \quad (\text{H3})$$

and corresponding equations for the right quarks. Let $A_{L,R}$ and $B_{L,R}$ be the momenta of the left and right particles in the unbroken phase. They are solutions to the quadratic equation

$$a_{L,R} p^2 - b_{L,R} p - c_{L,R} = 0. \quad (\text{H4})$$

Let us introduce new variables, which correspond to particle excitations in the unbroken phase with momenta $A_{L,R}, B_{L,R}$:

$$\Psi_1 = \left(i \frac{\partial}{\partial x} - B_L \right) \sqrt{a_L} \Psi_L, \quad \Psi_2 = \left(i \frac{\partial}{\partial x} - A_L \right) \sqrt{a_L} \Psi_L, \quad (\text{H5})$$

$$\Psi_3 = \left(i \frac{\partial}{\partial x} - B_R \right) \sqrt{a_R} \Psi_R, \quad (\text{H6})$$

$$\Psi_4 = \left(i \frac{\partial}{\partial x} - A_R \right) \sqrt{a_R} \Psi_R.$$

Now, the equations for these variables have the same form as in the usual case,

$$i \frac{\partial}{\partial x} \Psi = D R \Psi, \quad (\text{H7})$$

where the operator D and matrix R are Hermitian and defined by

$$R = \begin{pmatrix} \frac{\text{Re}d_L}{|d_L|^2} & \frac{i\text{Im}d_L}{|d_L|^2} & 0 & 0 \\ -\frac{i\text{Im}d_L}{|d_L|^2} & -\frac{\text{Re}d_L}{|d_L|^2} & 0 & 0 \\ 0 & 0 & \frac{\text{Re}d_R}{|d_R|^2} & \frac{i\text{Im}d_R}{|d_R|^2} \\ 0 & 0 & -\frac{i\text{Im}d_R}{|d_R|^2} & -\frac{\text{Re}d_R}{|d_R|^2} \end{pmatrix}, \quad (\text{H8})$$

$$D = \begin{pmatrix} A_L \text{Re}d_L & iA_L \text{Im}d_L & -\frac{1}{\sqrt{a_L}} \mathcal{M} \frac{1}{\sqrt{a_R}} & -\frac{1}{\sqrt{a_L}} \mathcal{M} \frac{1}{\sqrt{a_R}} \\ -iA_L^* \text{Im}d_L & -B_L \text{Re}d_L & -\frac{1}{\sqrt{a_L}} \mathcal{M} \frac{1}{\sqrt{a_R}} & -\frac{1}{\sqrt{a_L}} \mathcal{M} \frac{1}{\sqrt{a_R}} \\ -\frac{1}{\sqrt{a_R}} \mathcal{M}^\dagger \frac{1}{\sqrt{a_L}} & -\frac{1}{\sqrt{a_R}} \mathcal{M}^\dagger \frac{1}{\sqrt{a_L}} & A_R \text{Re}d_R & iA_R \text{Im}d_R \\ -\frac{1}{\sqrt{a_R}} \mathcal{M}^\dagger \frac{1}{\sqrt{a_L}} & -\frac{1}{\sqrt{a_R}} \mathcal{M}^\dagger \frac{1}{\sqrt{a_L}} & -iA_R^* \text{Im}d_R & -B_R \text{Re}d_R \end{pmatrix}, \quad (\text{H9})$$

$$d_{L,R} = \frac{1}{a_L} \sqrt{b_{L,R}^2 + 4a_{L,R} c_{L,R}}. \quad (\text{H10})$$

The conserved baryonic current is given by the usual expression

$$J^B = \Psi^\dagger R \Psi. \quad (\text{H11})$$

Now these equations can be solved with the help of formalism described in Appendixes A and G.

APPENDIX I: D_B AND SCATTERING LENGTH OF THE QUASIPARTICLES

One might think that with such a degree of concurrence among the estimates for the scattering length listed in Sec. X that we can be rather confident that $\lambda \sim (4-5)/T$. However when one considers the calculations leading to these estimates, one sees that the scattering length in those discussions is that of a particle with the typical momentum $\sim T$, while we need the scattering length of a

quasiparticle, with relatively low momentum. The quasiparticles are gauge singlets when viewed at a scale longer than some screening length, given by the inverse Debye or magnetic mass. Moreover at least in the one-dimensional problem, the quarks which produce the asymmetry, and thus the quarks whose diffusion length is relevant to determining $f_{\text{sph}}(\rho)$, have energies considerably lower than the thermal average. Let us therefore investigate whether the scattering length obtained in the references quoted above is a good approximation to the actual diffusion length which we require.

The diffusion of the quasiparticles is clearly a three-dimensional phenomenon, so we must consider the general problem in which the quarks incident on the domain wall have nonzero $p_{||}$. We first must decide whether, in the full three-dimensional problem, the quarks carrying the asymmetry current will have relatively low energies, as is the case for the 1D problem. Since we know that

the p_t of s quarks which reflect is in all cases low (see Appendix E), the only way these quarks could have an energy typical of the thermal medium would be if they have $p_{||} \gg \omega_0$. However quarks with this large value of $p_{||}$ see a bubble thickness of $\sim (p_{||}/p_t)a^{-1}$ which may be much larger than the expected mean free path $\sim 5/T$ of quasiparticles having typical thermal energies. If this is the case, these particles will experience many inelastic collisions in the scattering process and the purely quantum mechanical description of their scattering would be inapplicable. In fact, on account of the loss of quantum coherence, the contribution of such particles to the asymmetry should be very much reduced, since CP violation arises because of the difference in phases between δ_{CP} and the quantum mechanical scattering phase shift, which changes sign in going from particles to antiparticles.

Thus the particles whose scattering contributes to the asymmetry current have $p_{||}$ and $p_t \lesssim \frac{3}{2}(\omega_L - \omega_R) \sim 6$ GeV (see Appendix E), so the mean free path which is relevant to estimating the D_B which enters ρ , is the mean free path of a quasiparticle with physical⁴⁶ (energy, momentum) $\sim (50, 6)$ GeV. Denoting the typical energy of a collision mate by $\bar{E} \sim T$ and doing the angular average, one finds $\langle s \rangle = 2\omega\bar{E}$.

Now we need the effective Lagrangian governing the quasiparticle interaction. On account of Debye and magnetic screening of the color of the quasiquark, the propagator appearing in the matrix element is $\sim (q^2 - M_{\text{screening}}^2)^{-1}$. Taking the Debye screening length as a lower limit to this scale, $M_{\text{screening}}^2 > M_D^2 = \frac{(N_f + 2N_c)}{6} g^2 T^2$, and assuming the coupling constant to be just the ordinary QCD coupling appropriate for this energy scale, leads to [79]⁴⁷

$$\sigma_{qq} \lesssim \frac{\alpha_s^2 \langle s \rangle}{M_D^4} = \frac{\langle s \rangle}{(8\pi T^2)^2}, \quad (I1)$$

where we have made use of the fact that the squared momentum transfer is less than $\langle s \rangle/2$ and thus is small compared with M_D^2 . Now summing over quark and gluon collision mates, and noting that $\sigma_{qg} = \frac{9}{4}\sigma_{qq}$, we find

$$n\sigma = \sigma_{qq}(n_{q,\bar{q}} + \frac{9}{4}n_g) \lesssim 0.013T. \quad (I2)$$

The standard estimate of the mean free path in a gas is

$$\lambda = \frac{\bar{v}}{\bar{V} n\sigma}, \quad (I3)$$

where \bar{v} denotes the average speed of the particle whose mean free path is being computed and \bar{V} denotes its average speed relative to other particles in the gas. The diffusion coefficient for a gas is

$$D = \frac{\bar{v}\lambda}{3}. \quad (I4)$$

Taking the average speed of quasiparticles to be ~ 1 while taking \bar{v} , the average speed of the the low-momentum quasiparticle which is diffusing to be $\sim 1/3$, gives a low and thus conservative estimate⁴⁸ $D_B \gtrsim 3/T$ and $\lambda \gtrsim 25/T$. Hopefully this discussion has revealed that the problem of estimating λ and D_B require real understanding of the nature of the quasiparticles and their short- and long-distance interactions. Thus estimates of these quantities must be regarded as highly provisional. In the following we use the ranges $D_B \sim (3 - 5)/T$ and $\lambda \sim (4 - 25)/T$.

⁴⁶See Sec. VI for a discussion of the physical momenta of the quasiparticles. On account of averaging over all directions of incidence of its collision mate, the magnitude of the quasiparticle momentum is in any event irrelevant to estimating the average s of its collisions.

⁴⁷Their calculation included all tree level diagrams.

⁴⁸Another reason that the true D_B and λ may be larger than this estimate is that in modeling the effective Lagrangian we reduced just the range of interaction but not the effective coupling, as compared to the fundamental Lagrangian.

-
- [1] A.D. Sakharov, Pis'ma Zh. Eksp. Teor. Fiz. **5**, 32 (1967) [JETP Lett. **5**, 24 (1967)].
 [2] V.A. Kuzmin, Pis'ma Zh. Eksp. Teor. Fiz. **12**, 335 (1970) [JETP Lett. **12**, 228 (1970)].
 [3] V.A. Kuzmin, A.Yu. Ignatiev, N.V. Krasnikov, and A.N. Tavkhelidze, Phys. Lett. **76B**, 436 (1978).
 [4] M. Yoshimura, Phys. Rev. Lett. **41**, 281 (1978); **42**, 476(E) (1979).
 [5] S. Weinberg, Phys. Rev. Lett. **42**, 850 (1979).
 [6] S. Dimopoulos and L. Susskind, Phys. Rev. D **18**, 4500 (1978).
 [7] A.D. Dolgov and Ya.B. Zeldovich, Rev. Mod. Phys. **53**,

- 1 (1981).
 [8] E.W. Kolb and M.S. Turner, *The Early Universe* (Addison-Wesley, New York, 1990).
 [9] A.D. Dolgov, Phys. Rep. **222**, 309 (1992).
 [10] M.E. Shaposhnikov, Phys. Scr. **T36**, 183 (1991).
 [11] M. Shaposhnikov, in *1991 Summer School in High Energy Physics and Cosmology* (World Scientific, Singapore, 1992), Vol. 1, p. 338.
 [12] N. Turok, Technical Report No. IMPERIAL-TP-91-92-33, 1992 (unpublished).
 [13] A.G. Cohen, D.B. Kaplan, and A.E. Nelson, Annu. Rev. Nucl. Part. Phys. **43**, 27 (1993).

- [14] G. 't Hooft, Phys. Rev. Lett. **37**, 8 (1976).
- [15] G. 't Hooft, Phys. Rev. D **14**, 3432 (1976).
- [16] V.A. Kuzmin, V.A. Rubakov, and M.E. Shaposhnikov, Phys. Lett. **155B**, 36 (1985).
- [17] A.D. Linde, Phys. Lett. **70B**, 306 (1977).
- [18] F.R. Klinkhamer and N.S. Manton, Phys. Rev. D **30**, 2212 (1984).
- [19] D.A. Kirzhnits, Pis'ma Zh. Eksp. Teor. Fiz. **15**, 745 (1972) [JETP Lett. **15**, 529 (1972)].
- [20] D.A. Kirzhnits and A.D. Linde, Phys. Lett. **72B**, 471 (1972).
- [21] M.E. Shaposhnikov, Pis'ma Zh. Eksp. Teor. Fiz. **44**, 364 (1986) [JETP Lett. **44**, 465 (1986)].
- [22] M.E. Shaposhnikov, Nucl. Phys. **B287**, 757 (1987).
- [23] M.E. Shaposhnikov and A.I. Bochkarev, Mod. Phys. Lett. A **2**, 417 (1987).
- [24] J.-F. Grivaz, Orsay Technical Report No. LAL 92-59, 1992 (unpublished).
- [25] L. McLerran, Phys. Rev. Lett. **62**, 1075 (1989).
- [26] M.E. Shaposhnikov, Nucl. Phys. **B299**, 797 (1988).
- [27] N. Turok and J. Zadrozny, Phys. Rev. Lett. **65**, 2331 (1990).
- [28] N. Turok and J. Zadrozny, Nucl. Phys. **B358**, 471 (1991).
- [29] L. McLerran, M.E. Shaposhnikov, N. Turok, and M.B. Voloshin, Phys. Lett. B **256**, 451 (1991).
- [30] M. Dine, P. Huet, R. Singleton, and L. Susskind, Phys. Lett. B **257**, 351 (1991).
- [31] A. Cohen, D. Kaplan, and A. Nelson, Phys. Lett. B **245**, 561 (1990).
- [32] A. Cohen, D. Kaplan, and A. Nelson, Nucl. Phys. **B349**, 727 (1991).
- [33] A. Cohen, D. Kaplan, and A. Nelson, Nucl. Phys. **B373**, 453 (1992).
- [34] A. Cohen, D. Kaplan, and A. Nelson, Phys. Lett. B **294**, 57 (1992).
- [35] A.I. Bochkarev, S.V. Kuzmin, and M.E. Shaposhnikov, Phys. Lett. B **244**, 275 (1990).
- [36] A.I. Bochkarev, S.V. Kuzmin, and M.E. Shaposhnikov, Phys. Rev. D **43**, 369 (1991).
- [37] N. Turok and J. Zadrozny, Nucl. Phys. **B369**, 729 (1992).
- [38] S. Myint, Phys. Lett. B **287**, 325 (1992).
- [39] M. Pietroni, Nucl. Phys. **B402**, 27 (1993).
- [40] M. Dine, R. Leigh, P. Huet, A. Linde, and D. Linde, Phys. Lett. B **283**, 319 (1992).
- [41] M. Dine, R. Leigh, P. Huet, A. Linde, and D. Linde, Phys. Rev. D **46**, 550 (1992).
- [42] J.E. Bagnasco and M. Dine, Phys. Lett. B **303**, 308 (1993).
- [43] P. Arnold and E. Espinosa, Phys. Rev. D **47**, 3546 (1993).
- [44] M.E. Shaposhnikov, Phys. Lett. B **316**, 112 (1993).
- [45] M.E. Shaposhnikov, Phys. Lett. B **277**, 324 (1992); **282**, 483(E) (1992).
- [46] G.R. Farrar and M.E. Shaposhnikov, Phys. Rev. Lett. **70**, 2833 (1993).
- [47] M. Kobayashi and T. Maskawa, Prog. Theor. Phys. **49**, 652 (1973).
- [48] Particle Data Group, K. Hikasa *et al.*, Phys. Rev. D **45**, S1 (1992).
- [49] C. Jarlskog, Phys. Rev. Lett. **55**, 1039 (1985).
- [50] A.I. Bochkarev, S.Yu. Khlebnikov, and M.E. Shaposhnikov, Nucl. Phys. **B329**, 493 (1990).
- [51] J. Ellis, M.K. Gaillard, and D. Nanopoulos, Nucl. Phys. **B109**, 213 (1976).
- [52] M. Laursen, J. Ambjørn, and M.E. Shaposhnikov, Phys. Lett. B **197**, 49 (1987).
- [53] M. Laursen, J. Ambjørn, and M.E. Shaposhnikov, Nucl. Phys. **B316**, 483 (1989).
- [54] V.A. Kuzmin, M.E. Shaposhnikov, and I.I. Tkachev, Phys. Rev. D **45**, 466 (1992).
- [55] A.N. Tavkhelidze, V.A. Matveev, V.A. Rubakov, and M.E. Shaposhnikov, Usp. Fiz. Nauk. B **156**, 253 (1988) [Sov. Phys. Usp. **31**, 916 (1988)].
- [57] A.D. Linde, Nucl. Phys. **B216**, 421 (1983).
- [58] A.D. Linde, Rep. Prog. Phys. **47**, 925 (1984).
- [59] Y. Grossmann and Y. Nir (unpublished).
- [60] S.Yu. Khlebnikov, Phys. Rev. D **46**, 3223 (1992).
- [61] Bao-Hua Liu, L. McLerran, and N. Turok, Phys. Rev. D **46**, 2668 (1992).
- [62] L. McLerran, E. Mottola, and M.E. Shaposhnikov, Phys. Rev. D **43**, 2027 (1991).
- [63] S.Yu. Khlebnikov and M.E. Shaposhnikov, Nucl. Phys. **B308**, 885 (1988).
- [64] S.Yu. Khlebnikov, Phys. Lett. B **300**, 376 (1993).
- [65] O.K. Kalashnikov, Fortschr. Phys. **32**, 525 (1984).
- [66] V.V. Klimov, Yad. Fiz. **33**, 1734 (1981) [Sov. J. Nucl. Phys. **33**, 934 (1981)].
- [67] H.A. Weldon, Phys. Rev. D **26**, 2789 (1982).
- [68] V.V. Lebedev and A.V. Smilga, Ann. Phys. (N.Y.) **202**, 229 (1990).
- [69] E. Braaten and R.D. Pisarski, Phys. Rev. D **46**, 1829 (1992).
- [70] G. Baym and S.A. Chin, Nucl. Phys. **A262**, 527 (1976).
- [71] L.D. Landau and E.M. Lifshits, *Quantum Mechanics* (Nauka, Moscow, 1974).
- [72] Y. Nir and H. Quinn, Phys. Rev. D **42**, 1473 (1990).
- [73] P. Arnold and L. McLerran, Phys. Rev. D **36**, 581 (1987).
- [74] J. Ambjørn, T. Askgaard, H. Porter, and M.E. Shaposhnikov, Phys. Lett. B **244**, 479 (1990).
- [75] J. Ambjørn, T. Askgaard, H. Porter, and M.E. Shaposhnikov, Nucl. Phys. **B353**, 346 (1991).
- [76] D.I. Diakonov, Y.Yu. Petrov, and A.V. Yung, Phys. Lett. **130B**, 385 (1983).
- [77] L. Carson and L. McLerran, Phys. Rev. D **41**, 647 (1990).
- [78] J. Baacke and S. Junker, Mod. Phys. Lett. A **8**, 2869 (1993).
- [79] G. Baym, H. Monien, C. Pethick, and D. Ravenhall, Phys. Rev. Lett. **64**, 1867 (1990).
- [80] K. Kajantie, K. Rummukainen, and M. Shaposhnikov, Nucl. Phys. **B407**, 112 (1993).
- [81] M. Sher, Phys. Lett. B **317**, 159 (1993).
- [82] T. Walker, G. Steigman, D. Schramm, K. Olive, and H.-S. Kang, Astrophys. J. **376**, 51 (1991).
- [83] B.E.J. Pagel, E.A. Simonson, R.J. Terlevich, and M.G. Edmunds, Mon. Not. R. Astron. Soc. **255**, 325 (1992).
- [84] W.H. Press, B.P. Flannery, S.A. Teukolsky, and W.T. Vetterling, *Numerical Recipes* (Cambridge University Press, Cambridge, England, 1986).